Université Catholique de Louvain

Secteur des Sciences de la Santé

Institut de Neuroscience

École Doctorale en Sciences Biomédicales

METHODOLOGICAL APPROACHES FOR THE STUDY OF AUDITORY-TACTILE INTERACTIONS IN CONDITIONS OF ACTIVE TOUCH

Giulia Esposito

2025

Thèse de doctorat présentée en vue de l'obtention du grade de Docteur en Sciences biomédicales et pharmaceutiques.

Cover page illustration: Abstract drawing of a brain hemisphere and a fingerprint, with sound oscillations in the background. Generated with ChatGPT4o (May 2025). Special thanks to Solenn Gousset for the inspiration.

Jury

Promoteur : Prof. André Mouraux, Université Catholique de Louvain

Co-promoteur : Prof. Olivier Collignon, Université Catholique de Louvain

Président : Prof. Valéry Legrain, Université Catholique de Louvain

Secrétaire : Dr. David Gueorguiev, Université Catholique de Louvain

Prof. Sylvie Nozaradan, Université Catholique de Louvain

Dr. Luke Miller, Radboud University, Pays-Bas

Dr. Luigi Tamè, University of Kent, Grande-Bretagne

This thesis was funded by the European Union's Horizon 2020 Research and Innovation Program under Grant Agreement No. 860114 (MultiTOUCH).

Table of Contents

ABBREVIATIONS

EEG:	electroencephalography
ICA:	independent component analysis
MEG:	magnetoencephalography
TMS:	transcranial magnetic stimulation
MEL:	maximum likelihood estimation
RA1:	rapidly-adapting mechanoreceptors type 1
RA2:	rapidly-adapting mechanoreceptors type 2
SA1:	slowly-adapting mechanoreceptors type 1
SA2:	slowly-adapting mechanoreceptors type 2
PSF:	predicted sensory feedback
ERP:	event-related potential
FFT:	Fast Fourier Transform
fMRI:	functional magnetic resonance imaging
SEP:	somatosensory-evoked potential
S1:	primary somatosensory cortex
S2:	secondary somatosensory cortex
M1:	primary motor cortex
APC:	anterior parietal cortex
LPC:	lateral parietal cortex
PPC:	posterior parietal cortex
PRR:	parietal reaching region
DCN:	dorsal column nuclei

PV:	posterior ventral area
VP:	ventroposterior nucleus
VPL:	lateral ventroposterior nucleus
VPM:	medial ventroposterior nucleus
VPS:	ventroposterior superior nucleus
VPI:	ventroposterior inferior nucleus
PSE:	point of subjective equality
PSS:	point of subjective simultaneity
JND:	just noticeable difference
TOJ:	temporal order judgment
MMN:	mismatch negativity
T:	tactile
A:	auditory
AT:	audio-tactile

Acknowledgements

First, I'd like to thank the members of my jury. My internal committee, Valéry, Sylvie, David, and my supervisors, André and Olivier. You have followed me throughout these years and pushed me to think and to learn more and more every day. Your advice and support have been invaluable in making this work possible. Sylvie, thank you for trusting me to take the lead in the frequency-tagging study you so elegantly designed. You often humbly said you were not from the field and maybe your questions were naïve, but some of the questions you asked me have actually shaped my whole way of thinking about my topic. David, I often reached out to you throughout the years to ask for advice and help, and not once have you failed to selflessly help me and guide me with your expertise. Président Legrain, what can I say? You taught me so much about the P300, the N20, the MMN, and so much about Belgium, Charleroi (shout-out to Fabrizio le carolo) and good music! Thank you for overseeing my PhD and making sure everything ran smoothly and appropriately. Working with you has been an absolute pleasure. To the external members of the jury, Luigi and Luke. Thank you for the time you have taken to evaluate my thesis. Your questions and comments have helped me to learn even more, even in the limited time of the private defence. I would have continued discussing with you for another 3 hours! What even is active touch, after all? To all of you, thank you for giving me the chance to discuss my work in such an enlightening, thoughtful manner. It was probably one of the best days of the whole PhD, and an experience I will cherish forever.

To my supervisors, André and Olivier, thank you for your precious guidance and support during this sometimes-challenging journey. Thank you both for being so available, attentive, and approachable.

Olivier, thank you for always having such insightful comments and suggestions. You have tirelessly helped me and challenged me to make my work better, and inspired me to always look and think beyond the "obvious". Thank you for making me part of the CPP lab – whose energy and enthusiasm for science are unparalleled. Organizing and being part of IMRF2023 with you is one of the best memories I have of these PhD years – particularly the wild dancing afterwards!

André, thank you for praising me at my best, and for supporting me at my worst. I never took for granted how much you helped me, in so many ways, throughout these years, from sitting with me for hours going through my very counter-intuitive MATLAB codes, to always keeping your door open for my **many** "confessions" and "epiphanies". I think we are very different in many ways, but you perfectly understood the way I work, the way I manage (or sometimes not) stress, and whenever I was simply being "plus catholique que le Pape" and just needed some reassurance. You have my outmost respect and admiration, as a scientist, as a leader, and as a person. I hope we will get many chances to develop our ambitious ideas together in the future. To André's new PhD students: you are very lucky, *indeed*!

To my new PI, David. Thank you for believing in me and giving me a chance to continue working on this topic that I've come to love so much. I look forward to this new chapter with you and the Tangi Lab, and to moving the field forward together.

To the NOCIONS PIs, André, Valéry, Giulia. Thank you for providing us with such a safe, friendly, and thriving work environment. The way you manage your leadership and authority with such grace and humility is truly remarkable, and something we are all very thankful for.

Delia, Lieve, Manu, Carlo, Simone, Arthur, Domi. During all these years, you have been the most precious support network and the best friends I could have wished for. In all those moments I've felt like I was hanging by a thread, you never failed to lend your hand to pick me back up again, and for that I am forever grateful.

Delinini, thank you for always being there to answer my questions, both statistical and existential, and for making me laugh and feel like a happy kid whenever we were together. Thank you for listening to my absurd doubts for hours without ever judging me, and for teaching me to sometimes laugh about them. I will keep upgrading my sofa beds so that you will always have a second home, wherever life will take us. Ti voglio tanto bene piccola Delia!

Lieve, mamma Lieve. Madame la directrice du bureau des réclamations. I am so grateful you gave me a place in your life and heart. You ~~were~~ are my mentor, my safe port, my ray of sunshine through the clouds. You helped me carry the weight of my worry the night of my private defence (lovely sea urchins!) and stood by me

until 13.59 on the day. I even wore your shoes so I could have a little piece of you in there with me to give me strength! Our sunny (and rainy) balcony breaks have been the favourite part of my working days for almost five years! Thank you for your unconditional support, your weekend adventure stories in crazy Eupen, and for your contagious energy. Delia couldn't have said it better: "everyone deserves a Lieve in their life".

Manu, you are one of the best people I've ever met. Your intelligence, curiosity, and culture (and musical taste!) have been incredibly inspiring. You have unknowingly pushed me, time and time again, to try and be a better person myself, and I am so fortunate to have had you as my PhD brother, my mfi. I cannot wait to celebrate your own success with you and see all the amazing things you will achieve – even though I am already (and always will be) immensely proud of you.

Carlo, we spent four years of extreme closeness, literally, but I couldn't have asked for a better office mate to share 1 square meter with. Keep finding new passions, but please refrain from buying new gadgets even if I'm not there to supervise you!

Simone, you were my very first friend in Brussels. Thank you for the deep conversations, the wonderful Sicilian food, and the carefree weekend walks around Ixelles. Non ci disuniremo mai!

Arthur and Domi, thank you for letting me into your very exclusive club, and for all the beers and laughs. I will always cherish the wonderfully fun times we spent together. Arthur, thank for all your guidance, help, and patience. Domi, you brought a hurricane of joy and fun in my life. Keep shining bright, my beautiful potato!

Thank you to Vladimir, Alberto, Igor, Chiara, Artem, Gloria, Solenn, Avgustina, Roberta, Francesca, Filippo, Iqra, and to everyone else in the NOCIONS, SpacePain, Liberati, RnB and CPP teams for always brightening my days with your presence. It was a pleasure to work with each and every one of you.

Thank you to Julien, Cédric, Kevin, and everyone at NTMED for helping me develop my crazy setups, for their invaluable scientific and technical inputs, and for their patience when I sometimes changed my mind or had new ideas over and over again.

Special thanks also to Leila, Cathy, and Sonia, for the continued support and help they give to all of us.

Elisa, thank you for helping me find the light in myself when everything seemed to have gone dark. I owe you more than you can imagine.

Giuliano, fafu, pupi. I could write a whole book about how much I love you and how incredibly blessed I feel for having you as my life partner. I really did win the lottery by finding you. You are the love of my life, my best friend, my family, my joy, my sun, my all. All the things I should be proud of myself for, I could not have done any single one of them without you by my side, and I can never thank you enough for everything you have done and do for me every day. Ti amo da morire pupatello.

Papà e Andrea. Nella lontananza, nel dolore, nelle mancanze, nella gioia, al sole, al mare, non mi avete mai fatto sentire sola. Il vostro amore e il vostro calore mi hanno accompagnata e dato forza ogni giorno. Vi voglio un bene dell'anima.

Mamma, ce l'ho fatta. Spero che da qualche parte nell'universo tu mi veda e sia fiera di me.

Lastly, to my anxiety. You took a lot from me. You made me doubt every single thing I did. You made me think I was never good enough. But you also pushed me to be my best. You pushed me the night before my private defence to get up at 2am to read more about proprioception, because you knew I didn't know as much as I wanted to know. But then I could answer a very specific question about the exact thing you made me read. So, in a weird way, thank you. I hope we can live together in peace one day.

Freely adapted from Fleabag:

A PhD is painful. It's frightening. It makes you doubt yourself, it makes you judge yourself. Doing a PhD takes a whole lot of hope. So no wonder it's something we don't want to do on our own.

So, once again, to all of you incredible, talented, wonderful people, thank you for sharing a ride with me on this rollercoaster.

CHAPTER 1: General introduction.

1. General Introduction

Feeling the world by touch is a complex process. When we explore objects with our hands, sensory receptors respond to the different forces on our skin, such as vibration, pressure, or friction. This information is transmitted and processed along the somatosensory pathway of our nervous system, and these simple inputs are integrated to provide us with a rich, unified experience of our interactions with the object or surface we are exploring. Touch is often not a passive, static experience. In our everyday life, we perform different actions to extract tactile information from the world: we stroke a piece of clothing to appreciate its fabric, we push on materials to feel their softness, we trace the edges of an object to recognize its shape. This further complexifies touch, as somatosensory inputs arising from the skin-surface contact are also integrated with motor signals guiding our actions to perceive the environment by touch, as well as with proprioceptive inputs informing us about the position of our body in the external space relative to the position of the object or surface we are exploring. Tactile experiences are also often accompanied by signals from other sensory modalities, such as sound: we hear the sounds elicited by stroking a surface, or the transient sounds elicited when briefly contacting the edges of an object we are interacting with.

In the neuroscientific literature, relatively little is known about the cortical mechanisms that underly such complex multisensory experiences in conditions of active touch. How are inputs from touch and sound integrated when we actively explore a texture? How do transient sounds elicited by transient contacts between the skin and an object help us locate it? Scalp electroencephalography (EEG) is a non-invasive neurophysiological technique allowing to study cortical processes with high temporal fidelity, making it a good candidate to assess how brain responses to a given stimulation evolve over a small, sub-second time scale,

allowing us to investigate the temporal dynamics of processing of sensory inputs arising from multisensory active tactile experiences. Although EEG has poor spatial resolution, the fact that the primary somatosensory cortex (S1) is somatotopically organized, that is, each body part is represented within S1 within anatomically-defined regions, allows us to disentangle whether a sensory stimulus is processed early within the cortical somatosensory hierarchy, or within higher order multisensory areas. Indeed, if processing of a sensory stimulus mainly involves S1, the distribution of responses over the scalp would differ when the same stimulus is applied to the hand or to a different body location.

This doctoral thesis aimed to develop and validate three neuroscientific approaches to study auditory-tactile interactions in conditions of active, dynamic touch, focusing on perception and processing of edges and textures: psychophysics (Chapter 2), EEG frequency-tagging (Chapter 3), and recording of EEG event-related potentials (Chapter 4).

Chapter 1 will provide an overview of the relevant theoretical background. First, it will introduce the somatosensory system, focusing on the interplay of the sensory receptors involved in active tactile sensing and the hierarchical processing of tactile and proprioceptive inputs along the somatosensory axis. Next, the Chapter will delve deeper into processes that are specific to active tactile sensing, including sensorimotor control, gating of somatosensory signals, and integration of proprioceptive and tactile inputs during active tactile exploration. Then, the Chapter will specifically introduce the neuroscientific evidence for interactions between the auditory and tactile modalities, and the candidate techniques to investigate such interactions in conditions of active touch both behaviorally using psychophysics and at the cortical level using scalp EEG. Lastly, the Chapter will

introduce the aims and objectives of this doctoral thesis, and outline the experimental work implemented to meet such aims.

In Chapters 2, 3, and 4, the experimental work carried out during this doctoral thesis will be presented in detail, including the addressed questions, hypotheses, methodological approaches, and discussion of the results. Chapter 2 will present a psychophysical experiment in which we investigated auditory-tactile interactions in the context of localization of edge-like tactile stimuli in conditions of active touch. Chapter 3 will present an EEG experiment in which we investigated the role of S1 in processing fine-grained changes in vibrational patterns distinguishing different vibrotactile textures, in conditions of passive touch. Chapter 4 will present an EEG experiment in which we investigated time-locked responses to edge-like tactile stimuli in conditions of active touch.

Chapter 5 will summarize and briefly discuss the experimental work reported in the previous chapters and the possible future applications of the techniques validated during this project for the study of the cortical mechanisms of audio-tactile integration in conditions of active, dynamic touch. Lastly, the Chapter will critically evaluate the stimulation platforms that are currently available to investigate such questions, their advantages and disadvantages, and provide insights on the technical needs for a robust, systematic investigation of such processes using EEG techniques.

2. The somatosensory system

2.1. Sensory receptors

The sense of touch arises from the synergetic activity of sensory receptors located both within the skin and within deeper tissue structures, such as muscles, tendons, and joints. Such sensory receptors include skin mechanoreceptors, and joint, muscle, and tendon proprioceptors. Skin mechanoreceptors are located both within glabrous and hairy skin, and they convey exteroceptive mechanical information (i.e. coming from an external source), specifically mechanical skin deformations. Proprioceptors convey, as the name suggests, proprioceptive information, that is, information about the position of the body in the external space. The interplay between mechanosensation and proprioception is especially relevant to haptic experiences involving active, dynamic touch, as will be discussed in the next sections. Below, the main classes of skin mechanoreceptors and proprioceptors, and their functions, are described.

2.1.1. Skin mechanoreceptors

Tactile sensations including shape, texture, vibration, and object size are rendered by mechanical deformations of the skin, which activate specialized sensory receptors in the skin. These receptors are collectively known as skin mechanoreceptors, and are classified on the basis of the rate of adaptation and receptive field size of the afferent fibers that innervate them. Slowly-adapting mechanoreceptors type 1 (SA1) and slowly-adapting mechanoreceptors type 2 (SA2) both display sustained responses during mechanical skin deformations. On the contrary, rapidly-adapting mechanoreceptors type 1 (RA1) and rapidly-adapting mechanoreceptors type 2 (RA2) respond to transient changes in the rate of skin indentation or changes in the rate of the forces applied to the skin, respectively

(Delhaye et al., 2018; Johnson, 2001; Jones and Smith, 2014; ten Donkelaar et al., 2020). The type 1 vs. type 2 classification distinguishes the size of the innervating fibers' receptive fields, with type 1 having small receptive fields and type 2 having larger receptive fields. RA1 fibers are thought to innervate Meissner's corpuscles, RA2 fibers to innervate Pacinian corpuscles, SA1 fibers to innervate Merkel's disks, and SA2 fibers to innervate Ruffini corpuscles (Figure 1) (Johansson and Vallbo, 1979; Johnson, 2001; Jones and Smith, 2014; Vallbo and Johansson, 1984). However, besides Pacinian corpuscles, which have been well characterized thanks to their very large size, the exact association between mechanoreceptor morphology and afferent fiber is still debated (Jones and Smith, 2014).

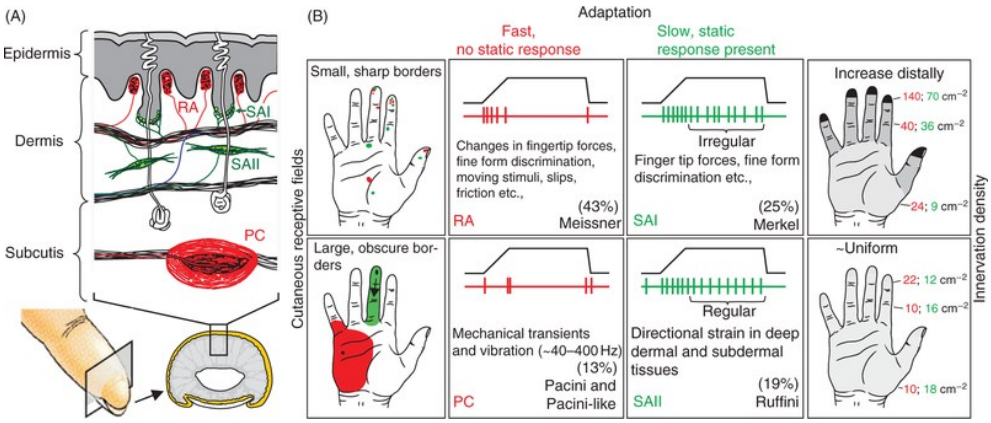

Figure 1. Skin mechanoreceptors within the hand. Different classes of skin mechanoreceptors are located at different depths within the skin (A) and differ in terms of their receptive field size and rate of adaptation (B), with type 1 receptors having small receptive fields and type 2 receptors having large receptive fields, while RA receptors respond to the onset and offset of stimulation and SA receptors display sustained responses. Type 1 receptors innervate the skin more densely at the fingertip than type 2 receptors, which display more uniform distribution throughout the hand. From Delhaye et al. (2018).

With regard to encoding of vibration, tactile fibers display time-locked responses to the frequency of vibratory stimuli, with SA1 fibers responding to

frequencies up to 5 Hz, RA2 being most sensitive to frequencies of around 250 Hz, and RA1 fibers responding to intermediate frequencies (Delhaye et al., 2018; Talbot et al., 1968). Due to their response properties, different classes of mechanoreceptors encode different aspects of textures. For instance, local skin deformations elicited by coarse textures such as Braille-dots activate SA1 (and RA1) fibers, which mediate encoding of such textures via a spatial code (Harvey et al., 2013; Weber et al., 2013). Similarly, the peripheral encoding of shape is given by the spatial pattern of activation of cutaneous mechanoreceptors (Khalsa et al., 1998; LaMotte and Srinivasan, 1996). On the other hand, encoding of fine textures such as sandpapers requires movement of the surface against the skin (Hollins and Risner, 2000). RA1 fibers are particularly implicated in the detection of skin motion and encode object slip and sudden changes in forces acting on the skin, thus also highlighting their important role in texture perception as well as grip control (Johnson, 2001). During exploration of fine textures, the skin vibrations elicited by dynamic skin-surface interactions activate RA1 and RA2 fibers, whose activity reliably reflects the properties of fine textures at the millisecond scale (Mackevicius et al., 2012; Weber et al., 2013).

Even though, for several years, each class of mechanoreceptor has been attributed a specific perceptual role, for example with SA mechanoreceptors being associated with the perception of shapes, RA1 mechanoreceptors being associated with the perception of textures, and RA2 being associated with the perception of rapid vibrations (Johnson, 2001), more recent views favor the idea that different classes of mechanoreceptors work together to transmit mechanical information about different forces acting on the skin (Saal et al., 2017; Saal and Bensmaia, 2014). Such models of population coding are discussed below.

2.1.2. Mechanoreceptors population coding

For years, there has been a general agreement on a one-to-one link between mechanoreceptor type and their contribution to the processing of a specific tactile submodality, such as shape, texture, motion, or friction (i.e., submodality segregation). For instance, SA1 fibers have long been associated with encoding information about shape, RA1 fibers to encode information about motion, and RA2 fibers to encode information about vibration (Johnson, 2001). However, the seminal work that has characterized the response properties and putative functions of tactile afferent fibers has relied on single-unit recordings (LaMotte and Srinivasan, 1996) or psychophysical experiments which exploited masking or adaptation of a specific class of afferent fiber (Bolanowski et al., 1988; Saal and Bensmaia, 2014). Single-unit recordings, while useful to model the behavior and properties of each individual fiber class, are limited by the fact that the activity originating from different classes of fibers cannot be measured simultaneously (Talbot et al., 1968; Vallbo and Hagbarth, 1968; Saal et al., 2017). Modelling studies are particularly useful to investigate population-level responses within different classes of fibers conveying somatosensory information (Saal et al., 2017). Indeed, in more recent years, such work has provided compelling evidence in favor of the view that instead, different afferent classes within a population act synergistically to process information about tactile stimuli (i.e., submodality convergence) (Deflorio et al., 2022; Saal et al., 2017; Saal and Bensmaia, 2014). For example, edge orientation, a spatial feature of tactile stimuli, is not solely encoded by the spatial pattern of activation of SA1 fibers. Indeed, while SA1 fibers do carry more precise information about edge orientation when their responses are measured in isolation, RA1 fibers also encode such information, and their greater density compensates for their less precise responsiveness. Indeed, modelling studies have shown that combining responses across the two fiber populations

significantly improves classification of edge orientation compared to relying on the responses of either population alone (Saal et al., 2017). Further evidence supporting the idea that shape processing does not solely involve the spatial patterning of SA1 responses comes from studies reporting that presenting letters using a sensory substitution device (OPTACON) that conveys shapes via arrays of vibrating pins (Goldish and Taylor, 1974) does not impair subjects' ability to recognize the letters, even though the device activates RA1 and RA2 fibers, but not SA1 fibers (Bliss et al., 1970; Gardner and Palmer, 1989). Texture is also conveyed by the activity of multiple classes of mechanoreceptive afferents. For instance, the patterning of SA fiber responses has been associated with conveying spatial information and the timing of RA fibers with conveying temporal information about skin indentation (Weber et al., 2013), and behavioral evidence has suggested that spatial and temporal codes underlie perception of coarse and fine textures, respectively (Hollins and Risner, 2000).

2.1.3. Proprioceptors

Proprioceptors are a specialized class of sensory receptors specifically encoding muscle, tendon and joint load, length, and stretches. Muscle spindles are structures of connective tissue embedded deep within mammalian skeletal muscle. Within muscle spindles, two classes of proprioceptors are found. Group Ia afferents encode muscle length and the velocity of change in muscle length, while group II afferents encode static muscle length (Proske, 1997; Proske and Gandevia, 2012; Tuthill and Azim, 2018). These two types of fibers work together to convey information about body position: group Ia fibers detect rapid changes in body position, and group II fibers encode larger scale postural changes (Hunt, 1990; Proske and Gandevia, 2012; Tuthill and Azim, 2018). Between muscles and tendons, a third group of proprioceptive afferents is found: type Ib fibers, called Golgi tendon

organs. These encode limb load and specifically fire in the presence of increased muscle tension. Within the joint, specialized mechanoreceptors fire at certain joint positions, often firing maximally at extreme positions. Joint mechanoreceptors are classified depending on their location within the joint: type I joint mechanoreceptors are located at the outer layers of the joint capsule and are slowly adapting. Type II joint mechanoreceptors are located in the deeper layers of the joint capsule and are rapidly adapting. Type III joint mechanoreceptors are found in ligaments and tendon ends near the joint capsule, and are slowly adapting. Lastly, type IV joint nociceptors convey painful information and are found throughout the joint capsule (Tuthill and Azim, 2018). Importantly, skin mechanoreceptors also contribute to movement and position senses (Edin, 2001; Edin and Abbs, 1991; Proske and Gandevia, 2012; Tuthill and Azim, 2018). Indeed, during limb movement and joint rotation, the cutaneous tissue on one side of the joint is stretched while the other is compressed, and SA2 fibers display sensitivity to such stretches (Aimonetti et al., 2007). Furthermore, microneurography studies have reported that both SA and RA mechanoreceptive fibers respond during natural movements of the hand and during knee rotation (Edin, 2001; Edin and Abbs, 1991). The reciprocal interactions between tactile and proprioceptive inputs will be discussed more in detail in Section 3.3.

2.2. Somatosensory pathways

From the periphery, sensory afferents bundle together into nerves and reach the dorsal root ganglia (DRG). From the DRG, afferent fibers ascend and form synapses with neurons within the dorsal column nuclei (DCN) of the brain stem (Delhaye et al., 2018; Smith and Deacon, 1984). Here, three nuclei are found: the cuneate and external cuneate nuclei receive inputs from the upper body, and the gracile nucleus receives inputs from the lower body. The cuneate nucleus

comprises a rostral, a central, and a caudal region, with the first two receiving predominantly proprioceptive (joint and muscle) input, and the latter also displaying Pacinian-like responses (Dykes et al., 1982; Loutit et al., 2021). The external cuneate nucleus, on the other hand, receives mainly proprioceptive input from muscles, tendons, and joints (Loutit et al., 2021). Lastly, the gracile nucleus is involved in processing of both proprioceptive and cutaneous inputs (Dykes et al., 1982; ten Donkelaar et al., 2020; Whitsel et al., 1969). The DCN is implicated in the transmission of afferent somatosensory signals with high temporal fidelity (Hsiao, 2008; Wang et al., 1995), and more recent evidence suggests that some level of feature extraction already occurs within this region, which is thus more than a simple relay station transmitting unprocessed signals (Bengtsson et al., 2013; Delhaye et al., 2018). Moving along the somatosensory hierarchy, the DCN projects onto the contralateral ventroposterior complex of the thalamus (ten Donkelaar et al., 2020). As in the DCN, somatosensory neurons in this region also display similar response properties to afferent fibers, suggesting that sensory processing at this stage is still minimal. The ventroposterior complex of the thalamus is divided into the ventroposterior nucleus (VP; further divided into lateral (VPL) and medial (VPM)), the ventroposterior superior nucleus (VPS) and the ventroposterior inferior nucleus (VPI) (Krubitzer and Kaas, 1992). Each of these regions displays an anatomically-defined contralateral map of the body (i.e., somatotopy) (Lenz et al., 1988). The VPL and the VPM both receive cutaneous input from RA1, SA1 and SA2 receptors (Lenz et al., 1988), with the first receiving it from the DCN and the second from the trigeminal nucleus. The VPS receives proprioceptive input, especially from deep receptors within muscle spindles (ten Donkelaar et al., 2020; Wiesendanger and Miles, 1982), while the VPI received nociceptive and thermoceptive input (Lenz et al., 1993). Neurons from the thalamus project to different areas and layers of

somatosensory cortices (Figure 2), described in the next section (Behrens et al., 2003; Delhaye et al., 2018; Krubitzer and Kaas, 1992).

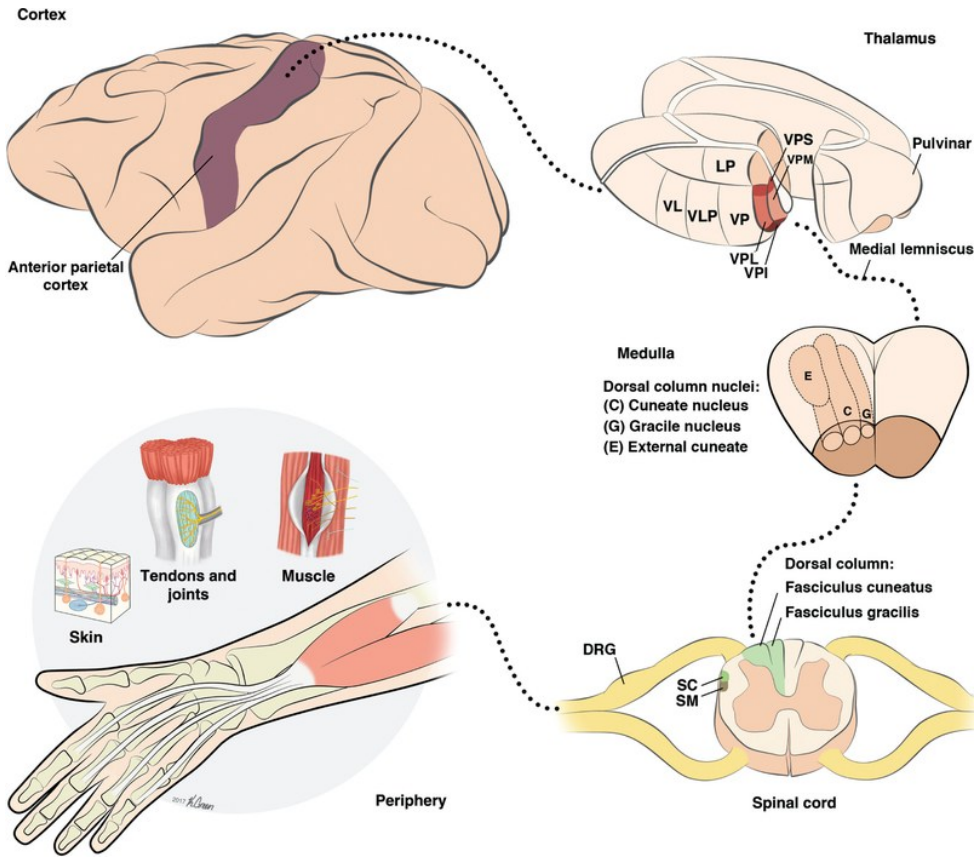

Figure 2. Overview of somatosensory pathways from the periphery to the cortex. From the periphery, afferent fibers within the skin, muscle, tendons, and joints project to the spinal cord through the dorsal root. At the spinal cord, they branch into two projections: one towards the dorsal horn and one towards the DCN, which projects contralaterally to the thalamus, which in turn projects to the somatosensory cortex. From Delhaye et al. (2018).

2.3. Somatosensory cortices

The hierarchical processing of somatosensory inputs continues at the cortical level (Iwamura, 1998). The first cortical region involved in the processing of tactile and proprioceptive inputs is the anterior parietal cortex (APC). The APC comprises four distinct areas: area 3a, 3b, 1, and 2, each of which is somatotopically organized,

(Iwamura, 1998; Jain et al., 2001, 1998; Kaas, 1983; ten Donkelaar et al., 2020). Area 3b represents the primary somatosensory cortex (S1) and it is the first cortical region receiving and processing tactile inputs (Kaas, 1983). Indeed, lesions to this area completely abolish tactile abilities, including shape and texture discrimination (Delhaye et al., 2018; Randolph and Semmes, 1974; Semmes and Turner, 1977). Neurons in area 3b respond to cutaneous stimulation and receive input from SA1, RA1 and RA2 fibers (Delhaye et al., 2018; Pei et al., 2009). Moving along the hierarchical organization of the somatosensory cortex, area 3b projects onto area 1 (Krubitzer and Kaas, 1990), where neurons also respond to cutaneous inputs, and have larger receptive fields compared to neurons in area 3b (Iwamura et al., 1993, 1983; Ploner et al., 2000). Following lesions to area 1, shape discrimination has been reported to be preserved, while texture discrimination is abolished (Carlson, 1981). Area 1 projects upstream to area 3a (Krubitzer and Kaas, 1990), where neurons mainly respond to proprioceptive inputs and display yet larger receptive fields than areas 3b and 1 (Iwamura et al., 1993). Area 3a projects to area 2, as well as the primary motor cortex (M1) and supplementary motor area (SMA) (Krubitzer and Kaas, 1990). The last area in the APC is area 2, which processes tactile and proprioceptive inputs, with some neurons responding to both modalities (Delhaye et al., 2018; Iwamura et al., 1993; Kaas, 1993; ten Donkelaar et al., 2020). Here, cells have even larger receptive fields, which can sometimes be bilateral, making somatotopy in area 2 less fine-grained than in the previous areas of the APC (Delhaye et al., 2018; Pons et al., 1985). Neurons in the APC encode vibrations through phase-locked activity (temporal code) as well as through increases or decreases in firing rate (rate code) in response to low frequency vibratory stimuli, while at higher frequencies, only a subpopulation of neurons still displays a phase-locked patterning of responses encoding frequency content (Delhaye et al., 2018; Mountcastle et al., 1969). The mechanisms of texture encoding in the APC are not

fully understood. Some neurons within the APC are sensitive to the spatial properties of tactile stimuli, thus possibly mediating encoding of coarse textures, whereas others respond to the temporal patterns of skin vibrations, thus possibly encoding finer textures (Connor et al., 1990; Connor and Johnson, 1992; Delhaye et al., 2018). The cortical processing of shape also begins within the APC, with neurons in areas 3b and 1 responding to specific orientations of skin indentation (Bensmaia et al., 2008; Delhaye et al., 2018). Area 2 displays responses to more complex features of shape compared to area 3b, such as curved shapes with multiple orientations (Delhaye et al., 2018; Yau et al., 2013). Similarly to tactile afferents, neurons in APC respond to the direction and magnitude of shear forces elicited during object manipulation or surface scanning, as well as encoding movement direction and speed when an object or texture slides against the skin (Costanzo and Gardner, 1980; Delhaye et al., 2018; Dépeault et al., 2013; Fortier-Poisson et al., 2016). APC areas project onto the lateral and posterior parietal cortices (LPC and PPC) (Krubitzer and Kaas, 1990; ten Donkelaar et al., 2020).

The LPC comprises two areas: the secondary somatosensory cortex (S2) and the parietal ventral area (PV) (Fitzgerald et al., 2004; ten Donkelaar et al., 2020). The LPC processes both cutaneous and proprioceptive inputs, and comprises neurons with large receptive fields and bilateral responses (Delhaye et al., 2018; Fitzgerald et al., 2006, 2004; Taoka et al., 2016; ten Donkelaar et al., 2020). With regard to frequency encoding, most LPC neurons display phase-locked responses to low frequencies up to 10 Hz, and frequency is more strongly encoded in this area by the neurons' firing rates (Burton and Sinclair, 1991; Delhaye et al., 2018; Salinas et al., 2000). In monkeys, it has been shown that neurons within S2 do not follow the temporal pattern of vibratory stimuli, but two frequency-dependent neuronal populations have been identified and implicated in frequency-discrimination (Romo et al., 2003). During texture processing, neurons in the LPC respond to

groove width, contact force, and/or scanning speed, and some neurons also encode the presence of a change in the spatial pattern of a texture (Jiang et al., 1997; Pruett et al., 2000). In the context of shape processing, LPC tuning for shape curvature is very refined and analogous to visual area V4 (Delhaye et al., 2018; Yau et al., 2009), and lesions to this area also impair shape discrimination in monkeys (Murray and Mishkin, 1984) as well as object manipulation in humans, suggesting its implication in sensorimotor integration (Roland, 1987). LPC is deeply interconnected with other cortical and thalamic regions, projecting to the insula, the posterior parietal cortex (PPC), the APC, the VPL, as well as premotor areas, and receiving inputs from the APC and thalamic areas (Delhaye et al., 2018; Disbrow et al., 2003).

The PPC comprises two areas: area 5 and area 7. Of these, area 5 includes two subregions: a lateral one, or area 5L, and a medial one, or parietal reaching region (PRR) (Delhaye et al., 2018; ten Donkelaar et al., 2020). Area 5L receives inputs from both the APC and the thalamus, and projects to area 5, area 7, LPC, motor cortices, and the superior temporal gyrus. It is thought to be involved in grasp and reaching behaviors associated with shape and texture exploration (Delhaye et al., 2018; Vingerhoets, 2014). The PRR is a multisensory region whose neurons respond both to proprioceptive and visual stimulation, receiving inputs from both area 5L and parietal visual areas. The PRR is involved in the planning and execution of reaching movements (Connolly et al., 2003; Delhaye et al., 2018; Filimon et al., 2009). The somatosensory subregion of area 7 is area 7b, which receives inputs from area 5, the LPC, the thalamus, as well as visual areas, and projects to premotor areas and the caudal PPC. Neurons in area 7b respond during both voluntary and passive limb movement, and to tactile, thermal, nociceptive, and visual stimuli, with some neurons responding to more than one modality (Delhaye et al., 2018; Dong et al., 1994; Leinonen et al., 1979).

3. Active touch

3.1. Active vs. passive touch

Gibson (1962) distinguished active and passive touch, defining passive touch as the perceptual experience of being touched, and active touch as touching, which is an effortful, intentional act to optimally extract information from the external world (Gibson, 1962). Part of the neural mechanisms involved in active tactile exploration are inherently different from those underlying passive tactile perception (Table 1). While passive touch mainly involves inputs from cutaneous receptors of the skin, active touch also encompasses proprioceptive and motor processes (Simões-Franklin et al., 2011). Passive touch can be static or dynamic. In passive static touch, a tactile stimulus, which can take the form of an electrical, pressure, or vibrotactile stimulation, is applied onto the subject's skin, and perception of the stimulus does not require any movement. In passive dynamic touch, which can be implemented, for example, to deliver textural stimuli, either the stimulus is displaced against the subject's skin while the subject's limb is kept static, or the subject's limb is displaced against the stimulus.

Table 1. Components distinguishing active dynamic touch from passive static and passive dynamic touch.

	Active dynamic touch	Passive static touch	Passive dynamic touch
Skin deformation	✓	✓	✓
Somatosensory inputs	✓	✓	✓
Limb displacement	✓	×	✓ / ×
Proprioceptive inputs	✓	×	✓ / ×
Sensorimotor control	✓	×	×
Volition	✓	×	×

By drawing parallels with engineering and computer science, active touch (and active sensing in general) can be seen as a mechanism by which the sensor (i.e., the skin coming into contact with the explored surface or object) moves against the stimulus to be measured while implementing and adapting its movement strategies depending on the feedback it receives, in order to maximize extraction of useful data and minimize the costs associated with active control (Bajcsy, 1988; Prescott et al., 2011). Indeed, during haptic exploration, subjects typically employ different exploration strategies depending on the task: stroking movements to extract textural features of different materials, pressing against a surface to assess its softness or hardness, sliding movements to explore the edges

of planar shapes, or even keeping the skin stationary against a surface to extract thermal information (Lederman and Klatzky, 1993). Thus, a crucial aspect distinguishing passive from active touch (as operationalized in this thesis) is the volitional aspect of the exploratory movements performed to extract tactile information from the external world. As such, one might even wonder if active touch, as discussed in this thesis, should be further described as "voluntary, active dynamic touch". Indeed, touch associated with movement is not always intentional. For instance, self-generated tactile input arises from several actions, such as clothes stroking against the skin while moving, or the sole of the foot pressing against the ground while walking. Even reaching for and manipulating an object, such as a cup, could be described as active, dynamic touch action lacking the volitional aspect specifically directed at extracting tactile information. While tactile information is undoubtedly necessary to perform such actions, it is not their final goal, as in the case of appreciating a piece of fabric or exploring the contours of a shape.

In the literature, several studies have aimed to characterize behavioral differences between active and passive touch in terms of perceptual advantages yielded by either condition as well as the neural factors potentially contributing to such advantages (or disadvantages). Seminal work on this topic has famously shown that active, dynamic touch was superior to passive touch, in that it provided a perceptual benefit reflected by shorter times necessary to correctly identify simple shapes compared to both passive static and passive dynamic touch (Heller, 1984). However, this effect has not always been observed when comparing behavioral performance between conditions of active and passive touch, and some conflicting evidence exists in the literature. For instance, early work on texture perception, in which subjects were required to report the perceived roughness of different materials reported no differences between the resulting magnitude

estimations obtained under conditions of active and passive touch, thus suggesting that active touch may not always offer a perceptual benefit over passive touch (Lederman, 1981). Other studies investigating texture perception also found no differences between active and passive touch and showed that discrimination of different surfaces rather appears to be affected by the roughness of the material being explored, such that accuracy was similar for fine and coarse textures, while performance was much lower for medium-roughness textures (Simões-Franklin et al., 2011). Possible mechanisms have been proposed to explain the underlying neural mechanisms that may be driving facilitation or suppression of tactile perception under conditions of active touch. However, one cannot but wonder whether merely comparing active and passive touch in terms of perceptual advantages or disadvantages offers a meaningful appreciation of the mechanisms of tactile perception guided by voluntary exploratory movements. The differentiation between passive and active touch as ''being touched'' vs. ''touching'' itself appears overly simplistic. Indeed, as mentioned above, active touch can be operationalized as a complex sensorimotor process by which the sensor (i.e., the exploring limb) is constantly adapted to its own state and to the environment to optimize the information to be extracted, by suppressing some signals and enhancing others, via a complex interplay of cutaneous, proprioceptive, and motor signals (Prescott et al., 2011). Furthermore, during active touch, tactile sensations are often accompanied by inputs from other modalities, such as the sound elicited by knocking on a door, or by stroking a textured surface.

In the next sections, we will discuss processes that are specifically associated with active tactile sensing, including sensorimotor control, movement-related gating of somatosensory signals, and the contribution of tactile and proprioceptive cues to tactile perception associated with voluntary movements.

3.2. Sensorimotor control during active touch

During active touch, fine-tuned sensorimotor control sees a balanced interplay between tactile inputs and motor outputs. Tactile inputs from afferent mechanoreceptive fibers provide information about the speed, intensity, and direction of forces acting on the skin, which are given by the object's size, shape, weight, and texture. In turn, the speed, direction, and force of the exploratory movements necessary to extract information from the environment are adapted to further enhance tactile perception (Jones and Smith, 2014). For example, when holding an object, grip forces and control are adapted depending on the object's weight or slipperiness and depending on the coefficient of friction between the skin and the object's surface. Indeed, object manipulation becomes a difficult task in the absence of or with disrupted tactile inputs (Augurelle et al., 2003), and adaptation and efficiency of precise grip control have been shown to be impaired when the palmar skin of participants' digits was covered by a thin layer of plastic material (Bilaloglu et al., 2016). Thus, during active tactile tasks such as object manipulation or feeling a texture by scanning movements, reciprocal influences occur between the somatosensory and motor systems.

When comparing active and passive touch, some suggest that active touch is "superior" to passive touch, in that it provides additional information to interpret the incoming sensory information (Sciutti et al., 2010). By its very nature, active touch comprises somatosensory, proprioceptive, and motor components. Thus, during haptic exploration, we receive afferent information from the periphery, but also from the motor commands necessary to initiate the exploratory movements (Deecke et al., 1976; Kornhuber and Deecke, 1985). The forward model of motor control suggests that the motor system predicts the arm trajectory and the sensory consequences of the movement (Kawato, 1999). Indeed, sensorimotor control

related to haptic tasks relies on predictive mechanisms whereby the motor output is adapted to the physical characteristics of the object or surface being explored, and afferent tactile input guides the timing and control of motor actions (Johansson and Edin, 1993). When trying to account to performance differences in conditions of active and passive touch, it has been hypothesized that, when we perform exploratory movements to extract information about a given object or surface, a copy of the motor command, also known as efference copy, or predicted sensory feedback (PSF), enables the sensorimotor system to predict the consequences of the exploratory action, thus potentially providing an additional channel of information regarding the surface or object being actively explored, compared to when the same surface or object is passively perceived (Sciutti et al., 2010). However, this facilitating effect of the PSF on haptic perception is not always clear. In a curvature discrimination task, where subjects were asked to judge the curvature of a virtual contour under both active and passive conditions, no differences were observed between the two for neither detection nor discrimination thresholds, suggesting that the PSF, while providing redundant sensorimotor information, does not improve haptic perception (Sciutti et al., 2010). In addition, some have suggested that the perceived timing of stimuli delivered under the two conditions would differ, and that sensory stimuli originating from active touch would be perceived before those originating from passive touch, as the PSF would be available to the brain about 290 ms prior to the incoming sensory information (Macefield et al., 1989; Winter et al., 2008). However, in a temporal order judgment (TOJ) task, no differences were observed for neither point of subjective simultaneity (PSS) nor for just noticeable difference (JND) under active and passive touch, suggesting that no clear temporal benefit arises from the presence of a copy of the motor command (Winter et al., 2008). Other accounts suggest that the PSF contributes to the attenuation of somatosensory perception

during self-generated movements (Bays et al., 2006), with evidence showing that self-generated taps were felt by participants as significantly less intense compared to taps generated by passive finger displacements (Kilteni et al., 2020). Given the limited evidence, whether, to what extent, and under which circumstances the PSF contributes to the sometimes-observed superior perceptual performance during active touch remains an open question.

3.3. Proprio-tactile interactions

During active, dynamic tactile exploration, information about the position of the exploring limb relative to the object or surface being explored is continuously processed and updated (Ghez et al., 1990; Rincon-Gozalez et al., 2012; Longo and Haggard, 2010). As introduced in the previous sections, along the somatosensory hierarchy, neurons within the VPS, area 3a and area 2 in the APC, PV and S2 in the LPC, area 5L, PRR, and the rostral part of area 7b in the PPC respond to both cutaneous and proprioceptive inputs (Delhaye et al., 2018). Functional magnetic resonance imaging (fMRI) investigations of proprio-tactile integration have shown that a very similar network of sensorimotor brain areas was activated when illusory limb motion is elicited by the tactile or proprioceptive channels, including the bilateral S1, the SMA, the inferior parietal lobule, the inferior frontal gyrus, the anterior cingulate cortex, and the insula (Kavounoudias et al., 2008). When the illusion was elicited by congruent proprioceptive and tactile inputs, areas activated selectively under bimodal stimulation were found in the inferior parietal lobule, the superior temporal sulcus, as well as subcortical regions, including the bilateral anterior insula and thalamus, and the right putamen (Kavounoudias et al., 2008). The interactions between proprioceptive and tactile cues during tactile exploration appear to be bi-directional, with tactile cues shown to improve the accuracy of estimations of hand location (Rincon-Gonzalez et al., 2011), and proprioceptive

cues manipulated by means of changes in posture shown to affect the perception of the timing of tactile cues (Heed and Azañon, 2014; Shore et al., 2005). Interestingly, when subjects have to judge the location of their hands when these are out of sight, they make constant and systematic estimation errors, suggesting the existence of a stable proprioceptive representation, or proprioceptive map, of the arm (Rincon-Gonzalez et al., 2011). In an experiment in which subjects had to judge the position of their finger after this was passively displaced at a specific location of a platform, it was shown that when they did touch the platform prior to making estimation judgments (i.e., when they also received tactile feedback) the pattern of such estimation errors remained stable, although tactile cues did reduce the magnitude of these errors, which was not the case for electrical stimulations applied at the fingertip without physical contact with the platform, suggesting that local mechanoreceptor activation and shear forces applied to the fingertip impact proprioceptive arm representation, without completely disrupting it (Rincon-Gonzalez et al., 2012). Furthermore, single-unit recordings in monkeys within area 1 and 3b in S1 showed that activity of cells responding to textural characteristics of the object being grasped can be modulated by the object's orientation in the external space (Rincon-Gonzalez et al., 2012).

It has been suggested that when subjects perform voluntary exploratory movements to discriminate angle width, they rely on two cognitive strategies: mental images of the whole angle and the pattern of cutaneous feedback when the finger reaches the angle intersection (likely with a strong contribution of SAI mechanoreceptors) (Voisin et al., 2002a). Angle discrimination performance was shown to be significantly reduced with local finger anesthesia, when subjects could only rely on kinesthetic inputs, and thus could not use information about skin deformation at the angle intersection. Angle discrimination performance was also significantly reduced in conditions of passive touch, when the angle was displaced

against the participants' finger in the absence of limb movement, suggesting that 2D shape perception in an integrative process drawing information from both inputs of cutaneous mechanoreceptor at the level of the fingertip and muscle and joint proprioceptors at the level of the shoulder (Voisin et al., 2002b).

Some studies have also attempted to investigate integration of position (proprioceptive) and force (tactile) cues within the framework of the maximum likelihood estimation (MLE) model of multisensory integration, according to which inputs coming from different sensory modalities carry different perceptual weights, which are given by their variance, and the final multisensory percept is a product of the weighted average of the estimates of each sensory cue (Drewing and Ernst, 2006; Ernst and Banks, 2002; Rohde et al., 2016). In these studies, it was shown that in the presence of a conflict between cues associated with the position of the finger following the geometry of an arch signaling one curvature and cues associated with the direction of the forces acting on the fingertip signaling a different curvature, the final curvature percept was a compromise between the two, suggesting that integration of force and position cues was achieved by a weighted average of their respective weights, as predicted by the MLE model (Drewing and Ernst, 2006; Drewing and Kaim, 2009). Cue combination between tactile and proprioceptive inputs is also particularly relevant for motor control, as evidenced by studies testing a well-validated tactile illusion of motion direction first reported in conditions of passive touch, where when participants explore a ridged surface, the perceived direction of movement is biased towards the axis perpendicular to the ridges (Bicchi et al., 2008; Pei et al., 2008). When subjects were asked to perform straight reaching movements against such ridged surfaces, they made trajectory errors in the opposite direction. When the tactile cues (i.e., the ridges on the surface) were made unreliable by having subjects wear a rubber

glove, the compensatory trajectory errors were reduced significantly (Moscatelli et al., 2019).

Together, these findings highlight the intricate relationship between touch, proprioception, and motor control in conditions of active, dynamic touch.

3.4. Gating of somatosensory responses during active touch

It has been frequently reported that, during movement execution, somatosensory processing is at least partially suppressed (Chapman, 1994). Investigations of differences between active and passive touch have reported that, at the neural level, a suppression of sensory signals occur when tactile perception is accompanied by movement, via a process called movement-related gating, or somatosensory gating (Jiang et al., 1991). In humans, gating of somatosensory-evoked potentials (SEPs) has been described using high resolution electroencephalography (EEG). Concomitant movement execution and medial nerve stimulation resulted in significantly reduced SEP components between 30 and 45 ms post stimulus (Rossini et al., 1999). The temporal aspects of somatosensory attenuation have also been investigated using transcranial magnetic stimulation (TMS) (Voss et al., 2006). Here, it was shown that cutaneous stimuli delivered to a moving finger had to be about 169% larger than stimuli delivered to the resting finger in order to be perceived of equal intensity. In addition, delivering a TMS pulse over M1 first determined an involuntary twitch, followed by a silent period which preceded the onset of voluntary movement. When the cutaneous stimulus was delivered during the silent period, a similar increase in point of subjective equality (PSE) was observed to that elicited by delivering the tactile stimulation during movement, therefore suggesting that central motor commands which precede movements play a significant role in somatosensory attenuation (Voss et al., 2006). While several studies have observed

a suppression of SEPs in correspondence of voluntary movements, one possibility remains that, when movement is necessary to extract features of the object or the surface being explored, the gating effects of movements are reduced. Early work in primates used single unit recordings to investigate the effects of voluntary movements on the activity of neurons both within and outside the receptive fields of the digit exploring a surface to perform a roughness discrimination task (Ageranioti-Bélanger and Chapman, 1992). Here, recordings revealed a convergence of activity in cells within the receptive fields of interest associated with the exploring digit, with more caudal areas more likely to show an increase in activation and less likely to show no modulation. In cells with receptive fields located elsewhere, an opposite trend was observed, with a decrease of activity observed going from rostral to caudal areas, and an increase in cells showing no modulation going towards caudal areas. These results suggest that, while tactile signals that are irrelevant to the task are subjected to somatosensory gating and are therefore filtered out at later stages of processing, signals that are relevant to the task are passed on to higher areas (Ageranioti-Bélanger and Chapman, 1992). In addition, recent investigations have reported that, in the presence of a task requiring detailed somatosensory information and accurate control of complex movements, gating of somatosensory signals is absent at later stages of processing (Wasaka et al., 2017). In a ball rotation task, which requires fine coordination of finger movements, early SEP components elicited by electrical stimulation of the median nerve were attenuated, in line with previous evidence of somatosensory suppression during movement. However, a later component (M38) was enhanced during the motor task, adding to previous evidence indicating that, when somatosensory information is necessary to control movements, SEPs are enhanced (Knecht et al., 1993; Wasaka et al., 2017). Behavioral evidence in favor of this view has been provided by studies showing that, while active movement significantly

decreases performance on a vibrotactile discrimination task when the reaching or exploring movement is irrelevant to the perception of the vibratory stimuli, active touch appears significantly superior to passive touch when the executed movements are relevant to the incoming sensory information (Juravle et al., 2013). Thus, it seems plausible to suggest that movement-related somatosensory gating represents yet another mechanism which is part of the optimal extraction of tactile information that characterizes active touch sensing, where irrelevant information is suppressed to facilitate processing of signals that are instead relevant to the sensorimotor task being performed.

4. Audio-tactile interactions in (active) touch

Haptic exploration and interactions with objects by touch are often accompanied by the sounds elicited by the skin acting on the surface being explored: tapping on a table, knocking on a door, stroking a textured surface, or typing on a keyboard are all inherently multisensory experiences encompassing touch and sound. Integration of touch and sound in conditions of active, dynamic touch has largely focused on the perception of textures. This seems reasonable if we consider hearing as being best suited to process the timing of stimuli, as opposed to vision, which is thought to be more relevant for spatial processing (Alais and Burr, 2004; Burr et al., 2009). Indeed, in the context of frequency-coding, the somatosensory and auditory systems are analogous in the way in which the temporal patterning of afferent responses reflects the frequency-composition of the incoming sensory information with high fidelity (Saal et al., 2016).

Texture perception is also strongly linked to the temporal aspect of the tactile percept, at least for finer-grained textures, which is thought to rely on a temporal neural code associated with the spike timing of RA mechanoreceptors (Harvey et

al., 2013; Hollins, 2001; Hollins and Risner, 2000). Evidence on the behavioral effects of audio-tactile interactions during texture perception is conflicting. Early findings of the effects of touch-produced sounds on tactile roughness perception revealed that, in the presence of both audition and touch, auditory cues are largely ignored, and magnitude estimation curves obtained under bimodal conditions appear highly similar to those obtained in tactile-only conditions (Lederman, 1979). When participants explored textured surfaces using a probe rather than their bare finger, on the other hand, a contribution of touch-produced sounds on roughness magnitude estimations emerged, although tactile cues still appeared to dominate perception under bimodal presentation (Lederman et al., 2002). Studies of audio-tactile integration under conditions of active touch have also revealed that modulating the frequency content of touch-produced auditory stimuli affects the perceived roughness/smoothness of tactile stimuli, namely through a phenomenon called the parchment-skin illusion (Jousmäki and Hari, 1998). In this illusion, the perception of hand dryness/wetness is affected when the sounds elicited by the subjects rubbing their hands against each other are amplitude-modulated, with amplification of high-frequency sounds leading to increased feelings of roughness/dryness, and attenuation of high-frequency sounds leading to increased feelings of smoothness/moisture (Jousmäki and Hari, 1998). Similarly, in the context of texture perception, high-frequency attenuation of sounds altered the perception of an actively explored textured surface, which was reportedly perceived as smoother, while high-frequency amplification of the touch-produced sounds led to the textured surface to be perceived as rougher (Guest et al., 2002). While most studies have employed auditory feedback by means of touch-produced sounds, some have also attempted to exploit artificial complex sounds, such as white noise, as these can be acoustically comparable with sounds produced by texture exploration, in order to determine whether auditory perception of complex

sounds is specifically associated with tactile perception of roughness, and not with other tactile percepts (such as length) (Suzuki et al., 2008). When comparing the effects of white noise and pure tones on the tactile perception of abrasive papers, it was shown that, while pure tones did not affect perception of roughness nor length, white noise influenced roughness perception (but not length perception), as revealed by significantly smaller magnitude estimation slopes compared to a control condition in which the auditory feedback consisted of short beeps. Thus, processing of complex sounds, such as white noise, and processing of roughness by touch appear to be related (Suzuki et al., 2008), further supporting the idea that, with regard to texture, the processing of auditory and tactile stimuli is more strongly related with the temporal aspects of stimulation. Neuroimaging studies have also reported that vibrotactile and pulse tactile stimuli presented in unimodal conditions activate the contralateral superior temporal gyrus more strongly than the ipsilateral superior temporal gyrus, and that vibrotactile-auditory co-activation is observed within the auditory belt area contralaterally to the hand receiving the vibrotactile stimulation (Schürmann et al., 2006). Importantly, concurrent somatosensory stimulation by means of sandpaper passively stroked against the participants' fingertips and auditory stimulation in the form of bandpass-filtered white noise resulted in stronger activation of the left superior temporal gyrus, compared to the summed activation from both modalities presented in isolation, thus indicating multisensory integration between sound and touch early within the primary auditory cortex (Foxe et al., 2002). EEG studies have also reported multisensory effects across the two modalities. Corroborating the fMRI findings, it has been shown that concurrent somatosensory (median nerve stimulation) and auditory (1000 Hz tones) led to multisensory ERP responses that were significantly stronger than the sum of unisensory ERPs between 50 and 79 ms post-stimulation. Interestingly, the scalp topography at around 50 ms was characterized by a

central/postcentral negativity, with a concurrent positivity which was strongest at the vertex, which is consistent with the hand representation within S1. The later component at about 70 ms, on the other hand, was characterized by a more anterior negativity and a concurrent occipito-central positivity, thus reflecting activity generating from the posterior auditory cortex. These results further support the view that integration of inputs from different sensory modalities, including audition and touch, are integrated at an early stage within the cortical hierarchy (Foxe et al., 2000).

Integration of sound and touch in the context of shape perception has been less extensively investigated compared to visuo-tactile integration. This is not surprising, since vision and touch are highly similar in the way in which they code spatial information both peripherally and centrally, with the spatial pattern of receptors in the retina and within the skin mirroring the spatial pattern of the stimulation (Saal et al., 2016). Indeed, previous work has shown that neurons in visual area V4 and in somatosensory SII are similarly sensitive to shape processing (Yau et al., 2009). Behaviorally, it has also been shown that, in the context of shape perception, vision and touch are integrated in a statistically optimal manner, as predicted by the MLE model of multisensory integration, and that activity in somatosensory area 2 is enhanced when visual information was manipulated to be less reliable (i.e., blurred) (Helbig et al., 2012; Helbig and Ernst, 2007). Being reflected by the pattern of cutaneous mechanoreceptor activation, more than by their spike timing, shape processing is a spatial process more than an auditory one. Nevertheless, research on multisensory interactions and sensory substitution has shown that an abstract representation of shape can be driven by the auditory modality (Kim and Zatorre, 2011, 2010). When coding artificial sounds to convey shape information, with frequency coding for the vertical dimension, and stereo panning and time coding the horizontal dimension, it has been shown that

participants were able to correctly match a shape explored by touch to its corresponding soundscape. Interestingly, this association also transferred to the visual modality, and subjects were able to correctly match a visually presented shape to its corresponding soundscape, with a high level of performance even for unfamiliar shapes (Kim and Zatorre, 2010). A subsequent fMRI investigation showed that the lateral occipital complex, which is typically associated with shape and object recognition via vision, was activated during both auditory and tactile shape recognition (Kim and Zatorre, 2011). However, in these studies, the soundscapes delivered during shape exploration were not time-locked to the exact moments in which the finger contacted the contours of the raised shapes. Thus, the cortical mechanisms of integration between transient sounds delivered concurrently with the transient contacts between the finger and the edges of a planar shape during free exploration remain to be investigated.

5. Methodological considerations for the study of auditory-tactile interactions in active touch and rationale for the chosen approaches.

5.1. Psychophysics

5.1.1. General terms in psychophysics

Psychophysics is the science investigating the link between physical characteristics of sensory stimuli and perception. In psychophysical experiments, a certain feature of a stimulus is varied, and participants are required to make specific judgments about the stimuli presented to them. Psychophysical tasks can be classified as *detection* tasks (*"Did you perceive a stimulus?"; "In which interval did you perceive a stimulus, interval 1 or interval 2?"*) or *discrimination tasks* (*"Which stimulus was more/less x, stimulus 1 or stimulus 2?; "Was the stimulus more x or y?"*). Typically, in psychophysical experiments, participants are not given the option

to respond ‘’I do not know’’. From this arises the nomenclature ‘’N-forced choice task’’, where forced-choice signifies that participants are given a certain number of response alternatives (typically 1, 2, or 3) from which they are obliged to choose, and N corresponds to the number of stimulus alternatives presented in each trial (*“Was the stimulus x or y?”*), as defined by Kingdom and Prins (2010).

From psychophysics experiments, psychometric functions are estimated based on participants’ performance on a given task. The psychometric function describes participants’ behavior (probability (p) of a given response) depending on the magnitude of variation of a given physical characteristic of the stimulus, such as intensity, position, brightness, contrast, and so on. The psychometric function comprises several parameters that describe its shape. The most often investigated parameters are the threshold (α) and the slope (β) parameters, which are associated with the underlying sensory mechanism (Kingdom and Prins, 2010). Two other parameters define the level of curve saturation at the extremes of the range of stimulus intensities used in the experiment. These are the guess (γ) and the lapse (λ) rates. The guess rate represents chance level performance for forced-choice tasks and the probability of reporting detection of a stimulus even if the stimulus is not there for yes/no detection tasks, i.e., by just guessing. The lapse rate represents the probability of not detecting a stimulus even at very high stimulus intensities and therefore reflects errors in judgment by the participants due to distraction, errors in reporting the intended answer, as well as errors by the experimenter in recording the reported answer. The threshold parameter, also referred to as bias, defines where the curve is placed along its x-axis (i.e., the levels of stimulus intensities). The threshold parameter can take the form of both an “appearance” measure, in tasks where there is no true correct or incorrect answer, such as tasks measuring the magnitude of a perceptual illusion, or a “performance” measure, where judgments about stimuli can be classified as correct or incorrect (as in the case of the

experiment we report in Chapter 2). Generally, in performance-based tasks, the threshold parameter describes how *accurate* participants are on a given task, that is, how close their perception is to the ''true'' reference intensity of the stimulus. The slope parameter, which represents the rate of change in perception per unit of change in stimulus intensity, describes how *precise* participants are on a given task, that is, how consistent they are when making their judgments. High accuracy but low precision would lead to a psychometric function having a shallow slope, but a 0.5 probability corresponding to the true reference value (e.g., a threshold value of 0). High precision but low accuracy would lead to a psychometric function having a steeper slope, but a biased 0.5 probability further away from the true reference value (e.g. a threshold value of 5) (Figure 3). Even in performance-based psychophysical tasks, both perceptual and response biases can occur, where the estimated threshold does not align with the true value of reference stimulus intensity (Kingdom and Prins, 2010). Therefore, the slope parameter can arguably be regarded as a more robust measure of participants' performance on a psychophysical task. Nevertheless, in performance-based tasks, the two measures both provide information about participants' ability to detect or discriminate the stimuli and should thus be considered.

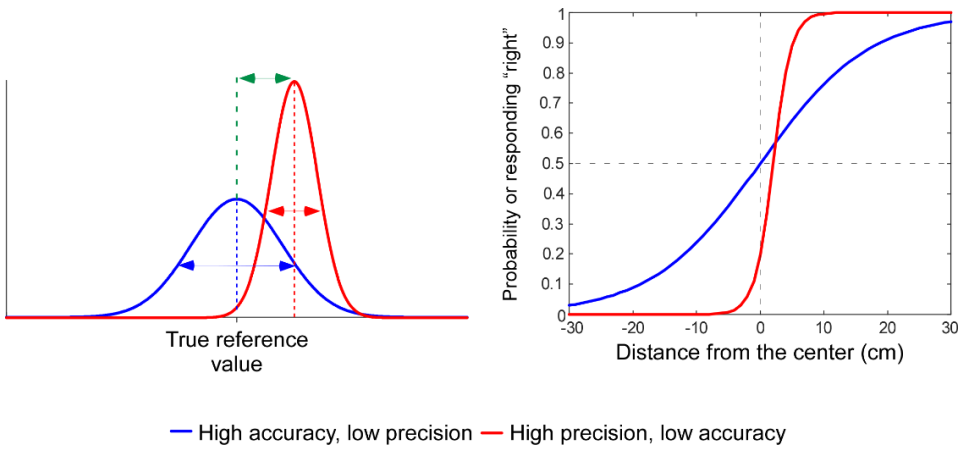

Figure 3. Accuracy (threshold) and precision (slope) in psychophysical experiments. The figure depicts two scenarios: one where accuracy is high but precision is low (blue distribution and psychometric function), and one where accuracy is low but precision is high (red distribution and psychometric function). In the left graph, the precision of the distributions is given by their spread. The dashed blue and red vertical lines represent the mean of the distributions. The mean of the high-accuracy blue distribution matches the true reference value (green dashed line), while the mean of the high-precision red distribution is displaced relative to the true reference value, thus displaying a bias (green arrow). This is reflected in the resulting psychometric functions (right graph): high accuracy but low precision would correspond to a curve displaying a threshold at or very close to the true reference value (e.g. the distance from the center in the experiment reported in Chapter 2, where participants had to report the location of their finger while they explored a ultrasonic haptic display relative to a visually displayed midline at the onset tactile, auditory, or audio-tactile stimuli), and to a shallower slope (i.e., more variance in the localization responses). High precision but low accuracy would be reflected by a threshold further away from the true reference value (here, the curve shows a 5 cm bias), but a steeper slope (i.e., less variance in the localization responses).

5.1.2. Psychophysical methods

Method of limits

The method of limits is used to estimate the threshold parameter. In this method, stimulus intensities are presented in both ascending and descending

sequences, where ascending sequences stop as soon as the subject reports perceiving the stimulus, while descending sequences stop as soon as the subject reports not perceiving the stimulus anymore (for detection tasks) (Gescheider, 1997; Jones and Tan, 2013; Kingdom and Prins, 2010). The method of limits as an important pitfall: the error of habituation. As the sequence progresses, the subject may become used to reporting that they perceive (or not) the stimulus, thus leading to wrong estimates of the threshold as lower or higher than the real threshold (Kingdom and Prins, 2010). Importantly, the method of limits does not allow to estimate the slope of the psychometric function, thus not allowing a full investigation of multisensory gain effects.

Method of constant stimuli

In the method of constant stimuli, a pre-defined range of stimulus intensities is presented a given number of times, such as 20 trials per stimulus intensity (Jones and Tan, 2013). It is important to design an appropriate range of stimulus intensities to be used during the experimental session, as selecting a too narrow range would not allow to properly model responses to barely perceivable or very intense stimulus intensities, thus impairing estimation of the slope parameter, while selecting a too wide range of stimulus intensities would either make the experimental session too long, or limit the number of times each intensity level can be presented, to avoid an overly long experimental session, thus impairing estimation of both the threshold and the slope parameters. Such pitfalls of the method of constant stimuli can be particularly problematic for designs involving more than one sensory modality, as at least three experimental conditions would be involved in such designs. Even more so, the very large number of trials and very long testing times needed to properly assess the psychometric function's

parameters through the method of constant stimuli are not appropriate for designs also implementing conditions of active, dynamic touch (Jones and Tan, 2013).

Adaptive methods

Adaptive psychophysical methods are aimed at optimizing estimation of the psychometric function's parameters while limiting the necessary number of trials. This is achieved by adjusting the level of stimuli presented on a trial-by-trial basis depending on what level allows to better gain information about the parameters of interest. Thus, unlike the method of constant stimuli, one does not have to present all stimulus intensities a pre-specified large number of times. Some adaptive methods only allow estimation of the threshold parameter. These include simple up-down staircases, where the stimulus intensity is adjusted after every trial depending on the participant's response on the previous trial. Similarly, running fit methods estimate the psychometric function at each trial depending on the responses on all previous trials, and the selected stimulus intensity corresponds to the best estimate of the threshold parameter, while no information is gained on the slope parameter. The psi method, on the other hand, is a Bayesian algorithm that selects the most efficient stimulus intensity on a trial-by-trial basis to gain information and estimate both the threshold and the slope parameters (Kontsevich and Tyler, 1999). With the psi method, prior distributions for the threshold and slope parameters are defined. During the experiment, the algorithm will update posterior distributions of the parameters based on the participants' response after every trial and considering the values defined in the prior distributions and select the next stimulus intensity as the one that will be more likely to allow gain of information about the parameters (Kingdom and Prins, 2010; Kontsevich and Tyler, 1999). A variant of the classical psi method, the psi+ method, also allows estimation of the lapse and guess rates (Prins, 2012). The advantage of the psi+ method is that

it does not require setting the guess and lapse rates at (arbitrary) fixed values. Indeed, when the actual values of these parameters differ from the pre-defined fixed values, both the threshold and slope parameter estimates can become biased (Prins, 2012). One possible disadvantage of the psi+ method is the fact that a larger than necessary number of trials may be used for the estimation of such ''nuisance'' (i.e., not associated with the underlying perceptual process) parameters. An alternative proposed by Prins (2013) is the psi-marginal method. Here, as in the psi+ method, prior distributions are also specified for the guess and lapse rates, but the algorithm will only estimate their posterior distributions when doing so aids the estimation of the primary parameters (i.e., the threshold and the slope) (Prins, 2013). Typically, for experiments employing the psi, psi+, or psi-marginal method, a total of 100 trials per experimental condition allows good estimation of both the slope and threshold parameters, which is dramatically less than the number of trials required with non-adaptive psychophysical methods (Courtin, 2022; Courtin et al., 2020). Sensory signals already being embedded in noise, it is crucial, for an estimation of the psychometric function's parameters that reflects true perception as closely as possible, that participants maintain a high level of attention and motivation throughout the duration of the task. In experiments involving active touch, participants are asked to repetitively perform the same or similar exploratory movements, and thus such designs face similar constraints as those faced by experiments involving painful or uncomfortable stimulations, where the number of trials has to be as limited as possible to ensure participants' comfort and compliance (Courtin et al., 2020). Thus, the psi method seems to represent the most efficient approach for the psychophysical investigation of tactile perception and multisensory integration in conditions of active, dynamic touch, thus motivating us to implement this approach for **Study 1**. Here, we used the psi+ method to investigate whether concurrent auditory stimulation improves

participants' performance in a task where they had to localize the finger used to perform exploratory movements while receiving haptic stimulation through an ultrasonic haptic display.

5.2. Neurophysiological methods

5.2.1. EEG frequency-tagging

EEG frequency-tagging is a technique based on the concept that a periodic stimulation or a periodic modulation of a stimulus elicits a periodic response in the EEG signal. Transforming the time-domain EEG signal to its corresponding frequency spectrum using a fast-Fourier transform (FFT) allows characterization of such periodic activity which becomes evident at the frequency of stimulus modulation and its harmonics (Lenc et al., 2021; Norcia et al., 2015; Nozaradan, 2014; Rossion, 2014).

EEG frequency-tagging is advantageous in that such responses will be constrained within specific frequency bands, and time-domain averaging will considerably reduce the impact on non-periodic noise and activity that is unrelated to the periodic stimulation (Norcia et al., 2015; Regan, 1989, 1966). EEG frequency-tagging is often used to investigate processing of higher-level perceptual categorization of high-level stimuli, such as faces, tools, or rhythm (Chemin et al., 2014; De Keyser et al., 2018; Lenc et al., 2021; Moungou et al., 2016a; Rossion et al., 2015; Rossion and Boremanse, 2011). Similarly, EEG frequency-tagging has also proven useful for the investigation of sustained, slow periodic painful thermic stimulations eliciting activity in slowly-adapting thermonociceptive C-fibers, which are not stimulated in isolation when using rapid, transient heat stimuli typically used to measure thermonociceptive ERPs (Colon et al., 2017). Perceptual categorization of textures arguably also involves a more sustained exposure to the

material than that required, for example, for the perception of a sharp edge, which represents a rather phasic interaction. Indeed, when exploring a surface to isolate its physical and perceptual attributes relating to texture (e.g. roughness vs. smoothness) we typically make relatively slow, repetitive lateral exploring movements, rather than rapidly pressing on the surface, a strategy linked to extraction of surface hardness information (Lederman and Klatzky, 1993). As such, EEG frequency-tagging represents a valid candidate technique for the investigation of the cortical processing of natural textures (Moungou et al., 2016a). Furthermore, EEG frequency-tagging can be implemented in combination with periodic oddball paradigms, where a periodic sequence of standard or unchanging stimuli is periodically embedded with oddball stimuli that differ, in some way, from the standard stimuli (Nozaradan et al., 2017). As such, the combination of the two approaches allows characterization of responses that are specific to the processing of *changes* in stimulation, such as rapid changes in auditory pitch, which is relevant to the study of speech perception and processing (Nozaradan et al., 2017). This motivated us to use this approach to investigate, in **Study 2**, the cortical underpinnings of categorization of features distinguishing different textures. Indeed, while the cortical processing of natural textures has been reported at the level of S1 using EEG frequency-tagging (Moungou et al., 2016a), whether the fine-grained vibrational features of different textures are processed within S1 is unknown. In Chapter 5, we discuss possible future applications of these techniques to investigate the cortical mechanisms of audio-tactile interactions in the context of the processing of natural textures.

5.2.2. Event-related potentials

Event-related potentials (ERPs) represent transient, discrete waveforms of cortical activity in the time-domain which are time-locked to the onset of a

transient stimulation (Sutton et al., 1965; Vaughan, 1982). ERPs have been well-characterized across sensory modalities, and can reflect low-level sensory processing steps as well as higher-level perceptual, attentional, and cognitive processes (Alain et al., 2013; Brandeis and Lehmann, 1986; Herrmann and Knight, 2001; Muzyka and Estephan, 2019; Yamada et al., 1980). SEPs have been extensively studied using different types of innocuous stimulation types in conditions of passive, static touch. These include short-, mid-, and late-latency SEPs, reflecting different stages of the cortical processing of somatosensory stimuli within S1 and S2 (Allison et al., 1991; Muzyka and Estephan, 2019). During active, dynamic touch exploring a planar shape would involve different exploration strategies compared to exploration of textures. These include strategies in which the subject remains in close vicinity of the shape's edge, which are named contour following strategies, as well as strategies in which the subject performs movements crossing more distant parts of the shape's contour, which are named contour scanning strategies. Contour following strategies involve linear exploration movements along the shape's edge, as well repetitive crossing of the shape's edges with oscillating movements Figure 4 (Lederman and Klatzky, 1993; Mizrachi et al., 2022).

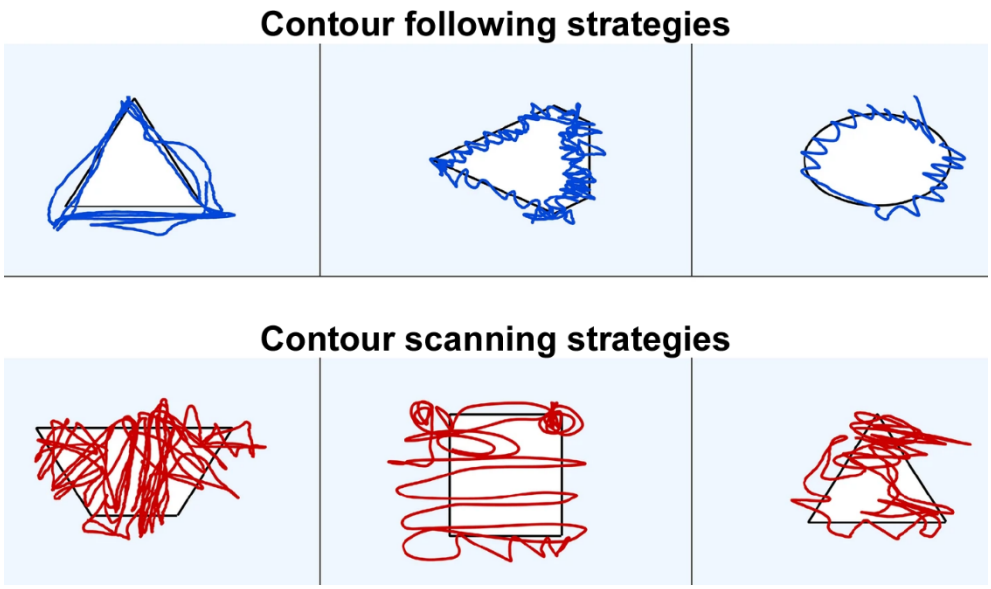

Figure 4. Planar shape exploration strategies during active touch. Exploratory movements associated with planar shape perception can broadly be classified in contour following (top blue panels) and contour scanning (bottom red panels) strategies. When adopting contour following strategies, subjects spend most of the exploration time in the vicinity of the shape's edges, and can either perform linear movements tangential to the shape's contour (top left), oscillatory movements perpendicular to the shape's contour (top middle), or a combination of the two (top right). When adopting contour scanning strategies, subjects spend a larger proportion of the exploration time further away from the shape's contour. Adapted from Mizrachi et al. (2022).

Recording of SEPs seems particularly useful for the characterization of cortical responses elicited via contour following with oscillating motion as well as via contour scanning, as in such cases, the tactile input is characterized by phasic contact with the shape's edge. To date, no studies have characterized SEPs elicited in response to transient tactile stimuli encountered by the subjects via exploratory sliding movements. Indeed, measuring SEPs in conditions of active touch in response to transient edged physical stimuli is particularly difficult, as the timing of stimulation is driven by the participants' exploratory movements, and it is not externally controlled by the experimenter. **Study 3** was a proof-of-concept

experiment in which we aimed to overcome some of the technical challenges associated with recording SEPs in conditions of active, dynamic touch, particularly those associated with precisely time-lock EEG responses to the onset of contact of the participants' finger with the tactile stimulus encountered during the exploratory movements. In Chapter 5, we discuss future possible applications of the setup we developed for the investigation of mismatch responses in the context of planar shape exploration as well as of how concurrent auditory stimulation affects the formation of mental representations of the explored shapes.

6. General aims of the thesis and overview of the experimental work

The investigation of tactile sensing and cortical processing of tactile stimuli in conditions of voluntary, active dynamic touch is a difficult endeavor. The main challenge associated with designs using voluntary, active dynamic touch lies in the fact that the experimenter does not have full control over the movements that participants perform to encounter and perceive the tactile stimuli. This challenge is especially relevant to EEG experiments and, possibly due to such difficulties, both the behavioral and electrophysiological evidence for integration of touch with sound in such conditions remains scarce.

The overarching aim of this doctoral thesis was to design and develop new methodological approaches for the study of multisensory integration under conditions of active, dynamic touch. This was achieved by investigating two areas of tactile perception: perception and processing of transient haptic stimuli (i.e., edges) and perception and processing of dynamic variations in the pattern of vibrations elicited at the skin-surface interface distinguishing different textures. Three neuroscientific approaches were employed to address our aims:

psychophysics (Chapter 2), EEG frequency-tagging (Chapter 3), and EEG recording of SEPs (Chapter 4).

In **Study 1** (reported in Chapter 2), we employed an adaptive psychophysical method (the Psi+ method) to assess whether multisensory enhancement effects can be observed when participants reconstruct the location of haptic stimuli perceived in conditions of voluntary, active dynamic touch when these are concomitantly presented with auditory cues compared to when they are presented in isolation. As this experiment allowed us to assess multisensory integration effects in conditions of voluntary, active dynamic touch, it represents an important milestone motivating further investigations to study such effects at the cortical level using scalp EEG.

In **Study 2** (reported in Chapter 3), we aimed to address the question of whether S1 is able to resolve fine variations in the spectrotemporal (frequency over time) content of vibrations distinguishing different tactile textures. To this aim, we used EEG frequency-tagging in combination with a periodic oddball paradigm, where we employed sequences of bandpass-filtered white noise that differed in their spectrotemporal content but not in their average frequency and intensity. As discussed in Section 4, multisensory effects between touch and sound have been reported in the context of texture perception, such as the parchment-skin illusion. However, the cortical mechanisms underlying such effects remain unknown. By using this novel paradigm to show that S1 activity reflects processing of complex vibration patterns associated with different textures, we open new avenues to investigate whether activity within S1 is altered when concomitant sounds change the roughness perception of the same texture remains to be determined. Possible developments of this design in the context of multisensory integration are discussed in Chapter 5.

In **Study 3** (reported in Chapter 4), we aimed to test the feasibility of recording SEPs elicited by physical edged tactile stimuli in conditions of voluntary, active dynamic touch. As discussed in Section 5.2.2, previous studies that have characterized SEPs have employed conditions of mainly static, passive touch. While this literature provides us with knowledge of the general cortical mechanisms of somatosensory processing, it does not allow a deep understanding of such mechanisms in ecological conditions of voluntary, active dynamic touch. However, measuring transient cortical responses to tactile stimuli using scalp EEG comes with several challenges, particularly associated with time-locking the onset of stimulation to the observed responses. Through this proof-of-concept study, we reported a method to overcome such challenges, laying the path to the study of SEPs in naturalistic conditions. Possible future applications of this novel experimental setup in the context of multisensory integration are discussed in Chapter 5.

Chapter 2: Integration of auditory and tactile inputs to localize haptic stimuli during active touch.

Abstract

Exploring our environment through touch often entails integration of tactile input with auditory and/or visual cues. The mechanisms by which mechanosensation integrates with other sensory modalities during active touch remain poorly understood, despite their ecological importance. Here, we investigated auditory-tactile integration in the context of edge localization during active tactile exploration. We assessed how accurately participants could determine the position of their moving finger in relation to the onsets of tactile, auditory, and auditory-tactile stimuli with respect to a visually displayed midline. We hypothesized that localization precision would be improved in the presence of combined auditory-tactile stimulation. In Experiment 1, the auditory, tactile, and auditory-tactile conditions were presented in separate blocks while in Experiment 2, they were interleaved within blocks. For both experiments, we found that concurrent auditory-tactile stimulation did not increase localization precision. We also observed across all modalities an inclination to localize the finger position towards the right, possibly due to a shift induced by the left-to-right finger movement. This bias was reduced in the auditory-tactile condition of the second experiment, suggesting that when modality was not predictable, integration of auditory and tactile input may have led to a more accurate representation of finger position at stimulation onset. In conclusion, we show that combined auditory-tactile input may reduce biases in reconstructing the spatial location of a tactile stimulus generated by sliding the finger onto a flat surface. These observations have potential implications for the design of haptic technologies involving active touch.

1. Introduction

Touch is a dynamic process: we explore the world, its shapes, textures, and materials by actively interacting with them. While passive touch is defined as the experience of being touched, active touch is defined as an intentional act performed to optimally extract tactile information from the external world (Gibson, 1962; Lederman and Klatzky, 1993). Localizing stimuli in the external world through active dynamic touch requires not only the ability to localize where tactile stimuli occur on the body surface, but it also entails the ability to integrate this somatotopic information with information on where the touched body surface was located in external space at the onset of tactile stimulation. This process often engages the integration of signals from proprioception (e.g., information on the location and movement of the exploring fingers), motor commands (e.g., the efference copy), and vision or audition when it is present (e.g. viewing the exploring fingers manipulating an object, or hearing the sounds generated by finger contact with a texture) (Gibson, 1962; Lederman, 1979; Prescott et al., 2011; Sciutti et al., 2010; Simões-Franklin et al., 2011). As such, active touch can be thought of as a dynamic, multisensory experience. However, studies investigating the integration of touch with other sensory modalities in the context of active tactile exploration remain scarce, despite their ecological validity (Matusz et al., 2019).

In the context of the spatial localization of auditory and tactile stimuli, some evidence exists for cross-modal effects in passive touch conditions. A well-established cross-modal interaction phenomenon in the spatial domain is the ventriloquist illusion (Bertelson and Aschersleben, 1998; Bertelson and Radeau, 1981), where localization of an auditory stimulus is biased towards the location of a concurrently presented visual stimulus (Alais and Burr, 2004; Bertelson and Aschersleben, 1998). Evidence for ‘’tactile ventriloquism’’ has also been reported,

with previous studies reporting that a sound can influence the perceived spatial position of touch (Bruns et al., 2011; Bruns and Röder, 2010; Caclin et al., 2002; Plöchl et al., 2016; Vercillo and Gori, 2015).

Even though such studies conducted in conditions of passive touch provide valuable information on cross-modal effects between touch and audition, they are of limited relevance for active touch. Indeed, in a static passive touch experiment, localization of the tactile stimulus relies solely on our ability to determine *where* it occurs on the body surface (spatial somatotopic discrimination) and where that body part is located in external space. In contrast, in conditions of active dynamic touch, where one is actively exploring the environment with the fingertip, spatial localization in external space of an object contacted by the fingers requires integrating information on *when* the tactile stimulus generated by the finger-object contact occurs (temporal discrimination) and *where* the exploring fingers are located in space (integration with proprioceptive, motor control, and/or visual information on finger position). Furthermore, the mechanical energy dissipated during a transient fingertip-object interaction in active touch will often generate – in addition to a tactile stimulus – a temporally-coinciding auditory stimulus (for example, the sound generated by knocking fingers on a door). In the context of multisensory integration in the temporal domain, temporal ventriloquism effects have been described, in which auditory stimuli can bias the perceived temporal onset of visual stimuli (Fendrich and Corballis, 2001; Morein-Zamir et al., 2003; Vroomen and De Gelder, 2004). Such temporal effects of multisensory interactions are particularly relevant to active touch where, as mentioned above, spatial information about limb position needs to be integrated with temporal information on the onset of a stimulus.

To investigate auditory-tactile interactions in conditions of active touch, we designed a psychophysical experiment aiming at evaluating the contribution and potential integration of transient tactile and auditory feedback during active sliding of the finger against a surface. A key feature of multisensory integration is multisensory enhancement, where behavioral performance in bimodal versus unimodal conditions improves the ability to detect and/or make judgements about stimuli and shortens reaction times (Stein and Stanford, 2008). For instance, in passive touch conditions, synchronously presented vibrotactile stimuli have often been shown to increase the detectability and perceived loudness of faint auditory tones (Gillmeister and Eimer, 2007). These findings are compatible with modern theories of perception which posit that, rather than being a simple read-out of physical stimuli, perception results from inferential processes integrating sensory evidence and prior knowledge (Aggelopoulos, 2015; Rohde et al., 2016). This integration is usually thought to be approximately Bayesian, meaning that the contribution of different sources of information (prior expectations, sensory evidence from various modalities...) are weighted by their precision (inverse uncertainty) (Ernst and Banks, 2002; Rohde et al., 2016). If two stimuli are presented at different spatial locations, or at different temporal onsets, the perceived location/onset would be a compromise between these locations/onsets, weighted by the relative precision of the modalities. If two stimuli are presented at the same location in space or close in time, precise localization should be easier when several sensory cues are available as compared to a single cue. In this study, our aims were to investigate how well participants can evaluate, during an active touch exploration task, the position of their moving finger relative to the onset of a tactile, auditory, or auditory-tactile stimulus. Specifically, we tested whether bimodal auditory-tactile stimulation improves localization precision compared to both unimodal tactile stimulation and unimodal auditory stimulation, which would

be consistent with multisensory enhancement effects. It is important to note that for active tactile exploration, localization refers to the process of integrating temporal (given by the onset of the stimulation) and spatial (given by proprioceptive, motor, and visual information about finger position) cues to determine where the exploring finger was at the time the stimulation was received.

2. Methods

2.1. Participants

The study received ethical approval by the UCLouvain Ethics Committee. Forty-five healthy participants (with no self-reported history of motor or auditory disorders, or loss of sensitivity at their hands) were recruited. Twenty participants were recruited for Experiment 1 (17 females, 3 males, aged 18 to 34), and twenty-five were recruited for Experiment 2 (18 females, 7 males, aged 18 to 35). Data collection had to be discontinued for 3 participants who were recruited for Experiment 2 because they struggled to perceive the haptic stimuli. Additionally, two participants who were recruited for Experiment 2 struggled to properly identify the stimulus types during the experiment, which led to many stimulus repetitions. For this reason, the data from these participants was excluded from the final dataset. Thus, the final sample for Experiment 2 included twenty participants. All participants gave written informed consent prior to participation. The choice of sample size was based on previous studies which used the Psi method to assess differences between experimental conditions in within subject designs (Courtin et al., 2023; Filbrich et al., 2017).

2.2. Experimental setup

Tactile stimuli were delivered using the E-VITA haptic display (Rekik et al., 2017) (Figure 1A). This device works by means of amplitude-modulated ultrasonic vibrations, which render tactile feedback upon dynamic touch by reducing the coefficient of friction between the finger and the glass plate of the display. By controlling the vibration amplitude as a function of fingertip position, monitored using an embedded capacitive touch screen (Banana-LCD-5''-TS, Marel, China, 50 Hz sampling frequency), the display can create tactile shapes or textures that are felt at the exploring fingertip at defined locations as it slides on the display (Rekik et al., 2017). The effect of ultrasonic vibration of the display on friction has not been completely elucidated, but might be mediated at least in part by ultrasonic lubrication and the ''squeeze film'' effect, where a thin layer of compressed air is created by the ultrasonic vibrations at the finger-surface interface (Wiertlewski et al., 2016).

An external infrared (IR) touch screen (model TOT104UIR009, active area dimensions: 213x161 mm) frame was used to detect finger position (position accuracy: 2 mm) and thereby trigger the auditory stimuli at a given finger location on the tactile display (Figure 1A).

2.3. Tactile, auditory and auditory-tactile sensory cues

The tactile (T) stimulus was a transient reduction of friction rendered by ultrasonic stimulation when the fingertip was located within an active area shaped as a vertical rectangle with a height of 100 mm and a width of 2 mm. In the context of planar shape exploration, a transient change in friction is expected to occur as the fingertip crosses the raised edges of the shape (Janko et al., 2018). The transient

change in friction rendered via the haptic display used in this experiment thus artificially reproduced part of the tactile experience of crossing an indentation.

The auditory (A) stimuli were bursts of white noise lasting 22.7 ms delivered using the Matlab Psychtoolbox. Transient white noise was selected because the sound elicited by the friction between a moving fingertip and a surface resembles white noise (Zahouani et al., 2009).

The bimodal auditory-tactile (AT) stimuli consisted of the same stimuli temporally synchronized and delivered when the fingertip reached a given position on the haptic display (Figure 1B). Importantly, the auditory stimuli were delivered through a single small speaker placed just behind the tactile display, and were thus not spatially modulated according to when they were triggered depending on the location of the exploring fingertip (i.e., they were always delivered in the same way via the external speaker). Similarly, the tactile stimulus also remained unchanged relative to the fingertip's location on the display (i.e., the same portion of fingertip skin was subjected to the transient change of friction). Localization of "where" the tactile, auditory and auditory-tactile stimuli occurred on the tactile display thus relied entirely on integrating temporal information about the onset of tactile and/or auditory feedback relative to spatial information about limb position provided by proprioceptive and/or visual feedback of fingertip location (Figure 1B).

To avoid stimuli from one modality being perceived more strongly, a standard one-up one-down staircase was used at the beginning of each experimental session, to match the perceptual intensities of the auditory and tactile stimuli. Participants were presented with AT stimuli and had to report which modality (tactile or auditory) was perceived as more intense. Since the intensity of tactile stimuli was kept constant across participants, only the volume of the auditory stimulus was adjusted with the staircase procedure. The staircase ended after ten

reversals and the volume for the auditory stimuli was set to the average volume of the last nine reversals.

2.4. Procedure

To allow participants to familiarize themselves with the stimuli and task, a brief training session was included. Participants were presented with stimuli placed at extreme distances from the midline (+/- 3.5 cm, with steps of 0.5 cm, six per modality), for a total of 18 training trials, as described below.

2.4.1. Experiment 1 (blocked design)

Participants were asked to slide the index fingertip of their dominant hand in a horizontal left-to-right direction along the surface of the haptic display. To allow for more ecological tactile exploration conditions, participants were not constrained to a fixed scanning velocity. They were instructed to slide their finger simply avoiding extremely fast or extremely slow scanning speeds, which would have impaired perception of the tactile feedback delivered with the haptic display. On the display, a black vertical line (0.5 mm width) was displayed against a white background to mark the midline position. At the end of each fingertip slide, participants were asked to report whether they had perceived the tactile, auditory or auditory-tactile stimulus while their finger was in the first half (left) or second half (right) of the display relative to the visual midline position (two-alternative forced-choice task). Participants were informed about what modality they would receive (T, A, or AT) prior to each block, and were encouraged to report lack of or incorrect detection of the stimuli (e.g., only hearing the A stimulus in AT trials), in which case the trial was repeated.

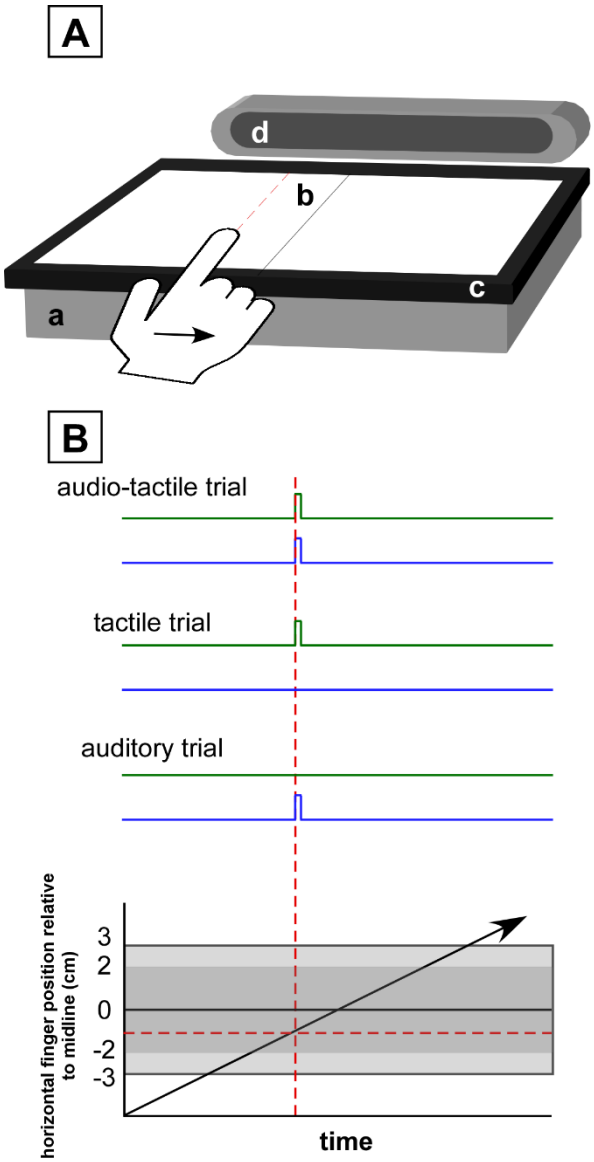

Figure 1. Experimental setup. (A) Participants were asked to slide from left-to-right their right index fingertip against a flat visuo-haptic display which renders tactile stimuli via friction-modulation (a). An infrared frame was placed on top of the display to monitor finger position and to trigger the auditory feedback (c), which was delivered via an external speaker placed just behind the haptic display (d).

Participants had to report, after each trial, whether they perceived the stimulation (tactile, auditory, or audio-tactile) while their finger was located to the left or to the right of a visually-displayed midline (b). The figure shows an example of a stimulus delivered while the fingertip was located to the left of the visually displayed midline (red dashed line). (B) Audio-tactile, tactile, and auditory stimuli were presented as follows. Participants performed horizontal left-to-right movements over the haptic display (bottom panel, diagonal arrow). Auditory (blue) and/or tactile (green) stimuli were triggered when the fingertip reached a given location on the haptic display (horizontal and vertical dashed red lines), relative to the visually displayed midline. The grey areas show the range of locations that were used to estimate the psychometric curves in the two experiments. In Experiment 1 (darker grey area) the range was -2 cm to + 2 cm. In Experiment 2 (lighter grey area) the range was -3 cm to +3 cm.

The distance relative to the midline of the T, A or AT stimuli was determined on a trial-to-trial basis using the psi+ method, run using the Palamedes toolbox in Matlab (Prins, 2012; Prins and Kingdom, 2018). The psi+ method is an extension of the original psi method proposed by Kontsevitch and Tyler (1999), a Bayesian adaptive algorithm aiming at optimizing stimulus placement to gain information on the psychometric function parameters: the threshold α (mid-point of the function), the slope β (rate of change parameter), and the lapse rate λ (determining the upper and lower asymptotes of the function). To do so, it keeps track of a joint probability distribution for the function parameters, selects stimulus placement to optimize entropy reduction on these parameters, updates the full joint distribution based on the response to the presented stimulus, and selects the next stimulus following the same approach for a given number of stimuli (Kontsevich and Tyler, 1999).

The method was run separately for the different conditions (A, T, AT). The psychometric function shape to be estimated by the algorithm was set to a cumulative Gaussian. Given the nature of the task, classification errors at both extremes of the stimulus range were considered lapses and the upper and lower asymptote values of the psychometric function were estimated jointly. The method was constrained to select stimulus locations relative to the midline ranging from –

2.0 cm to +2.0 cm in steps of 0.5 mm, and to consider threshold α values in the same range. It was also constrained to consider slope β values between 0.05 and 5, and lapse rate λ values between 0 and 0.2. Threshold (alpha) and slope (beta) priors were uniform on the predefined range. Lapse rate (lambda) prior was a half-normal with mean 0 and standard deviation 0.5, normalized to integrate to 1 on the predefined range.

The experimental session comprised a total of 300 trials (100 per modality), divided into twelve blocks of 25 stimuli, four for each modality (T, A and AT). The order of the blocks was pseudo-randomized across participants: to avoid too many repetitions of blocks of the same modality, the order of the blocks was randomized for every sequence of three blocks (e.g. block 1 = A, T, AT; block 2 = T, AT, A etc.)

2.4.2. Experiment 2 (interleaved design)

In Experiment 1, participants were informed about what modality would be presented to them prior to each block. Such a blocked design could have led participants to choose the sensory cue (tactile or auditory) that they perceived as more reliable during bimodal trials, thus disregarding the sensory cue from the other modality. For this reason, a follow-up experiment was conducted using an interleaved design mixing T, A and AT trials within each testing block. Participants were not informed about modality prior to each trial, and could therefore not choose to focus on one modality or the other during bimodal trials. The task performed by the participant was identical to Experiment 1. To ensure correct perception of each modality, participants were also asked, at the end of each trial, to report what type of stimulation they perceived (T, A or AT), in addition to reporting the perceived location of their finger at the time the stimulus was presented. In case of lack of detection or incorrect detection of a stimulus (for example, only perceiving a T or A stimulus during AT trials), the trial was repeated,

and participants were not informed that they would be presented with the same stimulus.

The same Psi+ adaptive procedure was employed. The stimulation and prior alpha ranges were increased compared to Experiment 1 from ± 2.0 cm to ± 3.0 cm as the results from Experiment 1 showed that, for some participants, the psychometric curve failed to saturate within the ± 2.0 cm range (Supplementary Fig. 1 and 2). The prior beta (slope) and lambda (lapse) distributions were the same as in Experiment 1.

The experimental session comprised a total of 300 trials. The experiment was divided into 10 blocks, each comprising 30 trials (10 of each modality). Within each block, the order of presentation of the three conditions was interleaved and pseudo-randomized for each participant: to avoid too many repetitions of the same modality, the randomization procedure was repeated every six trials, thus obtaining two repetitions of stimuli of each modality within twelve trials (e.g. A;T;A;AT;T;AT – T;AT;T;A;A;AT etc.).

2.5. Data analysis

Rather than using the estimates of the psychometric function's parameters returned by the psi+ method (threshold, slope, and lapse rate), we decided to use the raw stimulus-response pairs to fit new hierarchical models able to better account for the structure of the data (condition within participants, participants within group). This was motivated by the fact that independent psi+ runs need to be used for each participant and conditions, corresponding to untenable assumptions of total independence between participants and conditions, and by the fact that we would have to either drop the uncertainty of these estimates and treat them as single observations (rather than as the results of fitting a model to

100 trials) or use complicated meta-analysis techniques to weight these estimates by their uncertainty.

2.5.1. Model choice

Assuming sensory noise to be the sum of many independent sources, this noise should be approximately normally distributed in accordance with the Central Limit Theorem (Kingdom and Prins, 2010). For such theoretical reasons, we chose to use a probit (i.e. cumulative normal) regression model, which is regarded as *''perhaps the most justifiable form''* of psychometric function (Kingdom and Prins, 2010).

In order to assess within participants differences in threshold and slope with the modelling, the AT condition was chosen as the intercept of the linear predictors, and the difference between *AT* and *T* and between *AT* and *A* were modelled. As stimuli located at more positive values along the x-axis of the display (i.e., more to the right) should lead to a larger probability of reporting a stimulus on the right half of the screen, the slope was constrained to be positive by making it a base 10 exponential. As we did not expect the different conditions to affect lapses, the lapse rate was treated as a nuisance parameter, and was allowed to vary between participants, but not between conditions.

This gives us the following model:

$For\ i\ in\ 1\ to\ I$

$For\ k\ in\ 1\ to\ K$

$$y_i \sim Binomial\ (\varphi_i,\ n_i)$$

$$\varphi_i = \lambda_k + \frac{(1-2\lambda_k)}{2}.erfc\left(\frac{-\beta_k\ .(x_i-\alpha_k)}{\sqrt{2}}\right)$$

$$\alpha_i = coef_{\alpha\ AT_{k[i]}} + coef_{\alpha\ AT-T_{k[i]}}.\ isT_i + coef_{\alpha\ AT-A_{k[i]}}.\ isA_i$$

$$\beta_i = 10\text{^}\left(coef_{\beta\ AT_{k[i]}} + coef_{\beta\ AT-T_{k[i]}}.\ isT_i + coef_{\beta\ AT-A_{k[i]}}.\ isA_i\right)$$

$$\lambda_i = \frac{1}{1+e^{-coef_{\lambda_{k[i]}}}}$$

$$coef_{\alpha\ AT_k} \sim Normal(\mu_{\alpha\ AT},\ \sigma_{\alpha\ AT})$$

$$coef_{\alpha\ AT-T_k} \sim Normal(\mu_{\alpha\ AT-T},\ \sigma_{\alpha\ AT-T})$$

$$coef_{\alpha\ AT-A_k} \sim Normal(\mu_{\alpha\ AT-A},\ \sigma_{\alpha\ AT-A})$$

$$coef_{\beta\ AT_k} \sim Normal(\mu_{\beta\ AT},\ \sigma_{\beta\ AT})$$

$$coef_{\beta\ AT-T_k} \sim Normal(\mu_{\beta\ AT-T},\ \sigma_{\beta\ AT-T})$$

$$coef_{\beta\ AT-A_k} \sim Normal(\mu_{\beta\ AT-A},\ \sigma_{\beta\ AT-A})$$

$$coef_{\lambda_k} \sim Normal(\mu_\lambda,\ \sigma_\lambda)$$

Where K is the number of subject, k is a varying index corresponding to the subject identity, I is the number of data points, i is a varying index corresponding to the current data point, n is the number of stimuli presented at a given intensity, φ is the probability to report the stimulus on the right part of the visually displayed midline, λ is the lapse rate, α is the threshold, β is the slope, erfc is the complementary error function, isA and isT are binary variables taking 0 (false) or 1 (true) value depending on the type of stimulus being used (A: isA=1, otherwise, isA=0; T: isT=1, otherwise, isT=0)

2.5.2. Model fitting

The model was fitted in *Stan* (Stan Development Team, 2016) using the *Cmdstanr* package (Gabry et al., 2023) within the *R* statistical program (R Core Team, 2021) and the *R Studio* interface (Allaire, 2012). To fit the model, four chains of 5000 iterations (including a warm-up period of 2500 iterations, which was discarded) were used, leading to a total of 10000 draws from the posterior distribution.

Experiment 1

A total of 1958 stimulus response pairs, coming from 20 participants and 3 conditions, were used to fit the model. Priors on standard deviations (σ) were constrained to be positive. The hyperprior (prior on group level parameter) for the intercept of the threshold predictors ($\mu_{\alpha AT}$, $\sigma_{\alpha AT}$) was a normal distribution with mean 0 and standard deviation 1. The hyperpriors for the slopes of the threshold predictors ($\mu_{\alpha T}$, $\sigma_{\alpha T}$; $\mu_{\alpha A}$, $\sigma_{\alpha A}$) were normal distributions with mean 0 and standard deviation 0.5. The hyperprior for the intercept of the log10(slope) predictors ($\mu_{\beta AT}$, $\sigma_{\beta AT}$) was a normal distribution with mean 1 and standard deviation 0.5. The hyperpriors for the log10(slope) predictors ($\mu_{\beta T}$, $\sigma_{\beta T}$; $\mu_{\beta A}$, $\sigma_{\beta A}$) were normal

distributions with mean 0 and standard deviation 0.25. The prior for the group mean of the logit transformed lapse rate was a normal distribution with mean -4 and standard deviation 1.

Experiment 2

A total of 2067 stimulus response pairs, coming from 20 participants and 3 conditions, were used to fit the model. The hyperprior for the intercept of the threshold predictors ($\mu_{\alpha AT}$, $\sigma_{\alpha AT}$) was a normal distribution with mean 0 and standard deviation 1. The hyperpriors for the threshold predictors ($\mu_{\alpha T}$, $\sigma_{\alpha T}$; $\mu_{\alpha A}$, $\sigma_{\alpha A}$) were normal distributions with mean 0 and standard deviation 0.5. The hyperprior for the intercept of the log10(slope) predictors ($\mu_{\beta AT}$, $\sigma_{\beta AT}$) was a normal distribution with mean 1 and standard deviation 0.5. The hyperpriors for the log10(slope) predictors ($\mu_{\beta T}$, $\sigma_{\beta T}$; $\mu_{\beta A}$, $\sigma_{\beta A}$) were normal distributions with mean 0 and standard deviation 0.25. The prior lapse rate was a normal distribution with mean -4 and standard deviation 1.

2.5.3. Model diagnostics

Following model fitting, appropriate sampling of the posterior distributions was assessed using the *ShinyStan* (Stan Development Team, 2017): absence of divergent transitions, not reaching maximum tree depth, good alignment of energy diagnostic plots, E-BFMI larger than 0.2, effective sample size larger than 10% of the total sample size, Monte Carlo standard error smaller than 10% of the posterior standard deviation, and *Rhat* equal to or smaller than 1.01. Individual participant data fits were inspected visually as a posterior predictive check (see supplementary Figs. 1-4).

2.5.4. Differences between conditions

For both experiments, the presence of significant interindividual threshold or slope differences between conditions *(AT vs T*; *AT vs A*; *T vs A*) were assessed based on the posterior probability distributions of $\mu_{\alpha T}$, $\mu_{\alpha A}$, and $\mu_{\alpha A} - \mu_{\alpha T}$ (thresholds) and $\mu_{\beta T}$, $\mu_{\beta A}$, and $\mu_{\beta A} - \mu_{\beta T}$ (slopes). These distributions correspond to the population means of differences in threshold and slope between *AT* and *T, between AT and A*, and between *A* and *T*, respectively. These parameters were used to estimate the posterior probability (P) of our different null hypotheses by comparing 10^5 random draws from their posterior distributions with 0. When comparing threshold estimates across conditions, bilateral tests were used, as we made no predictions on the effects of modality on threshold values within participants. For estimation of interindividual differences in slope, we conducted unilateral tests when assessing differences between the two unimodal and the bimodal conditions, given our pre-registered (Experiment 1: https://doi.org/10.17605/OSF.IO/Y4GBN; Experiment 2: https://doi.org/10.17605/OSF.IO/X69UZ) hypothesis that concurrent auditory-tactile stimulation would improve precision, and bilateral tests when comparing the two unimodal conditions, since we did not have a pre-registered hypothesis on the slope difference between these two. We considered the null hypothesis to be rejected when its posterior probability was less than 0.05.

To better illustrate the psychometric function fitted from the posterior distribution of the model parameters, an expected function was constructed, for each condition. This was achieved by constructing 10^4 functions using random draws from the posterior distribution of the parameters and taking, for each temporal delay, the 50^{th} percentile of the stimulus detection probability. To get a sense of the uncertainty around these values, the pointwise 2.5^{th} and 97.5^{th} percentiles (95% credible interval) were also plotted. These psychometric functions

can be interpreted as the expected values for a new unobserved participant coming from the same population.

3. Results

3.1. Experiment 1 (blocked design)

The model diagnostics revealed appropriate sampling, and the model appeared to fit well to the individual participants' raw data (see supplementary Figs. 1 and 2).

As can be seen in Figure 2, when the different conditions were presented in separate blocks (Experiment 1), thresholds of all three stimuli (A, T, AT) tended to be negative, indicating that participants reported that their finger was to the right of the midline when stimuli were presented close to it. Furthermore, the threshold for the tactile-only stimulus T was significantly more negative than that of the auditory-tactile stimulus AT ($P_{(T \neq AT|data)}$=0.034). The threshold of the auditory-only stimulus A appeared less negative than the thresholds of the other stimuli, but these differences were not statistically significant ($P_{(A \neq AT|data)}$=0.708, $P_{(T \neq A|data)}$=0.107). The slopes of the AT and T psychometric functions appeared very similar ($P_{(T<AT|data)}$=0.581) and both were significantly greater than the slope of the A psychometric function ($P_{(A<AT|data)}$ = 0.001, $P_{(T \neq A|data)}$=0.004), indicating greater localization precision in the case of tactile stimulation (T or AT).

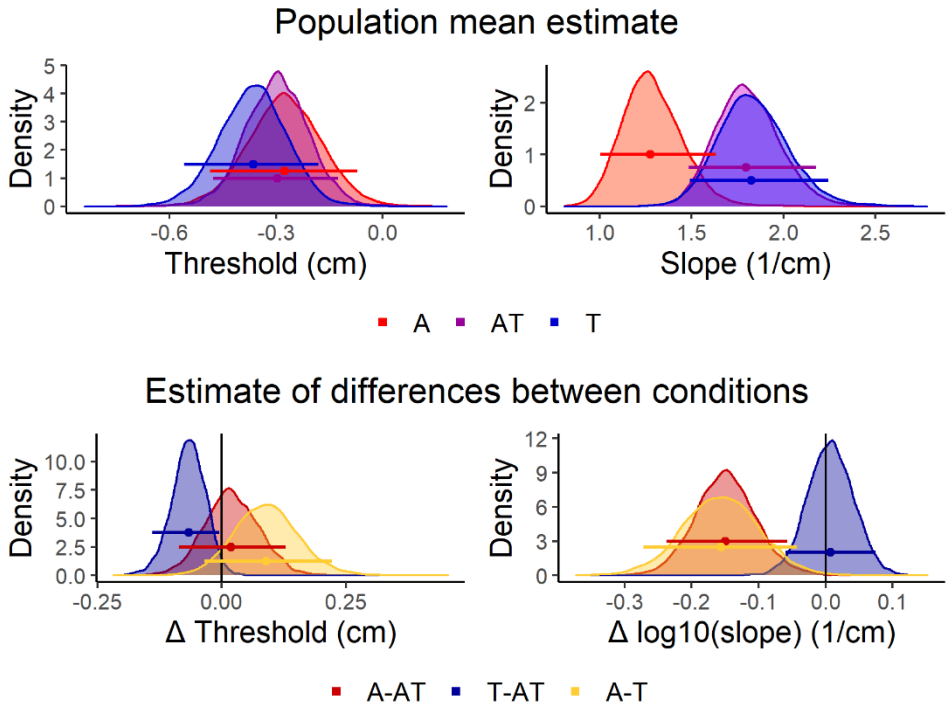

Figure 2. Posterior psychometric function parameter estimates for Experiment 1 (blocked design). The top row represents the population mean estimates for the threshold (left) and log10(slope) (right) for the three conditions. In the model, these parameters correspond to $\mu_{\alpha AT}$ / $\mu_{\beta AT}$ (AT), $\mu_{\alpha AT} + \mu_{\alpha T}$ / 10^($\mu_{\beta AT} + \mu_{\beta T}$) (T), and $\mu_{\alpha AT} + \mu_{\alpha A}$/ 10^($\mu_{\beta AT} + \mu_{\beta A}$) (A). The bottom row represents estimates of threshold (left) and log10(slope) (right) differences between conditions. In the model, these correspond to $\mu_{\alpha T}/\mu_{\beta T}$ (T-*AT*) and $\mu_{\alpha A}/\mu_{\beta A}$ (*A*-*AT*), and $\mu_{\alpha A} - \mu_{\alpha T}/\mu_{\beta A} - \mu_{\beta T}$ (*A*-T), where T-AT, A-AT, and A-T represent the population means of differences in threshold and slope between AT and T, between AT and A, and between A and T, respectively. In all cases, the horizontal lines represent the 95% highest probability density intervals of the posterior distributions and the dots represent the medians of the posterior distributions.

A posterior predictive psychometric function, corresponding to what can be expected for a new participant coming from the same population taking Experiment 1, is displayed in Figure 3.

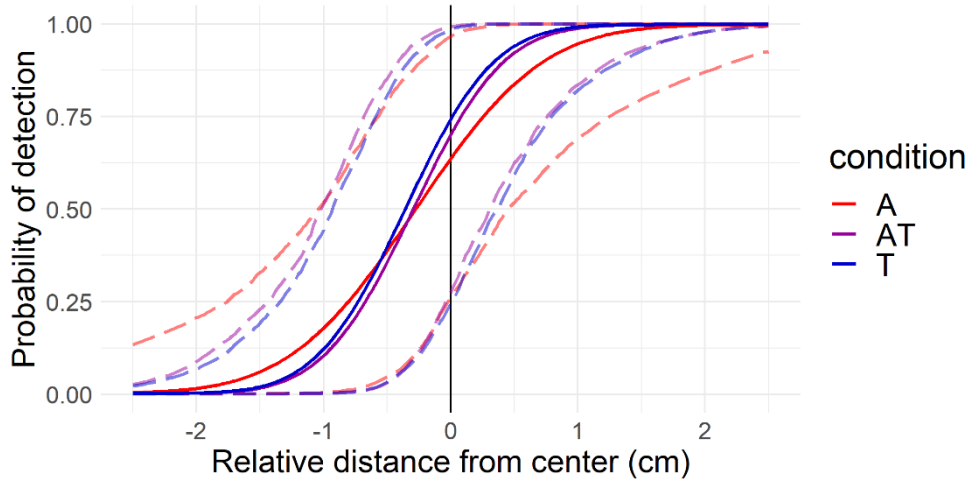

Figure 3. Posterior expected psychometric functions for Experiment 1 (blocked design). Bold lines represent the function constructed with the most likely parameter values (i.e. the median of 10^3 random draws from the posterior distribution of the model parameters). Dotted lines represent the pointwise uncertainty around the posterior expected function (95% highest probability density intervals).

3.2. Experiment 2 (interleaved design)

The model diagnostics revealed appropriate sampling, and the model appeared to fit well to the individual participants' raw data (see supplementary Figs. 3 and 4).

As can be seen in Figure 4, when the different stimulus conditions were intermingled within the same blocks (Experiment 2), the threshold of the auditory-tactile AT stimulus was significantly less negative (closer to the display midline) compared to the auditory-only A stimulus ($P_{(T\neq AT|data)}$=0.005) and the tactile-only T stimulus ($P_{(A\neq AT|data)}$<0.001), which were extremely similar ($P_{(T\neq A|data)}$=0.801). The slope of the AT psychometric function appeared steeper than the slope of the T psychometric function (not significant; $P_{(T<AT|data)}$=0.209) which itself was significantly steeper compared to the slope of the A psychometric function ($P_{(A<AT|data)}$=0.001, $P_{(T\neq A|data)}$=0.028).

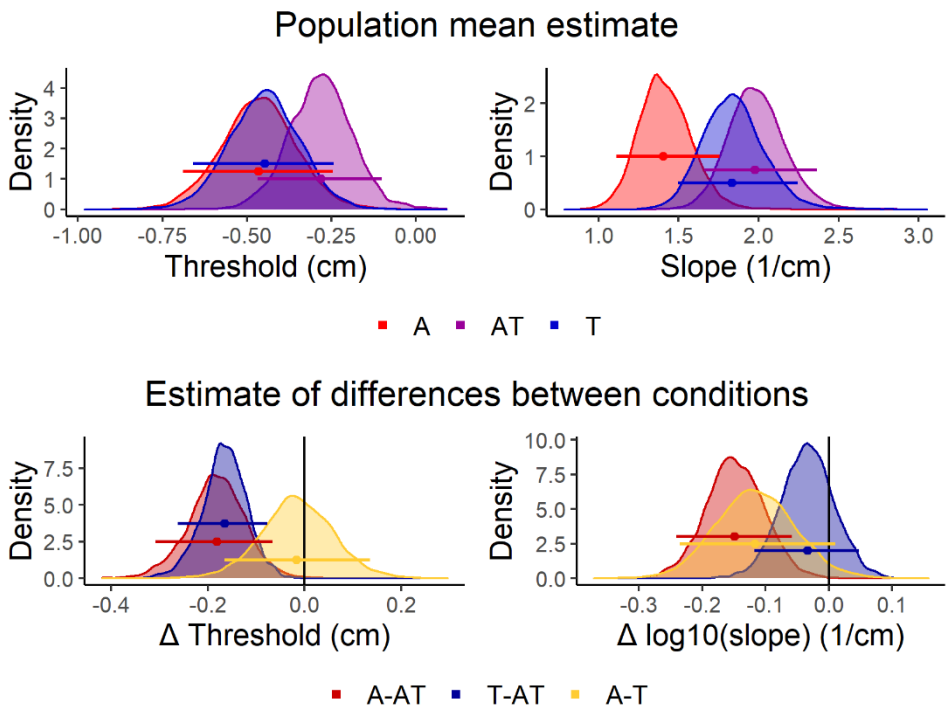

Figure 4. Posterior psychometric function parameter estimates for Experiment 2 (interleaved design). The top row represents the population mean estimates for the threshold (left) and log10(slope) (right) for the three conditions. In the model, these parameters correspond to $\mu_{\alpha AT}$ / $\mu_{\beta AT}$ (AT), $\mu_{\alpha AT} + \mu_{\alpha T}$ / 10^($\mu_{\beta AT} + \mu_{\beta T}$) (T), and $\mu_{\alpha AT} + \mu_{\alpha A}$/ 10^($\mu_{\beta AT} + \mu_{\beta A}$) (A),. The bottom row represents estimates of threshold (left) and log10(slope) (right) differences between conditions. In the model, these correspond to $\mu_{\alpha T}/\mu_{\beta T}$ (T-*AT*) and $\mu_{\alpha A}/\mu_{\beta A}$ (*A*-*AT*), and $\mu_{\alpha A} - \mu_{\alpha T}/\mu_{\beta A} - \mu_{\beta T}$ (*A*-T), where T-AT, A-AT, and A-T represent the population means of differences in threshold and slope between AT and T, between AT and A, and between A and T, respectively. In all cases, the horizontal lines represent the 95% highest probability density interval of the posterior distributions and the dots represent the medians of the posterior distributions.

A posterior predictive psychometric function, corresponding to what can be expected for a new participant coming from the same population performing Experiment 2, is displayed in Figure 5.

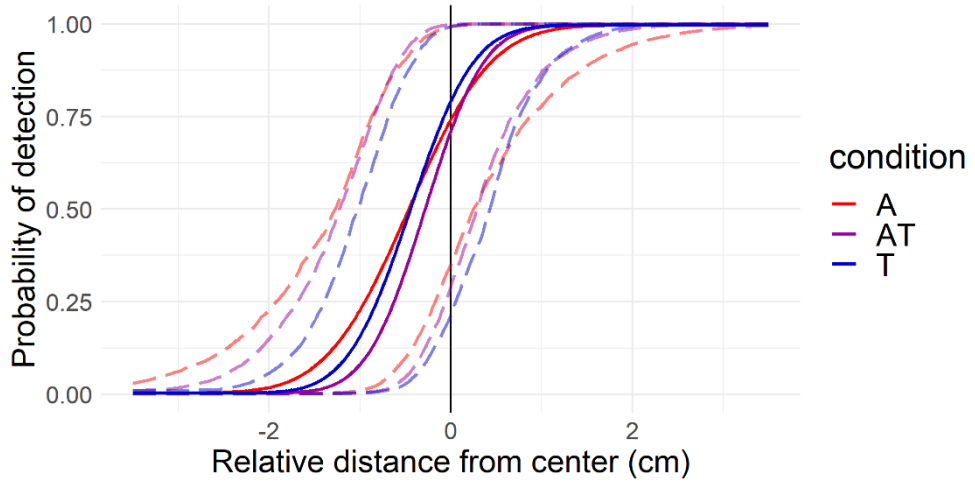

Figure 5. Posterior expected psychometric functions for Experiment 2 (interleaved design). Bold lines represent the psychometric function constructed with the most likely parameter values (i.e. the median of 10^3 random draws from the posterior distribution of the model parameters). Dotted lines represent the uncertainty around the posterior expected function (95% highest probability density intervals).

4. Discussion

In this study, we aimed to investigate how observers integrate the onsets of auditory and/or tactile feedback to localize events in external space occurring during active tactile exploration (sliding the fingertip against a surface). Specifically, we assessed whether concurrent auditory-tactile stimulation improves localization performance compared to unimodal-tactile and unimodal-auditory stimulation. To address this question, two experiments were performed. In a first experiment, participants received information on the modality of the incoming sensory information prior to each block (auditory, tactile or auditory-tactile). With such a design, participants could be inclined to ignore one of the sensory cues during bimodal trials, and simply respond to what they perceived as the most reliable cue. Therefore, in a second experiment, the three modalities were interleaved within

blocks, and participants did not receive any information about the incoming sensory information prior to each trial. Results from both experiments revealed better localization precision (indexed by the slope of the fitted psychometric functions) for unimodal tactile stimulation compared to unimodal auditory stimulation. This suggests that the onset of tactile cues during fingertip sliding was more informative on localization than the onset of auditory cues. Given the nature of the task, where participants used their finger to actively explore a surface, it seems reasonable to expect a finer grained spatial representation of where the finger is when a tactile stimulus is perceived at its extremity than when a concurrent auditory stimulus without somatosensory counterpart is perceived.

While we had hypothesized that the combination of tactile and auditory sensory cues would lead to an improvement of localization precision, this was not the case in Experiment 1. In this experiment, participants knew in advance what type of stimulus would occur. It is thus likely that some participants focused on the more informative tactile modality when receiving bimodal stimuli, which poses a significant limitation to the interpretation of the group-level results from the first experiment. For this reason, the rest of the discussion will focus on the interpretation of the results from Experiment 2.

In that experiment, participants did not know in advance what type of stimulus they would receive and therefore could not beforehand focus on a specific modality. In this experiment, the slopes for the different psychometric functions followed our hypothesis (auditory<tactile<auditory-tactile), but the slope estimates between the T and AT modalities were not significantly different, whereas the slope estimate for the unimodal A condition was markedly lower than the other two conditions. This suggests that such as in Experiment 1, tactile cues were more informative on localization as compared to auditory cues, and that combined auditory-tactile stimulation did not significantly improve localization precision.

The exploratory analysis of threshold estimates provides interesting insights in the effects of bimodal stimulus presentation on localization bias. In both experiments, and for all conditions, the psychometric curves were shifted towards negative threshold values. This indicates that, irrespective of modality, when stimuli were presented while the exploring finger was close to the midline, participants tended to respond that their finger was to the right of the midline. Several reasons could explain this effect. First, our results are consistent with leftward biases observed in bisection tasks (left side underestimation, or pseudoneglect) frequently reported in the literature in healthy subjects, who tend to place their perceived midpoint towards the left of the true midpoint of a line (Bradshaw et al., 1985; Varnava et al., 2002). Second, the haptic display used to deliver the tactile stimuli modulates friction of the entire fingertip contacting surface, rather than a specific fingertip location. This is due to the fact that ultrasonic vibrations are triggered across the whole plate once the finger is detected within a pre-defined active zone (Vezzoli et al., 2016). Given that the display was explored in a single left-to-right direction, and taking into consideration the size of the fingertip contacting surface, it is therefore possible that the bias in the tactile modality was influenced by the fact that participants perceived the change in friction on the entire fingertip surface as soon as it entered the haptic rectangle. Thus, for stimuli presented at short distances to the left of the visual midline, the friction modulation also occurred at locations on the fingertip skin that had already crossed the midline, biasing perception to the right. A further possibility is that delays between detection of finger position via the capacitive screen of the E-VITA haptic display as well as the infrared frame and triggering of both tactile and auditory stimuli also contributed to the observed bias. However, such delays would also have been present in the bimodal condition, and the bias reduction in this condition in experiment 2 still points towards the presence of multisensory effects. Lastly, the observed perceptual rightward bias may relate

to the effect of *representational momentum,* or forward displacement. This phenomenon occurs when, in the presence of motion, the localization of a stimulus is shifted towards the direction of movement (Freyd and Finke, 1984; Hubbard, 2018, 2005; Merz et al., 2020). More specifically, our findings appear to be consistent with a special case of representational momentum, the flash-lag effect, which is observed when the position of a stationary object is assessed relative to a moving target object (here the position of the finger sliding against the display) (Hubbard, 2013). Different accounts of the mechanisms underlying the flash-lag effect have been proposed, including a longer processing time for stationary than for moving stimuli (Whitney et al., 2000), and the effect has already been described for haptic stimuli (the buzz-lag effect) (Cellini et al., 2016; Drewing et al., 2018; Drewing and Vroomen, 2022), and for cross-modal stimuli (Alais and Burr, 2003). In our experiments, participants had to continuously integrate motor, proprioceptive, and visual inputs, to estimate the timing of stimulation relative to the estimated fingertip position, as neither the tactile nor auditory stimuli (corresponding to the flash in the flash-lag effect or the buzz in the buzz-lag effect) carried explicit spatial information in themselves (i.e. the somatosensory and auditory stimuli were identical regardless of where the finger was located on the haptic display). Since the task only involved left-to-right movements, it seems plausible that the estimated position of the exploring fingertip at the moment of transient auditory and/or tactile stimulation was shifted forward relative to the visually displayed midline, giving rise to a rightward perceptual bias in both experiments. In Experiment 2, where modality of the upcoming sensory cue was not predictable, bimodal stimulation led to a reduced bias compared to the unimodal auditory stimulation, suggesting that concurrent presentation of the auditory and tactile stimuli increased the temporal binding between the auditory-tactile stimuli and the estimated position of the exploring fingertip relative to the visually displayed

midline. Such cross-modal effects on temporal binding have also been previously reported in the context of the flash-lag effect between the visual and auditory modalities (Vroomen and De Gelder, 2004). In these experiments, it was shown that a sound concurrently presented with a visual flash significantly reduced the magnitude of the flash-lag effect, and that presenting the sound with an offset relative to the visual flash biased the effect linearly with the introduced delay, consistent with a temporal ventriloquism effect (Vroomen and De Gelder, 2004). In drawing parallels between auditory-visual and auditory tactile interactions in the context of representational momentum, a key difference is that, while in the flash-lag effect the moving target is passively presented to participants (i.e., a dot moving horizontally across a screen), during the buzz-lag effect as well as in our task, the moving target is voluntarily displaced by the participants (i.e., the exploring fingertip). Localization during active finger sliding movements therefore relies on dynamically integrating spatial information about limb position at a given time (given by visual and/or proprioceptive cues) and temporal information about the onset of the tactile and/or auditory stimuli. In contrast with our results, a study investigating the effects of modality on the buzz-lag and flash lag-effects across vision and touch found that the magnitude of the effect was not different between unimodal versus bimodal conditions (Drewing et al., 2018). However, a key difference with the present work is that we tested differences between a bimodal (temporally synchronized auditory and tactile stimuli) and unimodal (tactile- or auditory-only) stimuli, while both the stationary object (the visually displayed midline) and the moving object (the exploring finger) were always the same across our experimental conditions. In line with our results, Drewing and colleagues ((Drewing et al., 2018)) reported that the characteristics of the flash (e.g., its intensity or duration) modulate the magnitude of the illusion, as they represent a temporal trigger to estimate the moving object's position, and the time necessary

to trigger the estimation depends on the processing timing of the flashed object (Drewing et al., 2018; Hubbard, 2014). This is consistent with a redundant signals effect, which predicts that multisensory gain is reflected by faster response times in bimodal compared to unimodal conditions (Otto and Mamassian, 2017; Raab, 1962), and which has been reported in a large number of studies investigating audio-visual, visual-tactile and auditory-tactile interactions (Diederich and Colonius, 2004; Forster et al., 2002; Girard et al., 2013; Murray et al., 2001; Zampini et al., 2007). In line with such gain effects, it is possible that, in the bimodal condition of our study, participants made quicker decisions about the stimuli, and therefore were faster at reconstructing the position of their finger relative to when the stimulus was perceived, thus leading to a more accurate localization of finger position relative to the stimulation onset. However, since we have no measure of reaction times to the stimulations used in our experiment, it is not possible to evaluate whether the effects we observed on accuracy could result from simple statistical facilitation and be driven by the fastest modality (as predicted by the race model (Otto and Mamassian, 2017; Raab, 1962)), or whether sensory integration took place prior to the decisional process (as predicted by the co-activation model (Miller, 1982; Otto and Mamassian, 2017)). Furthermore, bimodal stimulation did not lead to significant improvements in precision (i.e., the slope of the psychometric function), possibly highlighting the fact that tactile stimuli provided sufficient information in isolation for participants to reach ceiling performance levels.

Importantly, the movement-related bias we observed could be intrinsic to different types of active tactile exploration. While the use of only one direction of movement does not allow us to fully exclude effects of left-side underestimation, previous studies that have reported buzz-lag effects in active touch employing both directions of movement have shown that the lagging effect occurs in both

directions (Cellini et al., 2016). Therefore, it seems plausible to suggest that the bias we observed is more closely related to representational momentum. Our finding that concurrent sound reduces such bias could therefore have important implications for the design of haptic technologies.

In conclusion, we show that, under our experimental conditions, concurrent auditory stimulation did not lead to a significant improvement of the localization precision of the fingertip at the time it receives a tactile stimulus in conditions of active touch, possibly due to the higher reliability and relevance of fingertip tactile input compared to auditory input during tactile exploration. Interestingly, however, our exploratory analysis revealed a localization bias compatible with the audiovisual flash-lag effect or the tactile-visual buzz-lag effect, which was significantly reduced under bimodal stimulus presentation. Therefore, cross-modal effects between sound and touch in conditions of active haptic exploration could increase the temporal binding between transient auditory-tactile cues relative to the estimated position of the moving fingertip. This more veridical perception of finger position when tactile stimuli are jointly presented with sounds can have implication for the design of efficient devices that need to be explored haptically.

Supplementary materials

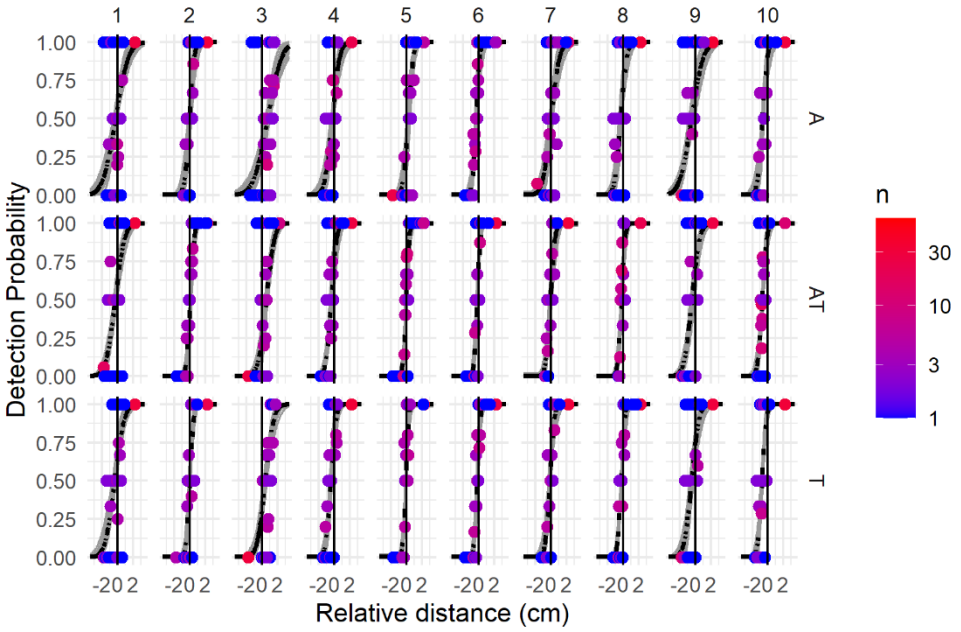

Supplementary Figure 1. Individual participants' fits of the model (experiment 1; Participants 1-10). For each participant (columns) and condition (rows), the detection probabilities for the various delays are depicted as dots, color-coded based on the number of trials used to compute the plotted probability. The PF constructed using the most likely parameter (median) is plotted in black. 100 PFs constructed using random draws from the posterior distribution of the parameters are plotted in grey (uncertainty around the true parameter values).

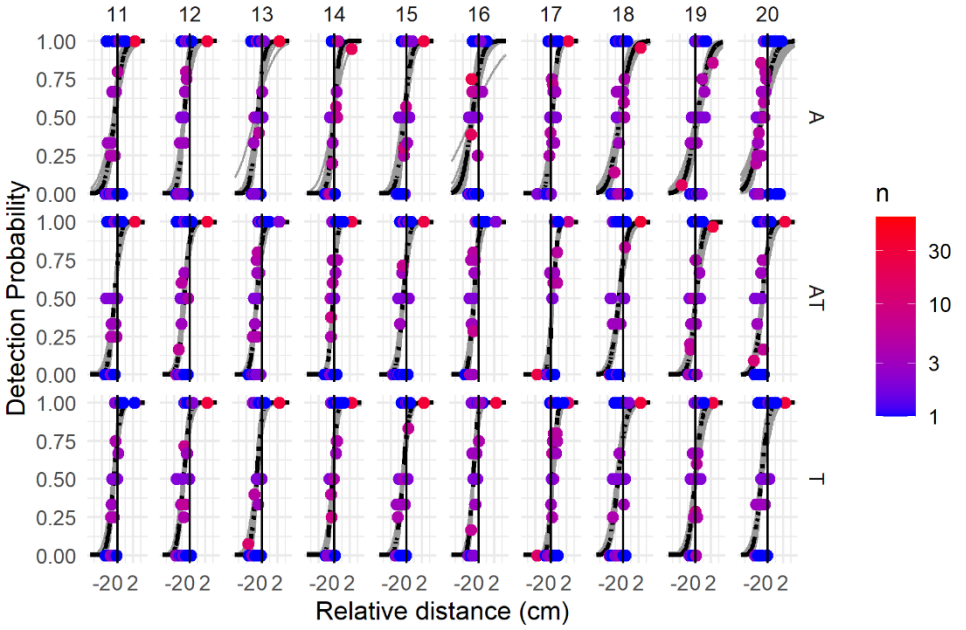

Supplementary Figure 2. Individual participants' fits of the model (experiment 1; Participants 11-20). For each participant (columns) and condition (rows), the detection probabilities for the various delays are depicted as dots, color-coded based on the number of trials used to compute the plotted probability. The PF constructed using the most likely parameter (median) is plotted in black. 100 PFs constructed using random draws from the posterior distribution of the parameters are plotted in grey (uncertainty around the true parameter values).

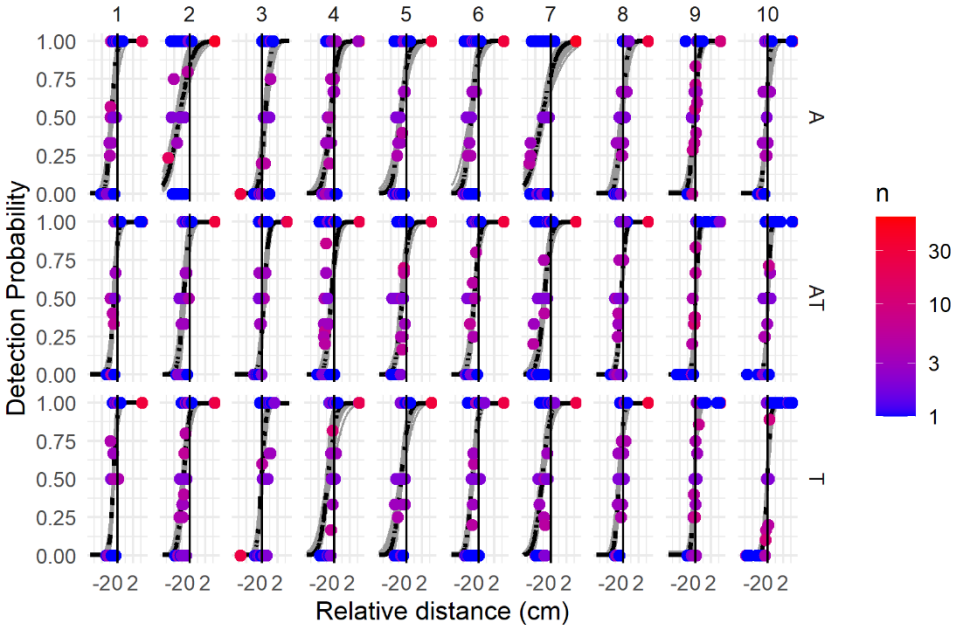

Supplementary Figure 3. Individual participants' fits of the model (experiment 2; Participants 1-10). For each participant (columns) and condition (rows), the detection probabilities for the various delays are depicted as dots, color-coded based on the number of trials used to compute the plotted probability. The PF constructed using the most likely parameter (median) is plotted in black. 100 PFs constructed using random draws from the posterior distribution of the parameters are plotted in grey (uncertainty around the true parameter values).

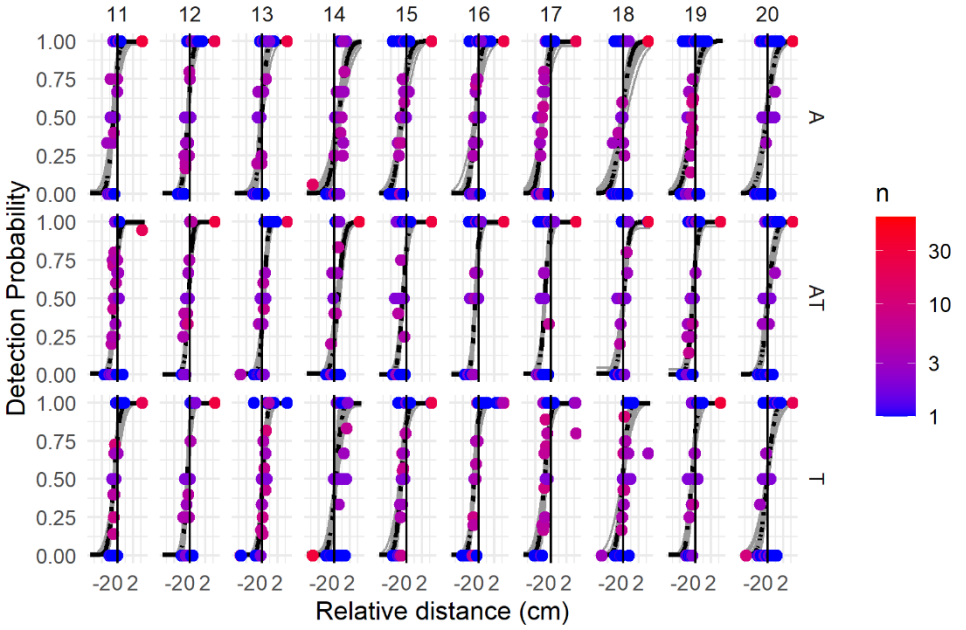

Supplementary Figure 4. Individual participants' fits of the model (experiment 2; Participants 11-20). For each participant (columns) and condition (rows), the detection probabilities for the various delays are depicted as dots, color-coded based on the number of trials used to compute the plotted probability. The PF constructed using the most likely parameter (median) is plotted in black. 100 PFs constructed using random draws from the posterior distribution of the parameters are plotted in grey (uncertainty around the true parameter values).

CHAPTER 3: Processing the fine-grained features of tactile textures involves the primary somatosensory cortex[1].

[1]Published as: **Esposito, G.,** Nozaradan, S., Kuzminova, A., Collignon, O., Mouraux, A. (2024) Processing the fine-grained features of tactile textures involves the primary somatosensory cortex. *Imaging Neuroscience*, 2: 1-15.

Abstract

Dynamic tactile perception and discrimination of textures require the ability to encode and differentiate complex vibration patterns elicited at the level of the skin when sliding against a surface. Whether the primary somatosensory cortex (S1) can encode the fine-grained spectrotemporal features distinguishing textures remains debated. To address this question, electroencephalography (EEG) frequency-tagging approach was used to characterize responses to vibrotactile oddball contrasts between two textures. In a first session designed to identify the topographical distribution of responses originating from the hand and foot representations in S1, standard and deviant stimuli were pure sinusoidal vibrations differing in frequency and intensity. In a second session, standard and deviant stimuli were two different snippets of bandpass-filtered white noise matched in terms of intensity and average frequency content, but differing in terms of their complex spectrotemporal content. Using the S1 functional localizer, we showed that oddball responses to a spectrotemporal contrast follow the somatotopical organization of S1. Our results suggest that the encoding of fine-grained spectrotemporal features associated with different vibration patterns involves S1.

Keywords: EEG, vibrotactile, frequency-tagging, texture, somatosensory, S1

1. Introduction

During tactile exploration of a textured surface, minute and complex deformations of the skin activate mechanoreceptors located within cutaneous and subcutaneous structures. It is believed that two main codes underlie our ability to discriminate textures: a spatial code, whereby texture information is conveyed by the differential activation of mechanoreceptors having small receptive fields, and a temporal code mediated by differences in the temporal dynamics of activity generated within rapidly adaptive mechanoreceptors (Connor et al., 1990; Connor and Johnson, 1992; Hollins and Risner, 2000; Muniak et al., 2007). Indeed, sliding the finger against a fine-grained textured surface generates mechanical vibrations at the skin-surface interface that preferentially activate rapidly adapting mechanoreceptors types I and II (Bensmaïa and Hollins, 2005; Hollins et al., 2001). Therefore, the frequency content and time course of skin vibrations during exploration of natural textures may carry information about individual texture identity (Manfredi et al., 2014). More specifically, the intensity of vibrations recorded at the level of the hand and wrist during dynamic exploration of a textured surface was shown to carry information about texture roughness for both periodic and non-periodic textures, while their frequency content allowed discrimination of different samples of periodic textures (Delhaye et al., 2012). In primates, several studies have reported temporal encoding of skin vibrations and fine textures within vibration-sensitive mechanoreceptors, with millisecond-scale precision (Mackevicius et al., 2012; Weber et al., 2013). The temporal pattern of activation of rapidly adapting types I and II fibers has been shown to reliably reflect individual texture identity, and has thus been suggested to mediate fine texture perception (Weber et al., 2013). Other studies conducted in non-human primates have shown that millisecond-level temporal patterning of responses to natural textures is also represented at the cortical level, in the primary somatosensory cortex (S1)

(Birznieks and Vickery, 2017; Harvey et al., 2013; Long et al., 2022). The cortical activity generated by high-frequency vibrations has been related to the envelope and the frequency content of skin vibrations elicited by surface scanning of the fingertip (Harvey et al., 2013).

In humans, scalp electroencephalography (EEG) can be used to non-invasively characterize brain responses to a sensory stimulus with a very fine time scale. However, measuring high-frequency cortical activity to high-frequency vibrations using scalp EEG is a challenging endeavor and, using pure sinusoidal mechanical vibrations, EEG responses have been previously shown to only be reliably recorded at stimulation frequencies below 100 Hz (Breitwieser et al., 2012; Srinivasan et al., 1990; Vialatte et al., 2009).

Besides the recording of event related potentials (ERPs) which allow characterizing synchronized and transient cortical responses to the onset of single sensory events, EEG can also be used to characterize cortical activity induced by the periodic and selective modulation of a property of the sensory stimulus using the frequency-tagging approach (Lenc et al., 2021; Norcia et al., 2015; Nozaradan, 2014; Rossion, 2014). In this approach, periodic modulation of a sensory feature elicits a periodic variation in cortical activity, which is expected to project at the frequency of the periodic modulation and its harmonics in the EEG spectrum (Nozaradan, 2014; Rossion, 2014). Therefore, an advantage of the frequency-tagging approach is the fact that it allows specific characterization and quantification of the elicited responses as they are constrained within exact narrow frequency bands determined by the rate at which the sensory feature is modulated (Norcia et al., 2015; Regan, 1989, 1966). Using this approach, Moungou et al. (2016a) were able to isolate and describe, in humans, cortical activity related to the processing of natural fine-grained textures. To do so, they periodically modulated

the envelope of high-frequency vibrations elicited at the fingertip by introducing a small 3 Hz sinusoidal vertical displacement of the textured surface while it was concurrently sliding against the finger. Besides showing that the EEG frequency-tagging approach was able to capture stimulus-related cortical activity tagged at the frequency of this vertical displacement, they also reported that the magnitude of these responses was related predominantly to the magnitude of the high-frequency vibrations recorded at the fingertip. Furthermore, the topographic pattern of the periodic texture-related activity was contralateral to the stimulated hand, suggesting an involvement of S1 (Moungou et al., 2016a). Classification of textures differing in their levels of roughness has also been recently achieved using EEG, indexed by variations in the total power of Mu- (8–15 Hz) and beta-band (16–30 Hz) oscillations (Eldeeb et al., 2020). Importantly, texture classification accuracy was highest around electrodes contralateral to the stimulation site (Eldeeb et al., 2020), further supporting tactile texture representation within S1. However, whether the processing and discrimination of different fine-grained textures are implemented within S1, or whether they require higher cortical areas remains unknown. In a recent investigation, decreases in alpha-band power were observed over bilateral sensorimotor areas in response to both smooth-to-rough and rough-to-smooth changes in textures in conditions of active, dynamic touch (Henderson et al., 2023), possibly suggesting involvement of areas beyond S1. Some neuroimaging studies have reported texture-selective activity in S1 (Lederman et al., 2001) as well as in the secondary somatosensory cortex (S2) and the insula (Kitada et al., 2005; Simões-Franklin et al., 2011). Neuroimaging studies have reported an involvement of S2 and the insula in the categorization of textures based on high-level texture characteristics, such as perceived roughness, while activity within S1 would be more closely associated with low-level differences in the physical characteristics of textures, such as their spatial period (Eck et al., 2016).

With some exceptions (Henderson et al., 2023, 2022; Moungou et al., 2016a), previous studies have largely relied on simple synthetic stimuli, such as raised dots or ridges, displaying very regular spatial characteristics. Such physical features poorly relate to the complex patterns of vibrations that are elicited upon scanning of natural textures. At the same time, previous work has largely focused on higher-level aspects of texture processing, for instance comparing rough and smooth textures. What thus needs to be further investigated is whether S1 is able to resolve minute variations in the frequency composition over time of vibrations that distinguish fine-grained textures, and, therefore, whether contrast-specific responses to spectrotemporal differences in vibrotactile input matching in terms of their overall intensity and spectral content involve S1.

Here we address this question using a variation of the EEG frequency-tagging approach referred to as periodic oddball stimulation. In this paradigm, a deviant or oddball stimulus periodically replaces a standard stimulus within a regular sequence repeated at a constant frequency (Norcia et al., 2015; Rossion, 2014; Rossion et al., 2015). The strength of the approach lies in the fact that it allows distinguishing EEG responses that are related to the processing of stimulus features that are shared across the standard and deviant stimuli from those related to processing the specific features distinguishing the standard stimulus from the deviant stimulus. Indeed, the first will appear in the EEG frequency spectrum as peaks at the frequencies corresponding to the base rate of stimulation— and its harmonics— whereas the second will appear as peaks at the frequencies corresponding to the rate of presentation of the deviant stimuli—and its harmonics (Nozaradan et al., 2017). The approach has been widely employed to characterize cortical processes involved in auditory (Nozaradan et al., 2017) and visual (Norcia et al., 2015; Rossion, 2014). To date, no studies have implemented periodic oddball

stimulation to investigate somatosensory processing of changes in vibrotactile stimulation.

The aim of this experiment was thus to explore whether it is possible to record EEG responses to fine-grained vibrotactile contrasts using the periodic oddball stimulation paradigm, and to examine whether these responses originate, at least in part, from the contralateral S1. In a first condition, the difference between the oddball and standard stimuli consisted in a low-level contrast in tactile vibration frequency and intensity. In a second condition, we implemented a higher-level fine-grained spectrotemporal contrast, where standard and oddball stimuli were complex bandpass filtered (40-200 Hz) white noise vibrations that did not differ in terms of their average intensity or average frequency content, but in the time course of their envelope and spectral content. Our main hypotheses were (1) that oddball EEG responses can be recorded to both frequency-intensity and spectrotemporal contrasts and (2) that the topography of the oddball responses to spectrotemporal contrasts would be consistent with activity originating at least partly from S1, based on recent evidence that fine-grained texture discrimination involves S1 (Moungou et al., 2016a). To test the second hypothesis, we stimulated two body sites that would allow assessing whether the topography of oddball EEG responses would follow the somatotopical organization of S1: the index finger of the right hand, for which we expected to observe responses clearly lateralized to the contralateral hemisphere, and the sole of the right foot, for which we expected responses localized at central scalp electrodes (Dowman and Schell, 1999; Heid et al., 2020). While somatotopy has also been characterized in areas beyond S1 such as S2 and the insula using functional magnetic resonance imaging (fMRI) and magnetoencephalography (MEG) (Björnsdotter et al., 2009; Del Gratta et al., 2002; Ruben et al., 2001), hand versus foot somatotopy in these higher-order areas is not

expected to generate marked differences in EEG scalp topography (Ruben et al., 2001).

2. Methods

2.1. Participants

Eighteen healthy participants (5 males, 13 females, aged 22-32 years) were recruited to participate in the study. Participants received information about the study and gave written informed consent. All participants confirmed they had no current or history of neurological or psychiatric disorders, and no loss of skin sensitivity at their hands or feet. The study was approved by the UCLouvain Ethics Committee. Data from one subject were excluded due to highly noisy EEG recordings. The final sample thus included 17 healthy participants (14 right-handed; 1 left-handed; handedness information missing from 2 participants).

2.2. Stimuli and apparatus

Vibrotactile stimuli were designed in MATLAB (version R2020b) and consisted of sequences of vibrotactile stimuli delivered according to an established (AAAAB) oddball pattern (Liu-Shuang et al., 2014; Nozaradan et al., 2017; Rossion, 2014). The base repetition frequency was 8 Hz. The frequency of the oddball B stimulus was 8/5 Hz = 1.6 Hz. For each trial, this pattern was looped 64 times, for a total of 40 s of periodic oddball vibrotactile stimulation. The rate of stimulation was chosen as, at 8 Hz, the 125 ms duration of individual stimuli was long enough to optimize contrast detection, but not so fast as to impair individual stimulus detection due to fusion effects, as vibrotactile stimuli modulated at frequencies up to 10-13 Hz are still perceived as individual events (Jurado et al., 2021; Park and Choi, 2011). Further, a relatively fast stimulation rate allowed presenting more stimuli in a short

amount of time, thus optimizing signal-to-noise ratio. These 40-s sequences were delivered in separate trials to the right index finger or the right inner midfoot.

2.2.1. Frequency–intensity contrast

In this first condition, individual A and B vibration stimuli were sine waves lasting 125 ms, with the amplitude of vibration linearly ramping up from 0 to 1 (full amplitude) and down from 1 to 0 during 15 ms at the beginning and end of each stimulus, respectively. The A stimuli had a frequency of 300 Hz and the B stimuli had a frequency of 200 Hz. These frequencies were chosen as responses to both A and B stimuli would be processed preferentially by rapidly adapting mechanoreceptors type II, responding maximally to frequencies in the 200–300 Hz range (Holmes and Tamè, 2023; Verrillo, 1985), and thought to largely contribute to the perception of fine textures (Bensmaïa and Hollins, 2005; Hollins et al., 2002). This condition was used to assess the feasibility of recording oddball responses to a low-level contrast in frequency and/or intensity of stimulation. Indeed, considering the frequency dependence of skin mechanoreceptors, changing the frequency of stimulation inevitably produces changes in the intensity of mechanoreceptor activation, and differential activation of different mechanoreceptor classes (Johansson and Vallbo, 1983). This condition was also used to obtain a topographic template of EEG responses to vibrotactile stimulation of the hand and foot, as described in Section 2.6.4.

2.2.2. Spectrotemporal contrast

In this second condition, A and B stimuli were also of 125 ms duration, with 15 ms ramps up and down. The only difference with the first condition was that A and B stimuli were made of broadband noise instead of sine waves. For each trial, A stimuli consisted of 125-ms white noise, and B stimuli were generated by shuffling

the amplitude values of noise A across time points. The two obtained white noise samples were then band-pass filtered between 40 and 200 Hz, to specifically stimulate within the preferred frequency band of rapidly adapting mechanoreceptors types I and type II (Johansson and Vallbo, 1983), and reduce potential confounding auditory stimulation elicited by high frequencies which would not concomitantly contribute to mechanoreceptor activation, which is typically observed at frequencies up to 1000 Hz (in the case of rapidly adapting mechanoreceptors type II) (Bell et al., 1994; Jones and Smith, 2014). Eight different trials were generated using eight random samples of white noise (stimulus A) and their shuffled version (stimulus B). For both conditions, A and B stimuli were RMS normalized to equalize their total energy. The A and B stimuli were thus matched in terms of energy and average spectral content, but differed in terms of envelope and spectral time course. All stimuli were delivered using a vibrating device (Minishaker Type 4810, Brüel & Kjaer) connected to a power amplifier (Type 2718, Bruel & Kjaer). A curved metal plate (45 mm length, 22 mm width) was attached to the top of the actuator using a 10-32 UNF screw. To maintain intensity of stimulation perceptually similar in both conditions, the amplitude of the frequency/intensity contrast sequences was set to about half that of the white noise sequences, as determined by pilot experiments. The stimulation laptop was connected to a digital-to-analog converter (USB 6363, National Instruments), which delivered the analog output to the amplifier and sent triggers to the EEG recording system at the onset of each trial. A custom platform was built to ensure participants received stimulation in an optimal manner while being in a comfortable position and to minimize finger and foot movements. The vibrating device was placed inside the platform, and support pistons allowed to adjust the height of the device. For hand stimulation, participants rested their forearms on the platform, placing their right index finger on the vibrating plate. For foot stimulation, participants rested

their right foot on the platform, placing their inner midfoot on the vibrating plate. The choice of location for foot stimulation was justified by previous studies reporting lower tactile perception thresholds for the inner midfoot compared with the big toe (Kekoni et al., 1989), which we reasoned would allow maximizing the EEG responses to foot stimulation.

2.3. Procedure

The experiment consisted of a total of 64 trials, divided into 4 blocks (2 for hand and 2 for foot stimulation). Within each block, 16 trials (8 frequency/intensity trials and 8 spectrotemporal trials) were randomly presented. During each trial, subjects listened to white noise played through headphones to cover any auditory noise generated by the vibrating device. To ensure participants did not hear the sequences, they were presented with one frequency/ intensity and one spectrotemporal sequence without concomitant tactile stimulation, and the level of white noise was adjusted until participants reported not hearing the sequences. To avoid any order effects, the order of stimulation location (hand or foot) was counterbalanced across participants. Subjects were asked to pay attention to the stimuli and to report, at the end of each trial, whether they were able to detect only one type of vibration (no contrast) or more than one type of vibration (contrast).

Prior to the experimental session, participants were presented with two example sequences, one with no contrast (only 47 Hz vibrations) and one with contrast (where A = 47 Hz and B = 197 Hz), to make sure they familiarized themselves with the oddball contrasts.

2.4. EEG data acquisition

Participants were instructed to relax, avoid moving their head and body as much as possible, and fixate on a point in front of them. A 64 Ag-AgCl electrode cap (ANT) was used for EEG recordings and placed on the participants' scalp according to the International 10/10 system. The signals were recorded using an average reference. Sample rate was set at 2,000 Hz and impedances were kept below 10 kΩ.

2.5. Spectrotemporal stimuli envelope dissimilarity analysis

For each of the eight spectrotemporal sequences, the A and B stimuli were designed to be matched in terms of total energy and average frequency content. However, they could differ both in terms of their temporal envelope (envelope contrast) or their fine-grained spectral content over time (spectrotemporal contrast). In order to investigate whether the oddball EEG responses to these stimuli could have been driven predominantly by differences in the time course of the envelopes of A and B white noise stimuli, a dissimilarity index was computed for each of the eight trials as the sum of the absolute point-by-point difference between the envelope of the A stimulus and its corresponding B stimulus (obtained by means of a Hilbert transformation of the A and B stimuli) in the time domain. As shown in Figure 1C, one of the eight sequences used (spectrotemporal sequence #2) exhibited a strong dissimilarity in envelope as compared with all other sequences.

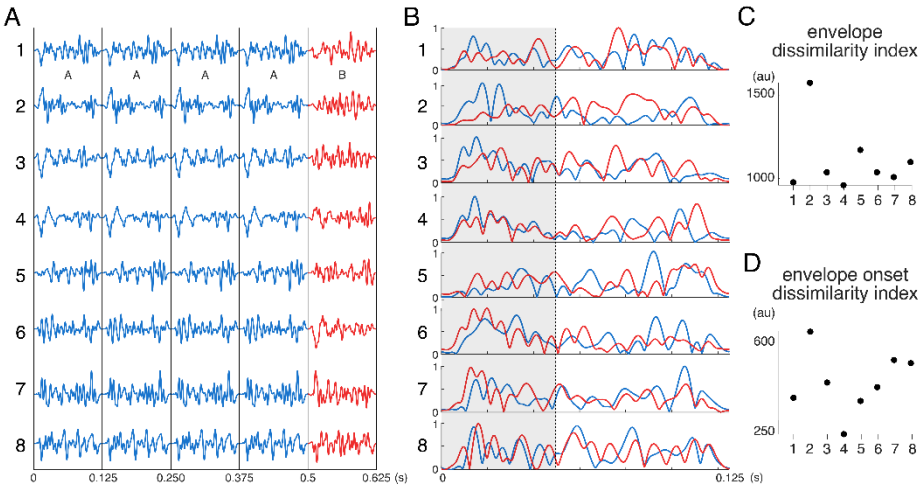

Figure 1. (A) Time course of spectrotemporal A and B stimuli 1-8 (x-axis: time in seconds.; y-axis: amplitude (AU), where 1 is maximum amplitude output). (B) Time course of the envelopes of spectrotemporal A and B stimuli 1–8 (x-axis: time in seconds.; y-axis: amplitude (AU), where 1 is maximum amplitude output). (C) Index of envelope dissimilarity between A and B stimuli 1-8. (D) Index of envelope onset (first 50 ms) dissimilarity between A and B stimuli 1–8.

The EEG analyses reported in the manuscript were performed excluding responses to the highly dissimilar spectrotemporal sequence 2. Results obtained using the dataset including spectrotemporal sequence 2, and additional analyses to explore whether oddball responses to spectrotemporal contrasts could have been driven by differences in the envelope of the A and B stimuli are reported as Supplementary Materials.

2.6. EEG Analysis

2.6.1. Preprocessing

EEG data preprocessing and analysis steps were performed using the Letswave (version 6; https://www.letswave.org/) Matlab toolbox for EEG signal

processing. First, a DC removal and linear detrend were applied on the continuous EEG traces to remove drifts in the signals. Next, a bandpass Butterworth filter (4th order) was applied between 0.1 and 40 Hz. To facilitate data handling, EEG traces were then downsampled to 500 Hz and segmented from 0 to 40 s relative to trial onset. Occasional noisy channels were identified visually and replaced by the average of the signals recorded at the three closest neighboring electrodes. A total of 12 channels were interpolated across 6 subjects. To remove ocular artifacts (eye blinks and eye movements), an independent component analysis (ICA) was performed using the RUNICA algorithm (constrained to 63-N independent components, where N corresponded to the number of interpolated channels). Independent components capturing electrooculographic activity were identified visually (based on their time course and topography) and removed. Finally, trials presenting remaining large-amplitude artifacts were automatically rejected using an amplitude criterion of 500 µV. A total of 47 trials were removed (14 and 9 trials for the frequency/intensity condition at the hand and foot; 19 and 5 trials for the spectrotemporal condition at the hand and foot) across 14 subjects. Finally, signals were re-referenced to the average of all scalp channels.

2.6.2. Frequency domain analysis

For each participant, stimulation type and stimulation site, EEG signals were averaged across trials in the time domain to reduce the contribution of signals that were not time locked with the trial onsets. A fast Fourier Transform (FFT) was applied to obtain amplitude spectra with a resolution of 0.025 Hz (i.e., 1/40 s), which allowed further analysis of responses at the frequencies of interest and their harmonics. To evaluate the periodic EEG response to the base and oddball stimuli, a baseline subtraction was applied to the single-subject amplitude spectra at each scalp channel by removing, at each frequency bin, the average of the 24

neighboring frequency bins (12 on each side, excluding bins immediately before and after the bin of interest). The baseline subtraction procedure minimizes the contribution of background EEG activity and noise to the activity at frequency bands of interest. In the absence of a periodic EEG response at the frequency of interest, baseline-subtracted amplitudes should tend toward zero (Chemin et al., 2014; Freeman et al., 2003; Mouraux et al., 2011; Nozaradan et al., 2017, 2011).

2.6.3. Significance testing of base and oddball EEG responses

For each participant, condition, and stimulation site, the baseline-subtracted frequency spectra were averaged across all scalp channels.

To assess whether a periodic response was elicited at the base frequency, baseline-corrected amplitudes at the base frequency and its harmonics were averaged up to 40 Hz (8, 16, 32, and 40 Hz). The resulting average values were tested against zero using a one-sample t-test (right tailed), separately for each stimulation type and stimulation site. Similarly, to test for the presence of an oddball response, baseline-corrected amplitudes at the oddball frequency and harmonics were averaged for frequencies up to 40 Hz—excluding frequencies corresponding to the base frequency and its harmonics— and tested against zero. Aggregation of harmonics is recommended as it allows to more effectively compare responses across conditions because different EEG response time courses may lead to different levels of amplitude at different harmonics, and inclusion of higher harmonics allows a better characterization of overall responses (Retter et al., 2021).

2.6.4. Topographic analysis of somatotopy

Next, we aimed to investigate our central hypothesis that a substantial part of the oddball EEG response to spectrotemporal contrasts originates from S1.

Because a periodic intensity modulation of vibrotactile input may be expected to generate a strong periodic variation in S1 activity, the base responses to the frequency/intensity sequences can be expected to predominantly reflect activity originating from S1 (Colon et al., 2014, 2012). Indeed, fMRI and MEG studies have shown that vibrotactile stimulation primarily activates the contralateral S1 (Kim et al., 2015; Stippich et al., 1998; Tuunanen et al., 2003), and that the magnitude of S1 responses increases with increasing amplitude of vibrotactile stimuli under task-free conditions (Nelson et al., 2004). Most importantly, and notwithstanding the fact that the vibrotactile stimuli are expected to generate activity beyond the contralateral S1, the differences in the scalp topography generated by vibrotactile stimulation of the hand versus the foot may be expected to predominantly result from the somatotopical organization of S1. The EEG responses to the base repetition of frequency–intensity contrasts were thus used to generate two weighted channel templates, one built using the base response during hand stimulation to capture the topographical distribution of activity originating from the hand representation within S1, the other built using the base response during foot stimulation to capture the topographical distribution of activity originating from the foot representation within S1. To construct each of the two templates, we first identified the base frequency harmonics exhibiting amplitude values significantly greater than zero when applying the frequency/ intensity stimulus to the hand or foot, respectively (t-test against zero using the frequency spectra averaged across all scalp channels). Then, amplitude values at each channel were averaged across significant harmonics. Negative amplitude values were set to 0, and the obtained channel template was divided by its sum across channels, such that the sum of the template would be equal to 1. In this way, a weight was assigned to each channel, depending on the relative amplitude of the base response across channels. This procedure allowed us to assess S1 somatotopy while maintaining the spatial

information provided by all electrodes, rather than by using an *a priori* selection, and at the same time by accounting for the relative contribution of each electrode (represented by the weight assigned in the templates) to the observed responses following hand and foot stimulation. Indeed, a similar topographical distribution of responses at both stimulation sites would lead to similar weights being assigned to the same electrodes. As such, even in the presence of differences in amplitudes following hand and foot stimulation, multiplying the amplitude of responses of one stimulation site by the weights of the two templates would lead to very similar results. However, in the presence of topographical differences at the two stimulation sites, different weights would be assigned to the same electrodes in the two templates, and multiplying the amplitude of responses of one stimulation site by the weights of the two templates would allow us to capture such differences of spatial distribution.

For each participant and stimulation site, the EEG response to the base frequency of the spectrotemporal contrast (average of baseline-subtracted amplitudes at base frequency and harmonics up to 40 Hz) and the EEG response to the oddball frequency of the spectrotemporal contrast (average of baseline-subtracted amplitudes at the oddball frequency and its harmonics up to 40 Hz, excluding frequencies corresponding to the base harmonic frequencies) were multiplied with each of the two weighted channel templates. The obtained weighted amplitudes were then averaged across all channels, yielding four values for each participant and stimulation site, corresponding to the base and oddball EEG responses weighted by the hand and foot templates, respectively.

Finally, the magnitudes of the responses elicited by hand versus foot stimulation weighted by the hand versus foot template were compared using a 2

by 2 repeated-measures ANOVA with the factors “stimulation site” (hand vs. foot stimulation) and “channel template” (hand template vs. foot template).

Our hypothesis was that, in the presence of S1 somatotopy, the repeated-measures ANOVA would reveal a significant interaction between the two factors, because the amplitude of the response elicited by stimulation of the hand weighted by the hand template would be significantly greater than the amplitude of that same response weighted by the foot template; whereas the response elicited by stimulation of the foot would be greater when weighted by the foot template as compared with the hand template. When significant, post hoc comparisons using paired-sample t-tests were used to compare, for each stimulation site, the amplitudes of the oddball response weighted by the hand template versus the foot template.

3. Results

3.1. Base and oddball EEG responses

Both for hand stimulation and foot stimulation, significant base responses (averaged across all harmonics up to 40 Hz) were observed for the frequency/intensity contrast condition (hand: mean = 0.005 μV; SD = 0.007 μV; $p = 0.004$; foot: mean = 0.003 μV; SD = 0.004 μV); $p < 0.001$) (Figure 2).

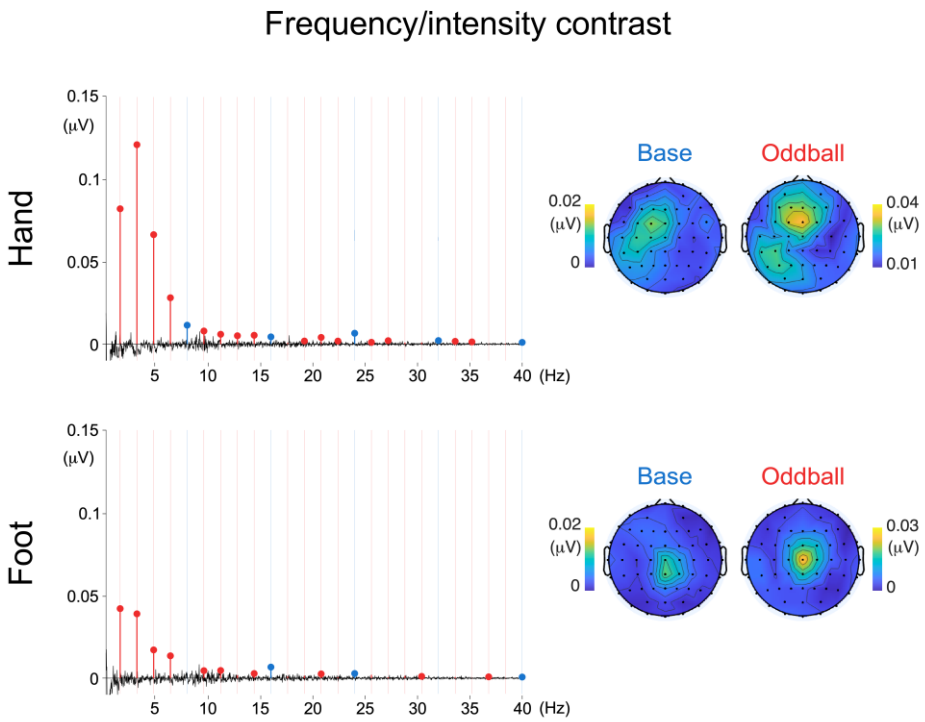

Figure 2. Baseline-subtracted EEG frequency spectra in the frequency/intensity contrast condition across hand and foot stimulation, averaged across participants and EEG channels. Harmonics are color-coded, with base responses depicted in blue, and oddball responses depicted in red. Filled dots depict harmonics with amplitude values significantly higher than zero (t-test, right-tailed). Vertical bars represent expected base and oddball frequencies. Topographical plots represent signal amplitude averaged across significant harmonics.

Significant base responses (averaged across all harmonics up to 40 Hz) were also observed the spectrotemporal contrast condition (hand: mean = 0.016 μV; SD = 0.015 μV; $p < 0.001$; foot: mean = 0.010 μV; SD = 0.008 μV; $p < 0.001$) (Figure 3).

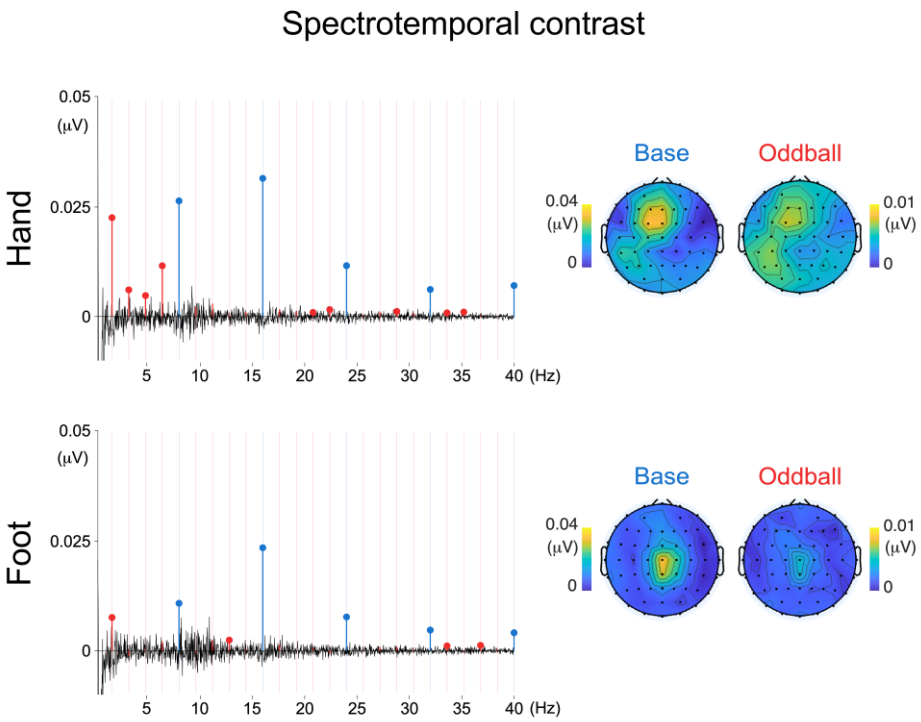

Figure 3. Baseline-subtracted EEG frequency spectra in the spectrotemporal contrast condition across hand and foot stimulation, averaged across participants and EEG channels. Harmonics are color-coded, with base responses depicted in blue, and oddball responses depicted in red. Filled dots depict harmonics with amplitude values significantly higher than zero (t-test, right-tailed). Vertical bars represent expected base and oddball frequencies. Topographical plots represent signal amplitude averaged across significant harmonics.

All base frequencies up to 40 Hz exhibited baseline-subtracted amplitude values significantly greater than zero in at least one stimulation condition or stimulation site (Figures 2 and 3).

Similarly, both for hand and foot stimulation, significant oddball responses (averaged across all harmonics, excluding base frequencies) were observed both for the frequency/intensity contrast (hand: mean = 0.017 μV; SD = 0.005 μV; $p <$

0.001; foot: mean = 0.007 µV; SD = 0.003 µV; p < 0.001) and for the spectrotemporal contrast (hand: mean = 0.003 µV; SD = 0.002 µV; p < 0.001; foot: mean = 0.001 µV; SD = 0.002 µV; p = 0.013). Oddball harmonics from 1.6 to 14.4 Hz and from 19.2 to 36.8 Hz exhibited amplitudes significantly greater than zero in at least one stimulation type (frequency/intensity or spectrotemporal contrast), at one or both stimulation sites (hand or foot) (Figure 2).

Visual inspection of the topographical distribution of the periodic EEG responses showed that, across both types of contrasts, both the base response and the oddball response were localized over central and parietal scalp electrodes contralateral to the stimulated limb. In contrast, for base and oddball responses to foot stimulation, the responses to both types of stimuli were localized over central scalp electrodes. Figure 4 shows the topography of the responses to hand stimulation using the spectrotemporal contrasts across clusters of oddball harmonics (1.6–6 .4 Hz; 9.6-14.4 Hz; 17.6-22.4 Hz; 25.6-30.4 Hz; 33.6–38.4 Hz), which remained stable and contralateral to the stimulated hand.

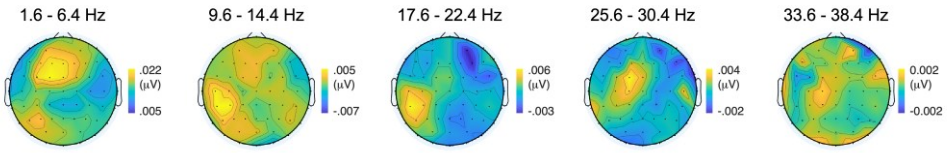

Figure 4. Topographical plots of the oddball EEG responses to the spectrotemporal contrast averaged across clusters of oddball harmonics (1.6 Hz-6.4 Hz; 9.6 Hz-14.4 Hz; 17.6 Hz-22.4 Hz; 25.6 Hz-30.4 Hz; 33.6 Hz-38.4 Hz).

3.2. Topographic test for somatotopy

Significant harmonic frequencies that were averaged to generate the weighted channel templates were 8, 16, 24, 32, and 40 Hz for hand stimulation, and 16, 24,

and 40 Hz for foot stimulation. The 10 channels showing maximum amplitudes in the hand template were FC1, FCz, C3, C1, FC3, CP3, F1, Fz, Cz, and CP5. For the foot template, they were CPz, Cz, CP2, C2, Pz, P1, CP1, FCz, FC2, and POz. The templates are shown in Figure 5.

3.2.1. EEG response to the base repetition of spectrotemporal contrasts

The repeated-measures ANOVA showed a significant interaction between stimulation site (hand vs. foot) and channel template (hand vs. foot template), indicating that the topography of the base response to the spectrotemporal contrast depended on the site of stimulation ($F = 14.666$, $p = 0.001$, $\eta^2 = 0.031$). Post hoc t-tests (one sided) showed S1 somatotopy: the base response to stimulation of the hand was greater when weighted with the hand template as compared with the foot template ($p = 0.003$, Cohen's $d = 0.784$), whereas the base response to stimulation of the foot was greater when weighted with the foot template than when weighted with the hand template ($p = 0.002$, Cohen's $d = 0.823$).

3.2.2. Oddball EEG response to the spectrotemporal contrasts

The repeated-measures ANOVA showed a significant interaction between stimulation site and channel template for the oddball EEG response to the spectrotemporal contrasts ($F = 23.442$, $p < 0.001$, $\eta^2 = 0.019$). Post hoc t-tests (one-sided) showed that the oddball response to stimulation of the hand was greater when weighted with the hand template than when weighted with the foot template ($p < 0.001$, Cohen's $d = 1.098$), and that the oddball response to stimulation of the foot was greater when weighted with the foot template than when weighted with the hand template ($p = 0.022$, Cohen's $d = 0.532$) (Figure 5).

Visual inspection of activity at a transversal subset of central electrodes (C1, C3, Cz, C2, and C4) confirmed that the topographical pattern of hand and foot base and oddball responses to the spectrotemporal sequences were maximal over contralateral central electrodes for hand stimulation (C1, C3), and maximal over the midline (Cz) for foot stimulation (Figure 5C).

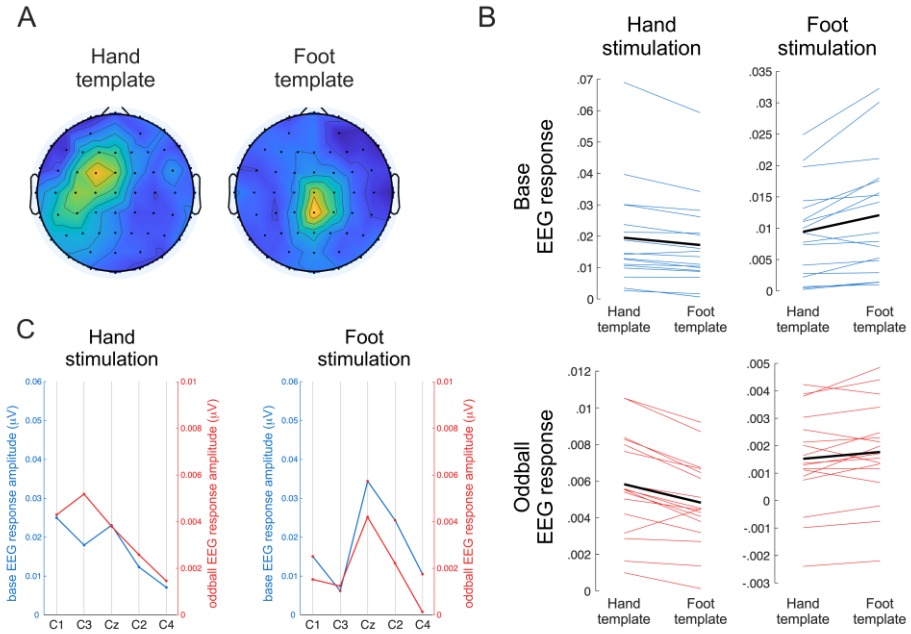

Figure 5. **Topographic test for somatotopy in the spectrotemporal contrast condition.** A. Weighted channel templates for hand and foot stimulation, generated using the base response to the frequency/intensity contrast. B. The left and right graphs show the responses to hand and foot stimulation, while the upper and lower graphs show the responses to the base and oddball EEG responses. Each graph compares the amplitude values weighted using the hand versus foot template. The thin blue and red lines display the data for each participant, and the thick black line shows the average across participants. Note that both for the base responses and the oddball responses, amplitude values following stimulation of the hand were greater when weighted with the hand template compared to the foot template, whereas amplitude values following stimulation of the foot

were greater when weighted with the foot template compared to the hand template. C. Visual comparison of base and oddball EEG responses to hand and foot stimulation at central electrodes C1, C3, Cz, C2, and C4. Individual data points represent the grand-average of the activity averaged across the base and oddball harmonics pre-selected in the main topographic test for somatotopy.

3.3. Behavioral results

Data from one subject are missing from the behavioral analysis due to issues with saving of behavioral responses. On average, participants reported perceiving the contrast within the sequence on 69.9% (SD: 28.0%) and 69.1% (SD: 28.9%) of the frequency/intensity contrast condition trials, for hand and foot stimulation, respectively. For the spectrotemporal contrast condition, participants reported perceiving the contrasts on 34.0% (SD: 24.7%) and 41.4% (SD: 28.1%) for hand and foot stimulation, respectively. A repeated measures ANOVA found no main effect of sequence on contrast detection within the spectrotemporal sequences for hand ($F = 0.789$, $p = 0.598$) nor for foot ($F = 0.829$, $p = 0.566$) stimulation.

To further assess whether explicit contrast perception in the spectrotemporal condition was related to the magnitude of the observed EEG responses, the pre-processed EEG trials of each participant following hand stimulation were categorized based on whether the participants had detected the contrast (two categories: detected and non-detected) and analyzed separately as described in Sections 2.6.3 and 2.6.4. For both detected and non-detected trials, we observed a significant base response (detected: mean 0.027 μV; SD = 0.0153; $p < 0.001$; non-detected: mean = 0.019 μV; SD = 0.013; $p < 0.001$) and, most importantly, a significant oddball response (detected: mean = 0.007 μV; SD = 0.008; $p = 0.0036$; non-detected: mean = 0.005 μV; SD = 0.003; $p < 0.001$) (Figure 6). A paired-sample t-test revealed no significant differences in the magnitude of the oddball responses collected in detected versus non-detected trials ($p = 0.506$; N = 13 participants with

both detected and non-detected trials), indicating that presence of an oddball response to the spectrotemporal contrast did not require conscious perception of the contrast.

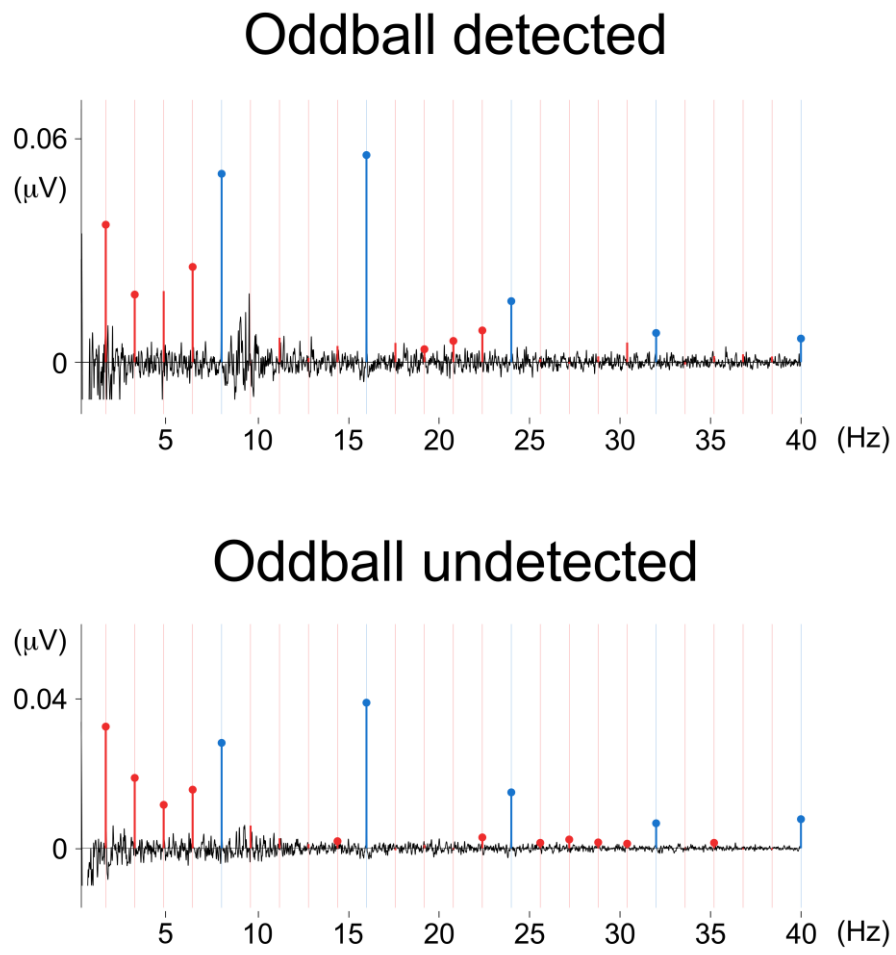

Figure 6: Baseline-subtracted EEG frequency spectra for detected and non-detected spectrotemporal contrast sequences, averaged across participants and EEG channels. Harmonics are color-coded, with base responses depicted in blue, and oddball responses depicted in red. Filled dots

depict harmonics with amplitude values significantly higher than zero (t-test, right-tailed). Vertical bars represent expected base and oddball frequencies.

4. Discussion

With this experiment, we aimed to characterize the cortical responses to fine-grained changes in the spectral pattern of vibrotactile textures (two different random noise vibrations matched in terms of average intensity, average spectral content and duration), and test the involvement of S1 by comparing these responses following stimulation of the hand and foot.

The spectrotemporal contrasts induced significant base responses (8 Hz and harmonics) and oddball responses (1.6 Hz and harmonics). When stimulating the right index finger, both responses were localized over contralateral parietal and frontal regions, compatible with the hand representation in S1. In contrast, when stimulating the foot sole, both responses were localized over central midline electrodes, consistent with the foot representation in S1 (Heid et al., 2020; Langdon et al., 2011; Moungou et al., 2016a; Snyder, 1992; Tobimatsu et al., 1999).

To further investigate the cortical origin of spectrotemporal contrast responses elicited by stimulation of the hand and foot, we implemented a simple approach to assess how closely their topographies matched -across all channels- the topographical distribution of the base response to hand and foot stimulation using the frequency–intensity contrast, used as a functional localizer of activity originating from the hand and foot representations within S1, respectively. The analysis showed that the topography of the oddball response to spectrotemporal contrasts delivered onto the hand matched more closely the S1 hand representation as compared with the S1 foot representation, while the opposite was observed when stimuli were delivered onto the foot. Taken together, and

without excluding a contribution of cortical areas outside S1, these results indicate an involvement of S1 in the processing of fine-grained contrasts in the pattern of complex vibrations such as those elicited during the tactile exploration of textures. Interestingly, despite their topography being highly similar, the base responses to the frequency/intensity sequences were overall lower than the base responses to the spectrotemporal sequences. While we did not expect such differences in the magnitude of activation, it is possible that these results are linked to the frequencies used for the standard and oddball stimuli in the frequency/intensity contrast condition. Indeed, seminal work has shown that the detection threshold of vibrotactile stimuli across different frequencies follows a U-shaped curve, being lowest at around 200 Hz (Mountcastle et al., 1972), corresponding to the frequency of the oddball stimulus used in the current experiment. Thus, it is possible that a stronger response to the oddball stimulus within the frequency/ intensity contrast condition led to a weakening of the response to the base stimuli. Furthermore, in the frequency/intensity contrast condition, the response at the fundamental frequency of 8 Hz was not significant. This is not necessarily surprising, as the sinusoidal periodic stimulation is not expected to elicit an EEG response that is sinusoidal, due to the non-linearity of the system. Instead, the response is expected to project onto a number of harmonics of the periodic repetition rate when analyzed in the frequency domain, with a distribution of amplitudes over these harmonics depending on the shape of the periodic response (Chemin et al., 2018; Lenc et al., 2024). Furthermore, in our experiment, the sharp ramps at the onset and at the offset of each tactile event likely generated strong onset and offset responses within rapidly adapting mechanoreceptors, which could partly explain the larger peak observed at 16 versus 8 Hz.

Interestingly, the somatotopical scalp topography of the oddball response to spectrotemporal contrasts was present across all harmonic frequencies, indicating

a contribution of S1 to both the slower and the faster EEG signals triggered by the oddball stimuli.

The standard and oddball stimuli constituting the spectrotemporal sequences were matched in terms of their average intensity and spectral content. However, they varied in terms of both their envelope and their spectral time course. A supplementary analysis was thus conducted to evaluate whether the observed oddball responses to the spectrotemporal sequences could have been driven solely by differences in envelope time course (Rossion et al., 2015). This analysis revealed that one of the spectrotemporal sequences exhibited a much stronger envelope dissimilarity than the other sequences, and that the oddball EEG response to that specific sequence was greater than the EEG responses to the other sequences, suggesting a contribution of envelope dissimilarity to the elicited EEG response. However, the analysis also showed that the oddball EEG response was present in each of the seven other spectrotemporal sequences, and that there was no significant relationship between envelope dissimilarity and the oddball EEG response across these seven sequences, indicating that the EEG response to the contrast was not solely driven by envelope dissimilarity. Such *a posteriori* exploration of the respective contributions of envelope versus spectrotemporal contrast across a limited number of sequences should be interpreted cautiously.

Future studies are thus necessary to further establish the specific features contributing to the spectrotemporal oddball response. One approach could be to employ sequences where standard stimuli would be a random sequence of different natural textures differing greatly in terms of their low-level properties such as intensity and frequency content, while the oddball stimulus would correspond to the same texture or texture category repeated throughout the

sequence— possibly also using scrambled versions of the stimuli (see De Keyser et al., 2018).

The magnitude of oddball responses to the spectrotemporal sequences when participants explicitly perceived the contrasts was not significantly different from the magnitude of oddball responses to the spectrotemporal sequences when the contrast was not perceived, suggesting that emergence of an oddball EEG response to the spectrotemporal contrasts did not require conscious perception of that contrast. Confirming that periodic oddball responses to fine-grained vibrational contrasts can occur in the absence of any explicit contrast perception will require further psychophysical studies. Indeed, in this experiment, participants were simply asked to report, at the end of each trial, whether they had perceived a contrast within the sequence, and no further controls such as sequences without oddball stimuli were implemented.

In conclusion, we show that minute and often unperceived variations in the spectrotemporal content and envelope of complex vibration patterns similar to those generated during the tactile exploration of textures generate a differential response within the contralateral S1. This finding indicates that fine-grained tactile texture discrimination involves or modulates S1 (or upstream subcortical structures relaying somatosensory input to S1). Most interestingly, distinguishing the oddball stimuli from the standard stimuli within the spectrotemporal sequences required to build a representation of the temporal pattern of vibrotactile stimuli (i.e., frequency content over time or intensity over time), indicating that S1 may have the ability to build such complex representations. Thus, similarly to the mechanisms underlying change-specific ERPs such as the P300 (Polich, 2007) or the mismatch negativity (Kekoni et al., 1997; Näätänen and Escera, 2000), over repeated presentation of the standard stimulus, a mental representation of the vibrotactile

texture may be formed and maintained at the level of S1. In turn, presentation of the oddball vibrotactile texture, whose spectrotemporal features differ from that of the standard stimulus and, hence, the formed mental representation, would elicit a differential S1 response.

By demonstrating that the frequency-tagging approach, in combination with a periodic oddball paradigm, can be used to capture cortical responses to fine-grained changes in the spectrotemporal content of complex vibrotactile stimuli, our results open new avenues to study how the somatosensory system processes natural textures during dynamic touch.

Supplementary Materials

Contribution of envelope dissimilarity to the spectrotemporal contrast EEG responses

First, we quantified the amplitude of the base and oddball EEG responses as described above (averaging across the same harmonics that were selected for the main analysis, and across channels using the weights from the S1 functional localizer constructed in the main analysis), but separately for each of the eight spectrotemporal sequences. We then carried out a linear regression analysis between the magnitude of the EEG responses to each spectrotemporal contrast and the index of envelope dissimilarity between the A and B stimuli, separately for each stimulation site. We hypothesized that if differences in envelope directly drove the oddball response, greater oddball responses would be observed for sequences exhibiting a stronger envelope dissimilarity.

An important feature of the stimulation envelope may be its attack segment. Therefore, the same analysis of envelope dissimilarity was performed considering only the first 50 ms of the A and B envelopes, to assess the potential contribution of envelope dissimilarity at the onsets of the A and B stimuli.

Analysis of the EEG responses to each individual spectrotemporal contrast revealed significant base and oddball responses for all eight sequences and for both stimulation sites (Supplementary Fig. 1).

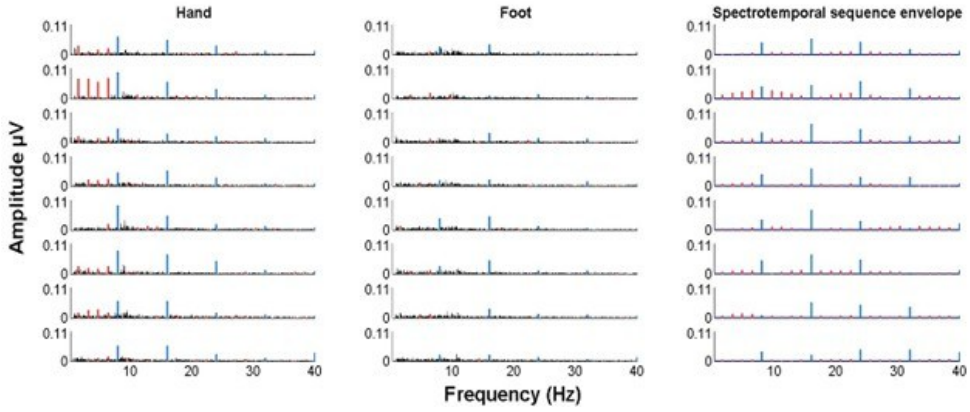

Supplementary Figure 1: Baseline-subtracted EEG frequency spectra of the responses to each spectrotemporal contrast sequence (1 to 8, top to bottom) for hand stimulation (left) and foot stimulation (middle). Harmonics with amplitude significantly higher than zero (t-test, right-tailed) are color-coded, with base responses depicted in blue, and oddball responses depicted in red. The right panel shows baseline-subtracted frequency spectra of the individual AAAAB sequence envelopes.

As shown in Supplementary Fig. 2, the envelopes of the A and B stimuli of the spectrotemporal sequence #2 exhibited a strong envelope dissimilarity as compared to the other sequences. When including this outlier sequence, the linear regression analysis showed a significant correlation between envelope dissimilarity and magnitude of the oddball EEG response for hand stimulation (R^2= 0.360, p= 0.007), and for foot stimulation (R^2= 0.049, p= 0.01). In contrast, no significant correlation was found when the spectrotemporal sequence #2 was excluded from the linear regression analysis (hand stimulation: R^2= 0.010, p= 0.271; foot stimulation: R^2= 0.003, p= 0.578).

Similarly, a significant correlation was found between envelope dissimilarity at the onset of the A and B stimuli and magnitude of the oddball EEG responses for hand stimulation

(R^2= 0.182; p<0.0001), but not for foot stimulation (R^2= 0.012; p= 0.200). When excluding spectrotemporal sequence #2, no significant correlation was found for either stimulation sites (hand: R^2= 0.0002; p= 0.872; foot: R^2= 0.007; p= 0.372).

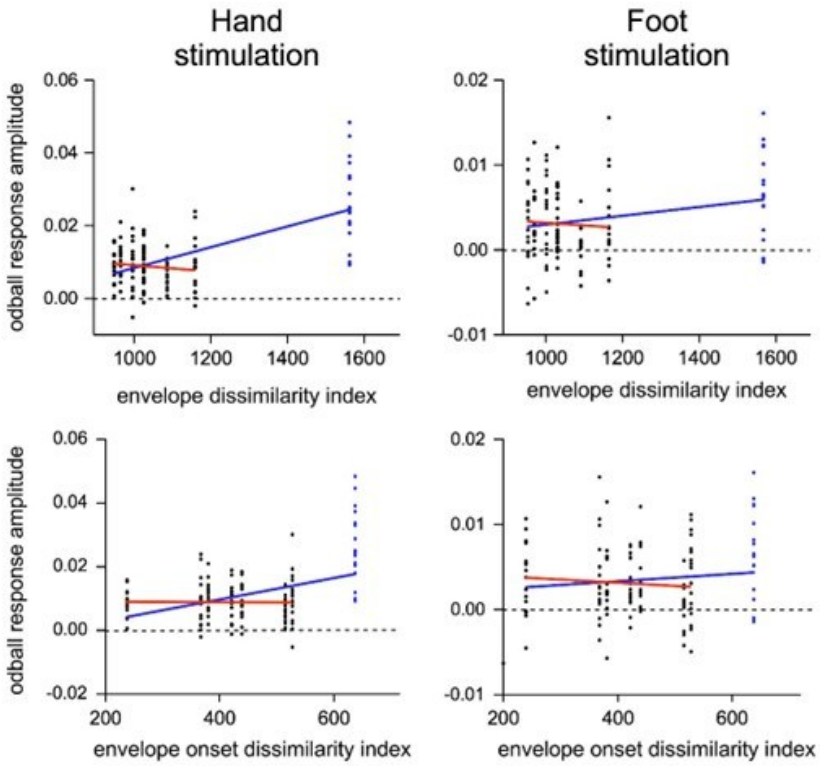

Supplementary Figure 2: Relationship between magnitude of the spectrotemporal oddball EEG responses and sequence envelope dissimilarity (top) and sequence envelope onset dissimilarity (bottom), following stimulation of the hand (left) and the foot (right). Individual dots represent single subject baseline-subtracted amplitudes, averaged across significant oddball harmonics (excluding corresponding base harmonics) and across channels, weighted according to their corresponding template. Linear regression analyses were performed including (red lines) or excluding (blue lines) spectrotemporal sequence #2 (blue dots).

Chapter 4: Investigating Somatosensory-Evoked Potentials in Conditions of Active touch.

Abstract

Exploratory movements are a key component of tactile sensing to extract haptic information from the external world. While much of the research in the somatosensory field has employed artificial tactile stimuli delivered in passive touch conditions, more recently, much interest has been put in the study of active, dynamic touch. An ecological study of tactile processing during active touch comes with several challenges, particularly with regard to electrophysiological techniques, such as scalp electroencephalography. Here, we report a novel experimental setup to record somatosensory evoked potentials in conditions of active, dynamic touch, where participants performed voluntary and minimally controlled exploratory finger-sliding movements against a surface to come into contact with an edged haptic stimulus. Our results showed that it is possible to record cortical responses to a physical, transient haptic stimulus. The pattern of responses revealed early-latency components with a contralateral topography, consistent with activity originating from the primary somatosensory cortex, followed by later components displaying a more central/bilateral pattern of activity, consistent with activity originating from higher-order areas. In summary, our results reveal the feasibility of recording time-locked cortical responses to tactile stimuli in conditions of active touch, with important implications to study somatosensory processing related to active tactile sensing.

Keywords—electroencephalography, somatosensory-evoked potentials, active touch

1. Introduction

Touch is often a dynamic process, and we actively perform exploratory movements to extract haptic information from the external world: ‘’Is this fabric rough or smooth?’; ‘’Is there a bump or indentation on this surface?’.

Much of the work investigating the sense of touch has employed tactile stimulations delivered in conditions of passive touch, especially when exploring the cortical processing of somatosensory inputs using scalp electroencephalography (EEG) (e.g., Guidotti et al., 2023; Hämäläinen et al., 1990; Schubert et al., 2006). Although passive touch can be both static and dynamic, it is inherently different from active touch. In active touch conditions, the subject performs voluntary, dynamic movements to explore the texture or shape being presented to them (Gibson, 1962). As such, active touch is a complex process which involves integration of somatosensory and proprioceptive inputs, as well as sensorimotor control (Simões-Franklin et al., 2011).

In passive static touch, no movement of the subject’s limbs is required to perceive the tactile stimulus, which can take the form of a pressure, vibrotactile, or electrical stimulation applied onto an area of the subject’s skin. In passive dynamic touch, a haptic stimulus, such as a piece of fabric, can be moved against the participant’s skin (e.g. Moungou et al., 2016b, 2016a), or the movement of the subject’s limb can be externally guided, for example using a robot. Thus, while both active and passive touch involve mechanical deformation of the skin, in passive touch conditions either the stimulus is displaced against the skin, or the subject’s limb is passively displaced against the stimulus, while the key feature of active touch is the voluntary component associated with displacement of the skin against a surface. Crucially, active touch is characterized by a purposeful act aimed at

optimally extracting haptic information from the external world (Gibson, 1962; Prescott et al., 2011).

Event-related brain potentials (ERPs) represent discrete waveforms of cortical activity recorded using EEG following the onset of a sensory stimulus. ERPs are classified based on the polarity of the signal (P= positive; N= negative), and the latency at which they occur following stimulation onset (e.g., the P300 is a positive defection occurring around 300 ms following the onset of stimulation) (Nelson and McCleery, 2008; Sutton et al., 1965; Vaughan, 1982). Several waveforms representing somatosensory-evoked potentials (SEPs) have been described, in conditions of passive touch. Among these, short-latency SEPs are often recorded in paradigms implementing direct transcutaneous electrical stimulation of a peripheral nerve at the level of the wrist or of the fingertip skin, such as the N20/P20 complex elicited by median nerve stimulation (Deiber et al., 1986; Desmedt and Bourguet, 1985; Shaw, 1986). These early responses have been shown to be localized over contralateral parietal and central scalp electrodes, indicating involvement of the hand representation within the primary somatosensory cortex (S1) (Allison et al., 1991). Mid-latency SEPs have also been recorded in response to vibrotactile stimuli (Dionne et al., 2013; Eimer and Forster, 2003). These include the N30, P50, N70, and P100 waveforms (Allison et al., 1992). The first three peaks have been shown to be stronger and to display shorter latencies at contralateral compared to ipsilateral electrodes, suggesting that they also represent activity originating at least partly from S1 (Allison et al., 1992). The P100, on the other hand, is characterized by bilateral activation, suggesting that it might predominantly reflect activity originating from higher somatosensory areas, such as (bilateral) activation of the secondary somatosensory cortex (S2) and/or multimodal areas. Thus, somatosensory areas appear to be sequentially activated during the processing of somatosensory stimuli (Hämäläinen et al., 1990).

To date, no studies have characterized SEPs in conditions of active, dynamic touch, when participants perform voluntary exploratory finger-sliding movements to generate the tactile stimulation. Several technical challenges arise when investigating SEPs in ecological conditions of active, dynamic touch. Indeed, in experimental designs involving active touch, the experimenter has little to no control over exactly when and how the stimulation is delivered to the subjects: it is their free, dynamic movements that will lead them to encounter the haptic stimulus. Importantly, since the timing of stimulation is not controlled by the experimenter, time-locking the exact moment at which the stimulus is delivered (i.e. encountered by the subject performing the movement), which represents a crucial aspect of EEG experiments, is a difficult endeavor.

In this study, we aimed to test the feasibility of recording SEPs when participants actively performed sliding movements on a flat surface using the index finger of their dominant hand and encountered physical edged tactile stimuli. Investigating cortical responses to transient, edged tactile stimuli in such conditions is particularly relevant to the study of processing and perception of planar shapes. When exploring planar shapes, we typically employ exploration strategies such as contour following with oscillating motion, where the finger crosses the contours of the shape while remaining in their proximity via small back and forth movements, or contour scanning, where the finger crosses the contours of the shape via relatively large movements reaching further away from the shape's boundaries (Lederman and Klatzky, 1993; Mizrachi et al., 2022), similarly to the sliding movements that participants performed in our study to encounter and to cross the tactile stimuli. Here, we describe the experimental setup, methodology and EEG analysis steps, and characterize the main waveforms recorded using our design. We hope that our novel methodological approach and experimental setup will help

fellow haptics researchers develop and design new approaches for the study of the cortical processing of tactile stimuli in ecological active touch conditions.

2. Methods

2.1. Participants

Seventeen healthy participants (7 females, 10 males; aged 22 to 47; 4 left-handed) with no self-reported history of neurological, psychiatric, or motor disorders volunteered to take part in the experiment. All participants gave written informed consent prior to participation. Data from one participant was excluded due to technical issues that led to very low signal-to-noise ratio of the recorded signals. Data collection had to be discontinued from another participant due to technical issues with the experimental setup. The final sample thus included data from a total of fifteen participants. The study received ethical approval from the Saint-Luc - UCLouvain ethics committee (approval number: 2023/11AVR/177).

2.2. Experimental Setup

The haptic stimulus was a small 3D-printed trapezoidal prism (3.2 mm x 14 mm) strip of plastic mounted on the upper face of a wooden parallelepiped (145.6 mm x 25 mm x 25 mm) via 10 mm rods, 90.5 mm from the left edge. The height of the tactile stimulus was 0.6 mm (Figure 1b). To monitor finger position and generate trigger events in the EEG recording upon participants' reaching the haptic stimulus with their exploring finger, a parallel-plane laser light-based position tracking sensor (Neonode NNAMC1220PCEV (122 mm), Neonode Inc., Sweden, Figure 1a) was placed at 25 mm distance behind the wooden platform. This tracking device generated a continuous 200 Hz stream of values depending on the position of the finger onto the plate. Using as threshold the value of the position tracking sensor

corresponding to when the finger was positioned over the plastic edge, the position of the finger was monitored during each trial to generate a trigger marking when the finger slided above the plastic edge.

To more precisely identify when the finger encountered the plastic edge, an accelerometer (amplifier Nexus 2696A-0S4, tri-axial accelerometer type 4524-B, Brüel & Kjaer, Denmark) was attached via double-sided tape to the nail of the index finger that participants used to perform the exploratory movements. To stabilize the accelerometer sensor, participants wore two plastic elastic ring bands around their index finger, to ensure that the wire attached to the sensor remained in place. The accelerometer was used to record the vibrations generated when the sliding finger encountered the edged stimulus

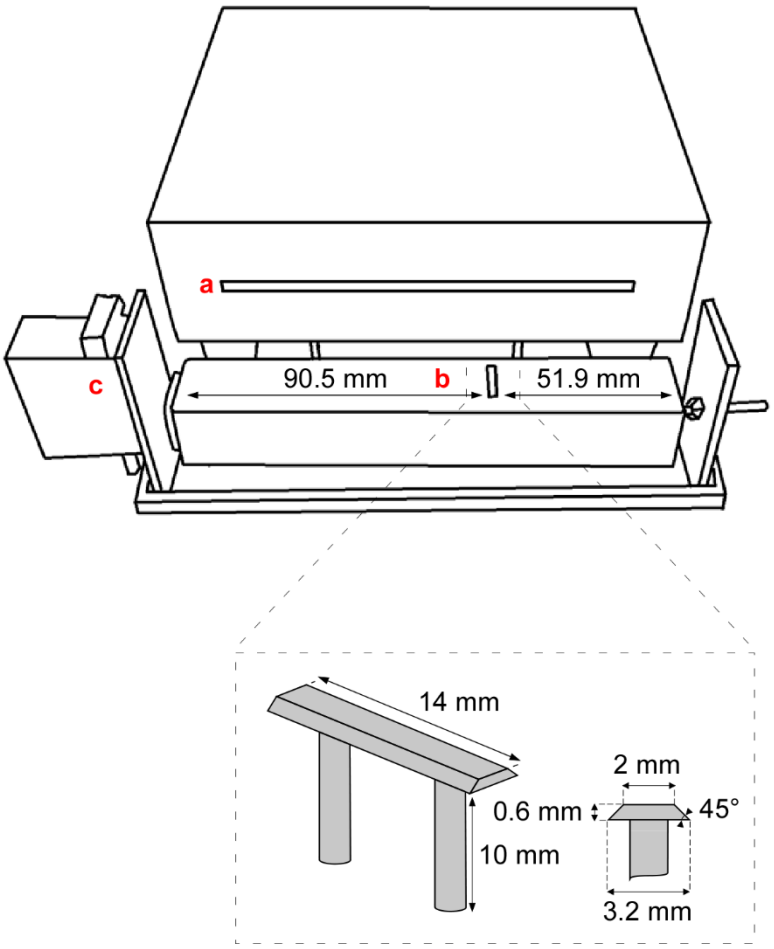

Figure 1. Experimental setup. The wooden platform onto which participants performed fingertip sliding strokes was fixed in front of a position sensor (a) used to send trigger events to the EEG recording system when the exploring finger reached the location of the haptic stimulus (b), which was mounted onto one face of the wooden platform via 10mm rods. The wooden platform was connected to a DC stepper motor (c), which allows to rotate the platform to display 3 faces, where additional stimuli at different locations may be fixed. For this proof-of-concept study, only one of the faces and one stimulus location was used. The section below shows a detailed view of the tactile stimulus and its dimensions.

2.3. Procedure

Participants were asked to use the index fingertip of their dominant hand to perform horizontal left-to-right strokes on the platform. To avoid any visual feedback, the platform was placed inside a wooden box presenting an opening at the front where participants could place their hand to perform the exploratory movements. The location of the platform inside the box was adjusted so that both the platform and the participant's hand were outside of the participants' field of vision. To avoid any auditory feedback, participants wore earphones through which white noise was played. Two participants were not presented with white noise. However, the auditory feedback from the finger encountering the haptic stimulus was very faint (as it was not produced by an external motor or stimulation device), and these participants never reported hearing a sound associated with the change in friction upon questioning.

Participants were instructed to perform the strokes maintaining a relatively stable but natural exploration velocity, avoiding very fast or very slow strokes. After each stroke, participants were instructed to remove their hand from the box, and to wait for a signal from the experimenter before re-contacting the platform and initiating the next stroke. When re-contacting the platform, participants were allowed to look at their hand to properly position their exploring finger at the starting position. To ensure a baseline period of minimal accelerometer signal variations, participants were instructed to wait about a second after contacting the platform prior to initiating the next stroke. The number of trials was set to 150, divided in three blocks of 50.

Pilot tests had revealed a delay between the trigger event sent via the position sensor and the actual contact onset of the finger with the tactile stimuli which was tracked via the accelerometer recording. This delay appeared to be variable and

dependent on the velocity of exploration. For this reason, the accelerometer recording was used to create new trigger events marking the precise onset of stimulation for each participant, as described in the next section.

2.4. Alignment of Trigger Events with Accelerometer Recordings

Within the vertical (z-axis) accelerometer recordings, we expected to see a transient change in signal amplitude occurring when the fingertip pad of the exploring finger contacted the edge of the rectangular stimulus. In most trials, a clear onset could be observed upon visual inspection (Figure 2, top left). For some trials, the accelerometer signal was noisier, and we could not observe clear contact onset (Figure 2, top right). Figure 2 (bottom panel) shows the rectified accelerometer signals averaged across all trials included in the EEG analysis, illustrating how, on average, the 0 ms time point following alignment of trigger events corresponded to a sharp change within the accelerometer recordings.

To identify the contact onset within the z-axis accelerometer signals, a 200 ms baseline was defined upon visual inspection of each individual trial for each participant. The chosen start time of the baseline was defined depending on the noisiness of the signal in the 1000 ms prior to the position sensor trigger event, as well as the delay between the position sensor trigger event and the change in accelerometer signal corresponding to the time of contact of the finger with the haptic stimulus. By default, the baseline started at -400 ms relative to the position sensor trigger event, and was adjusted on a trial-by-trial basis for each participant, with a starting time ranging from -800 to -250 ms prior to position sensor trigger event. The time of the first peak in the accelerometer recording (corresponding to the onset of contact between the finger and the haptic stimulus) was identified as the time in which the absolute amplitude of the signal exceeded x times the standard deviation of the baseline (x*SD threshold). The default value of x was set

to 3. Due to the high trial-by-trial variability of the accelerometer signals, the value of x value was adjusted on a trial-by-trial basis using values ranging from 3 to 8, as follows. The accelerometer signal was plotted, with the accelerometer-derived trigger event displayed as a vertical line. If, upon visual inspection, the new trigger event did not correspond to a clear change in the accelerometer amplitude, the baseline and/or x*SD threshold parameters were adjusted (Figure 2). Both the baseline and the x*SD threshold were adjusted as needed, due to trial-by-trial variability of signal noisiness. The corresponding time points were then added to the EEG recording file as new trigger events, and subsequently used to segment the EEG signals for further analysis.

Lastly, the accelerometer signals were segmented between -500 to +1000 ms relative to the new event trigger. Next, each epoch was visually inspected to determine whether the accelerometer signals allowed determination of the new trigger events. When participants performed the exploring movements, they would occasionally hit the metal support located at the end of the platform. This would not only generate a strong peak in the accelerometer recording (visible in Figure 2, top panels), but also potentially a subsequent somatosensory response, as participants would receive a rather strong tactile input by the sudden contact with the metal support on the side of their fingertip, which could therefore translate to an additional response in the EEG recording. For this reason, trials were excluded whenever the time interval between the event trigger and the end of the movement was less than 200 ms.

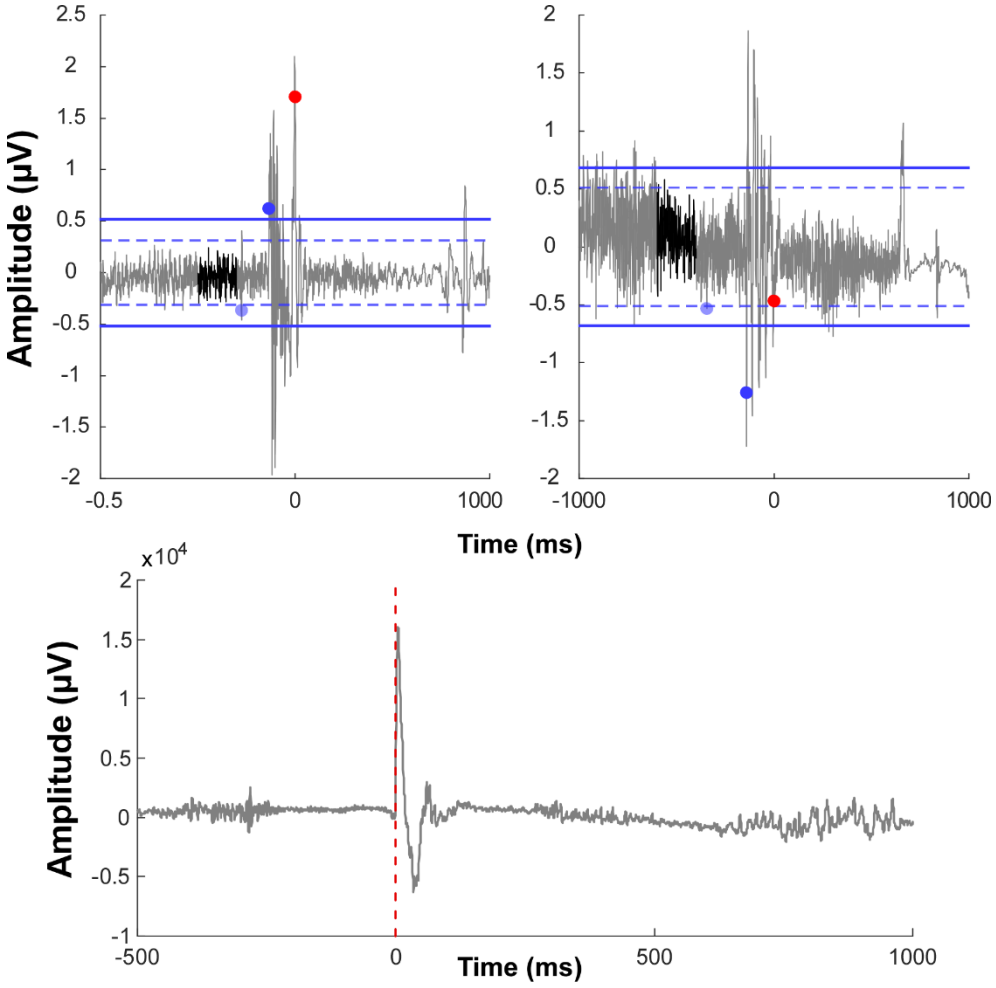

Figure 2. Determination of contact onsets from the accelerometer z-axis displacement recording. The top left panel shows the accelerometer signal recorded in a trial displaying clear onset/offset peaks. The top right panel shows a recording with a lower SNR. The red dots represent the trigger events generated by the position sensor. Note that the accelerometer signals show that the actual onset of stimulation due to fingertip contact with the plastic edge preceded that trigger, justifying the use of the accelerometer signal to mark the actual stimulation onsets. The chosen baseline interval is plotted in black. Horizontal dotted blue lines represent the default +/- 3*SD threshold, Light blue dots represent the time of contact onset found using this default threshold. Horizontal blue lines represent the +/- x*SD threshold selected to define the time of contact onset. Dark blue dots represent the accelerometer-derived time of contact onset using this adjusted threshold. The bottom panel shows

the group-average of rectified accelerometer signals, aligned relative to the accelerometer-derived triggers (dotted red line).

2.5. EEG Recordings

Participants were instructed to relax, avoid moving their head and body as much as possible, and fixate their gaze on a fixation cross placed in front of them. An EEG recording system (ActiveTwo, Biosemi, the Netherlands) and a 64 Ag-AgCl electrode cap with pre-amplified electrodes (Biosemi, the Netherlands) was used for EEG recordings. The cap was placed on the participants' scalp according to the International 10/10 system. Sample rate was set at 2048 Hz and impedances (electrode offsets) were kept below 20 mV.

2.6. EEG Preprocessing

First, the EEG signals were re-referenced to the average of all scalp electrodes. Next, a 0.1 Hz filter (4th order Butterworth filter) was applied to the continuous EEG signals. This type of filter is typically used to characterize early, transient components (<100 ms) (Cruccu et al., 2008; M. Rossini et al., 1981). However, the noisiness of the resulting waveforms and the fact that, upon visual inspection, we did not observe any distinct transient waveforms motivated us to instead apply a bandpass filter between 0.1 Hz and 40 Hz (4th order Butterworth filter), which is commonly used for the recording of SEPs using different types of stimulation when the focus is not specifically on short-latency components (Guidotti et al., 2023; Hämäläinen et al., 1990; Miller et al., 2019). This filtering window, however, revealed strong slow drifts in the EEG signals, which were likely due to expectation of the stimulus during the sliding movements. Given the presence such drifts in the signals, the EEG signals were also bandpass-filtered between 3Hz and 40Hz (Figure 3).

The following pre-processing steps were applied to the 0.1 Hz highpass-only, and to the 0.1 Hz – 40 Hz and the 3 Hz – 40 Hz filtered signals. An additional notch FFT filter (50 Hz, 100 Hz, 150 Hz, 200 Hz; notch width: 2 Hz; slope cutoff width: 2 Hz) was applied. The continuous EEG signals were then segmented from –200 ms to +600 ms relative to the accelerometer-based onset of contact with the haptic stimulus. A DC removal and linear detrend was then applied to the epoched signals. Ocular artifacts (eye blinks and lateral eye movements) were removed following an independent component analysis (ICA) (calculated from the 0.1 Hz – 40 Hz filtered signals). This led to the removal of a total 27 ICs across 13 participants (mean= 1.8; SD= 1.08). To remove further artifacts, epochs were excluded when the signal exceeded 100 μV in the interval between –200 ms and +400 ms relative to the accelerometer-based onset of contact with the haptic stimulus. A baseline correction (-200 ms to 0 ms) was then applied to the epoched data. For left-handed participants, left and right electrodes were flipped. Lastly, trials were averaged in the time domain and grand-averaged across participants for visualization.

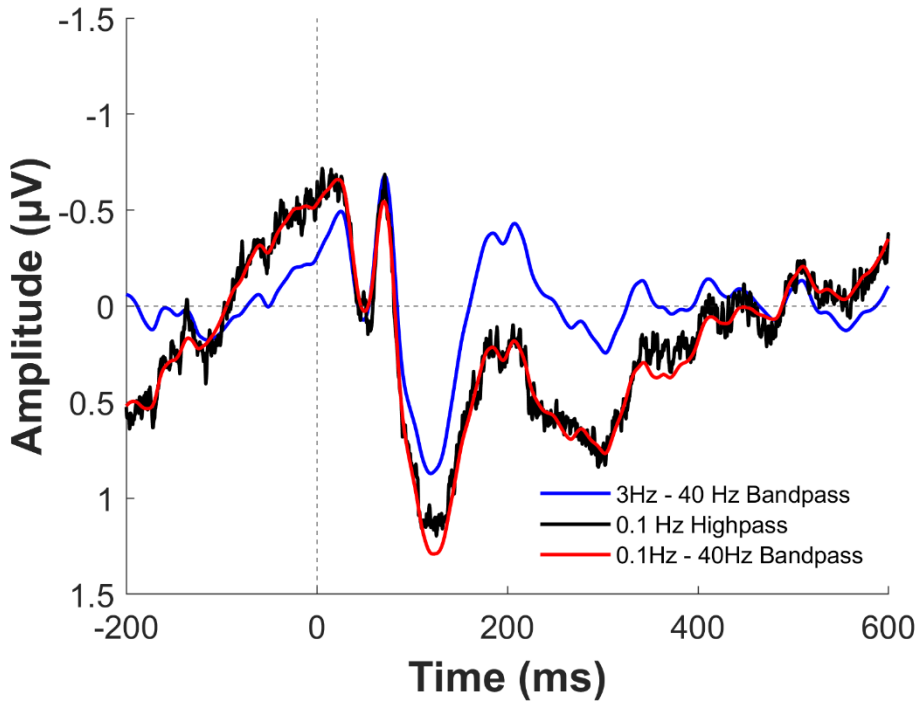

Figure 3. Signal filtering procedure. The three lines represent group-level average of activity at electrode CP3 preprocessed using a highpass only and two different highpass cutoff frequencies in the bandpass filter applied to the continuous EEG recordings. The signal noisiness was high when only a highpass filter was applied to the data (black trace). When the cutoff highpass frequency was set to 0.1Hz, a strong drift was visible in the pre-stimulus interval (red trace), which was attenuated in the 3-Hz high-passed signals (blue trace).

2.7. Assessment of Significant Responses

To assess the presence of significant ERP waveforms, a cluster-based permutation test against 0 was performed as follows, using the 3 Hz – 40 Hz filtered signals. Individual participants' trials were averaged in the time domain. Next, a non-parametric point-by-point cluster-based permutation test was performed to identify, at each channel, time-intervals of the averaged ERP waveforms that deviated significantly from zero across participants (Maris and Oostenveld, 2007;

van den Broeke et al., 2015). The approach assumes that stimulus-evoked amplitude changes in the signal will tend to occur over contiguous time points (Groppe et al., 2011). First, the ERP waveforms were compared using a point-by-point t-test against zero. Then, clusters of contiguous time points above the critical t-value corresponding to a p-value of 0.05 were identified, and an estimate of the magnitude of each cluster was computed by summing the t-values constituting each cluster. Random permutation testing (2000 permutations) was then used to obtain a reference distribution of maximum cluster magnitude. As cluster magnitudes could be negative or positive depending on the polarity of the signals, clusters in the observed data were regarded as significant when their magnitude was either above the 97.5th percentile or below the 2.5th percentiles (corresponding to a 2-sided test).

2.8. Differences across Contralateral and Ipsilateral Electrodes

To assess whether the ERP components exhibited hemispheric lateralization, a paired cluster-based permutation test was performed as described in Section 2.7, comparing the signals recorded at the following electrode pairs: C3 vs. C4 and CP3 vs. CP4.

3. Results

For nine participants, a few trigger events were missing due to faulty tracking of the position sensor. Three participants performed an extra trial due to an error by the experimenter in tracking the number of performed trials. One participant reported looking at their hand during the first seventeen trials. These trials were excluded and the participant performed seventeen extra trials at the end of the experiment. One participant performed an extra block at the end of the experiment, as he performed very rapid movements in the second block. However,

since visual inspection of the signals showed that the velocity they used was acceptable, the trials from the extra block were not included in the analysis. A total of 92 epochs across 13 participants were excluded from the dataset. Of these, 35 represented extra triggers accidentally sent by the position sensor when participants displaced their finger between trials, or extra triggers sent by position sensor within the same trials. The remaining 57 epochs represented actual trials that were excluded (among 12 participants) due to unclear determination of the accelerometer-derived trigger because of noisy signals or because participants performed excessively rapid exploration movements. Among real trials, the accelerometer signals allowed marking contact onsets in most cases (mean= 97.4%, SD= 2.5%). In total, 2152 trials were included in the final dataset for further processing (average per participant= 143.5, SD= 5.9). Following EEG artifact rejection, a total of 23 trials were removed across 5 participants in the 0.1 Hz – 40 Hz filtered signals, and a total of 7 trials were removed across 3 participants in the 3 Hz – 40 Hz filtered signals.

3.1. SEP Responses Across Pre-Selected Electrodes and Topographical Distribution of Activity Over Time

Based on previous studies characterizing SEPs in static touch conditions, we expected early-latency responses originating from the contralateral S1, and later responses having a central topographic distribution. Therefore, here we report the results across six pre-selected electrodes: C3 and CP3 (contralateral to the stimulated finger); Fz and Cz (fronto-central); C4 and CP4 (ipsilateral to the stimulated finger) (3 Hz – 40 Hz bandpass-filtered signals).

Visual inspection of the responses between -200 ms and +400 ms relative to the accelerometer-based event triggers revealed SEP responses across contralateral, fronto-central as well as ipsilateral electrodes. Visual inspection of

the topographies over time between 0 and 240 ms revealed that, earlier components (before ~120 ms) were characterized by a clear lateralization, contralateral to the exploring finger. Later, components (between ~120-220 ms) appeared to be characterized by a more central/bilateral scalp topography (Figure 4).

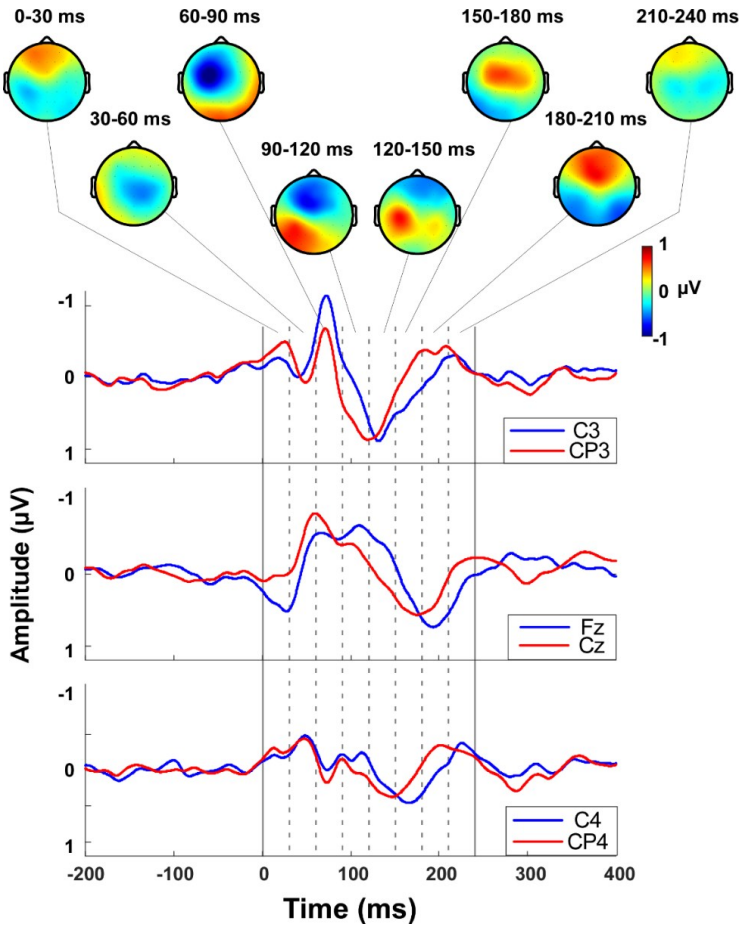

Figure 4. Group-level averaged topographical maps and time course of the signals recorded at contralateral (C3, CP3), fronto-central (Fz, Cz), and ipsilateral (C4, CP4) electrodes. Each topographical map represents scalp activity within 30 ms intervals between 0 and 240 ms (top panel). The bottom panels represent EEG responses in the time domain. Dashed lines mark the 30 ms intervals.

3.2. Assessment of Significant Responses

The cluster-based permutation test revealed several time-intervals where activity was significantly different from 0 ($p<0.05$) at contralateral (C3, CP3), fronto-central (Fz, Cz), and ipsilateral (C4, CP4) electrodes (Figure 5).

The onset, offset, peak, and cluster statistics (p-values) of the time intervals where activity was significantly different from 0 are reported in TABLE 1.

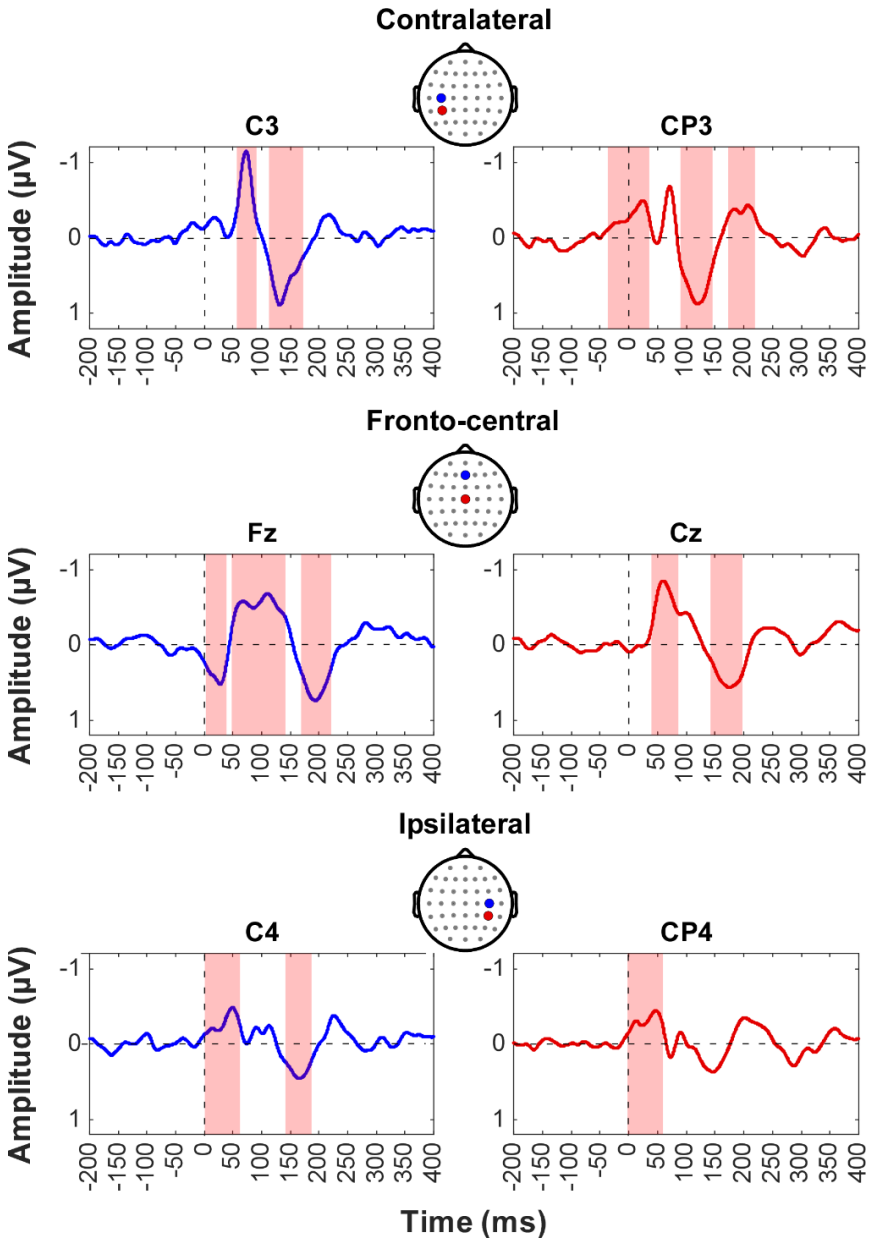

Figure 5. Group-level averaged waveforms across contralateral (C3, CP3), fronto-central (Fz, Cz), and ipsilateral (C4, CP4) electrodes. Shaded red areas represent time intervals of activity that were significantly different from 0 (point-by-point cluster-based permutation test; $p<0.05$).

TABLE 1. One-sample cluster-based permutation test statistics across contralateral (C3, CP3), fronto-central (Fz, Cz), and ipsilateral (C4, CP4) electrodes.

Electrode	Onset (ms)	Offset (ms)	Peak (ms)	Cluster p-value
C3	57	91	72	0.008
	113	172	131	0.002
CP3	-35	36	25	<0.001
	90	146	119	0.003
	173	221	207	0.029
Fz	2	39	27	0.021
	48	141	109	<0.001
	169	221	193	0.002
Cz	39	86	59	<0.001
	142	199	174	0.002
C4	0	62	48	0.002
	139	186	165	0.006
CP4	-2	59	47	<0.001

3.3. Lateralization of SEPs

Cluster-based permutation paired tests revealed time-intervals where activity was significantly different between contralateral and ipsilateral electrode pairs (C3 vs. C4; CP3 vs. CP4) (Figure 6).

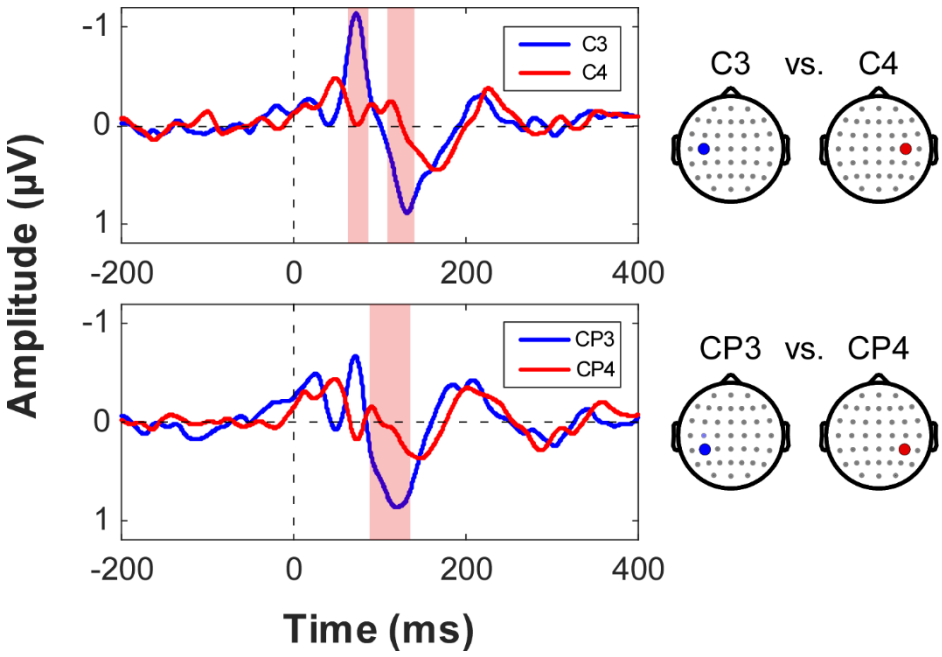

Figure 6. Comparison of group-level averaged waveforms between pairs of contralateral and ipsilateral electrodes (C3 vs. C4; CP3 vs. CP4). Shaded red areas represent time intervals where activity differed significantly between electrode pairs ($p<0.05$).

The onset, offset, and cluster statistics (p-values) of the time intervals that differed significantly between ipsilateral and contralateral electrode pairs are reported in TABLE 2.

TABLE 2. Paired-sample cluster-based permutation test statistics between pairs of contralateral and ipsilateral electrodes (C3 vs. C4; CP3 vs. CP4).

Electrode comparison	Onset (ms)	Offset (ms)	Cluster p-value
C3 vs. C4	62	86	0.020
	108	140	0.019
CP3 vs. CP4	88	135	0.002

4. Discussion

The current experiment aimed to record, for the first time, SEPs elicited in conditions of active, dynamic touch, in response to physical edged haptic stimuli. In recent years, research in the field of haptics and tactile perception has seen a growing interest in the study of tactile sensing in conditions of active, voluntary dynamic touch (e.g., Brahimaj et al., 2023; Casado-Palacios et al., 2023; Eldeeb et al., 2020; Henderson et al., 2023, 2022; Moungou et al., 2016b). However, the cortical responses to haptic stimuli delivered in conditions of active dynamic touch remain unknown, possibly due to the technical challenges associated with measuring such responses while participants perform voluntary movements. Perhaps the most important challenge for recording ERPs in such conditions is the difficulty of time-locking responses to the actual onset of the mechanosensory stimulation produced by the subjects' free movements. Here, to overcome this challenge, we developed a novel experimental setup that allowed us to align EEG responses to the moment at which the subject's fingertip encountered the physical edged haptic stimulus. Our analysis revealed that our experimental setup successfully allowed us to identify the onset of stimulation and thereby record SEP components, with a topographical sequence consistent with hierarchical

somatosensory processing, starting within the hand representation of the contralateral S1, and then progressing towards bilateral responses possibly originating from S2 and/or multimodal areas (Iwamura, 1998; Whitehead et al., 2019).

The earliest component we identified was a negative deflection appearing at 25 ms at contralateral centro-parietal electrode CP3. The scalp distribution of this early negativity resembled the N20 component, one of the earliest SEPs that can be measured using scalp EEG, which reflects early stages of stimulus processing within S1 (Allison et al., 1991). This component is characterized by a dipolar configuration, with a concurrent positivity observed at frontal electrodes (Deiber et al., 1986; Desmedt et al., 1987), which is consistent with the topography we observed at this latency, as we found a concomitant significant positivity at frontal electrode Fz. However, the N20 component is typically recorded in response to electrical stimuli generating a highly synchronized afferent volley. Furthermore, the latency of the components we identified must be interpreted cautiously as mechanosensory stimulation may have initiated before the accelerometer-derived trigger. Thus, despite similarities in latency and scalp distribution, it is premature to interpret the early negativity we observed in our study as an equivalent of the somatosensory N20 observed after transcutaneous electrical stimulation of the median nerve. Nevertheless, the latency and topography of the response clearly indicates that it reflects early stages of somatosensory processing originating primarily from the hand representation of the contralateral S1.

The second component we recorded was a negativity appearing at 72 ms at contralateral electrode C3. This deflection displayed a similar latency and scalp topography as the somatosensory N70 component, which is typically localized around central and posterior contralateral electrodes (Hämäläinen et al., 1990) and

is thought to also originate from the contralateral S1 (Allison et al., 1992). Unlike the N20, the N70 component has also been reported in response to mechanical stimulation (Eimer and Forster, 2003; Guidotti et al., 2023). At this time interval, we also observed a significant lateralization when comparing the signals recorded at electrodes C3 and C4, further suggesting that this peak is compatible with a mid-latency SEP whose activity likely originates from S1.

Next, we observed a central bilateral positivity, peaking at 119 ms at CP3 and at 131 ms at C3. Positive deflections at this latency are often reported as the somatosensory P100, which is associated with explicit perception of somatosensory stimulation (Schubert et al., 2006). This component is thought to originate within S2 bilaterally and to be associated with a bilateral pattern of scalp distribution (Forss et al., 1996; Hogendoorn et al., 2015). Compared to what we observed, the P100 is usually reported at shorter latencies in response to both electrical/nerve (80-110 ms) (Hogendoorn et al., 2015; Miller et al., 2019) and single slow, large amplitude mechanical pulse stimulation (97 +/- 3.6 ms) (Hämäläinen et al., 1990), although some studies involving mechanical finger stimulation have reported windows between 100 and 125 ms (Eimer and Forster, 2003), which is closer to the latency we observed in the current study. However, as discussed for the earlier components, given the novelty of our stimulation paradigm, which involved dynamically self-generated somatosensory inputs, whose exact duration and intensity depended on the nature of participants' free exploration strategy (such as the pressure they applied on the platform and the speed with which they explored it) the exact latencies of SEPs we measured should be interpreted cautiously, as discussed below.

Furthermore, when assessing lateralization of the SEP waveforms we recorded, we did find a statistically significant difference between both pairs of

contralateral and ipsilateral electrodes (C3 vs. C4; CP3 vs. CP4), suggesting a contribution of activity originating from the primary somatosensory cortex at these later latencies.

At fronto-central scalp electrodes, we measured a negativity peaking at 109 ms at Fz and at 59 ms at Cz, followed by a positivity peaking at 174 ms at Cz and at 193 ms at Fz. This is consistent with the N1/P2 component, or the vertex potential, which has been reported in response to both innocuous mechanical and painful somatosensory stimulation, as well as auditory stimulation (Guidotti et al., 2023; Mouraux and Iannetti, 2009), and is thought to be an index of higher-level stimulus processing, mainly associated with the saliency of the stimulus irrespective of modality (Mouraux and Iannetti, 2009).

The temporal evolution of topographical distribution of activity revealed that, for earlier components, responses were strongly lateralized over the contralateral scalp hemisphere, consistent with early stages of somatosensory processing mainly occurring within S1. After ∼120 ms, responses were characterized by a central and bilateral scalp distribution, consistent with activity originating from higher cortical areas, such as S2. These results are consistent with sequential activation of somatosensory areas (Hämäläinen et al., 1990), and resemble previous reports investigating SEPs in conditions of passive touch that used mechanical tactile stimulation of different sites on the hand (Guidotti et al., 2023). However, the exact latencies we report are less consistent with such previous reports. Our stimuli differ from phasic short-lasting electrical, mechanical, or vibrotactile stimuli employed in passive touch paradigms, since the somatosensory input was dynamically self-generated by participants in our study. The skin is an elastic organ, and during sliding complex spatiotemporal patterns of skin deformation and strain occur, which in turn give rise to complex patterns of

mechanoreceptor activation (Delhaye et al., 2016). Importantly, it has been shown that fingertip strains vary with the normal force applied against the fingertip as well as with the velocity with which the stimulus (a flat glass plate) was displaced against the fingertip (Delhaye et al., 2016). Furthermore, scanning speed has been shown to affect vibrations elicited at the fingertip during texture exploration, which would also in turn affect responses of mechanoreceptive afferents (Greenspon et al., 2020). Importantly, the movements performed by subjects in our study were minimally controlled. No specific constraints were imposed on subjects, besides instructions to avoid very fast or very slow movements. Thus, it is likely that the pattern and magnitude of mechanoreceptor activation self- generated by participants in our experiment was influenced by the pressure used by subjects when sliding their finger on the platform, as well as their speed of exploration. Such variations are not only to be expected between participants, but some variability is also likely to occur on a trial-by-trial basis within participants. Thus, compared to passive touch designs, we can expect more variability in the amplitude as well as the latency of the recorded SEPs. To address such questions, future efforts should be made to characterize the exact dynamics of fingertip deformation during sliding and contact with a physical edged tactile stimulus, for example using high-speed cameras (Doumont et al., 2025), and subsequently using microneurography and modeling approaches to elucidate the exact nature of afferent responses during such conditions.

One potential limitation of our stimulation setup lies in the determination of contact onset from the accelerometer z-axis recordings. While we defined contact onsets as the first time point associated with a sharp change in accelerometer signal, it is possible that contact of the finger with the edge and hence onset of mechanosensory stimulation had already occurred some milliseconds before the accelerometer-derived trigger. Thus, it is possible that a

small delay was still present in the event triggers we defined *a posteriori*, thus leading to shorter SEP latencies. Furthermore, it is also possible that the tactile input was strongest when the pulp of the fingertip was in full contact with the tactile stimulus, thus leading to longer recorded SEP latencies. For this reason, as discussed above, the exact latencies reported in this study have to be cautiously interpreted. Nevertheless, the overall pattern and cortical distribution of responses we observed is consistent with well-characterized SEP components triggered, for example, by transcutaneous electrical nerve stimulation. To obtain more robust and reproducible results on the exact timing of SEPs in conditions of active, dynamic touch, future efforts should be made into assessing the exact dynamics of finger displacement during active sliding movements to determine the most appropriate method to define true contact onset of the exploring fingertip with the haptic stimuli. During pilot experiments, unsuccessful attempts were made to assess true contact onset by measuring the impedance between the finger and the edge printed using electrically-conductive plastic.

Our results have important implications to address questions in the field of active tactile sensing and processing. For instance, it is widely known that cortical responses to somatosensory stimuli are suppressed or reduced during voluntary movement, via a mechanism known as movement-related somatosensory gating (Chapman, 1994; Rossini et al., 1999). However, in most studies reporting such an effect, the active movements were unrelated to the concomitantly delivered tactile stimulation. Early work on primates has in fact shown that, when movements are necessary to perceive the somatosensory stimuli, activity in S1 neurons having receptive fields associated with the fingertip performing the exploratory movements is enhanced, rather than suppressed. Specifically, the proportion of neurons showing enhanced activity increases along the hierarchical rostral-to-caudal sequential processing within S1, with increasing activation going from area

3b, to area 1, to area 2. An opposite pattern of modulation is instead observed for neurons with receptive fields outside of the digit coming into contact with the tactile stimuli (Ageranioti-Bélanger and Chapman, 1992). Our setup could help further investigate movement-related somatosensory gating in humans by implementing matched active and passive dynamic touch conditions, as done by Moungou et al. (2016b).

A key issue to consider is that, in active touch conditions, it is difficult to disentangle motor signals from purely tactile signals, and that, in such conditions, motor-related activity may reduce the signal-to-noise ratio of the recorded responses. Nevertheless, previous studies have been able to characterize EEG responses to both textures (Eldeeb et al., 2020, 2019) and to transient changes in friction during active touch (Moungou et al., 2016). Importantly, Moungou and colleagues (2016) showed that periodic EEG responses were comparable (although smaller in amplitude) to those recorded in matched passive touch conditions (Moungou et al., 2016). While such work has investigated EEG responses in the frequency and the time-frequency domains, we believe that such similarities should also be observable in the time domain through recordings of SEPs. Thus, compared to such previous EEG investigations of tactile processing during active touch, the main contribution of our study is the characterization of the temporal pattern of time-locked responses to a single tactile event. Having time-locked responses precisely to the onset of contact with the tactile stimulus, as well as the similarity of the SEPs we recorded with well-characterized SEPs recorded in conditions of passive touch make us confident that the responses we observed were largely somatosensory in nature. However, it is still possible that sliding over the tactile stimulus triggered some reaction of motor-related activity, which would have also been time-locked to the stimulation onset. To further investigate this possibility and fully disentangle motor-related activity from purely somatosensory responses,

future work should include electromyography recordings, as well as normal and tangential force measurements. Furthermore, future studies should also aim to perform similar active-passive touch matching conditions to Moungou et al. (2016) to investigate how responses to tactile edges vary with and without voluntary movement.

In conclusion, our study sets the basis for overcoming important methodological challenges associated with measuring cortical responses to naturalistic tactile stimuli encountered by participants via voluntary exploratory movements. With the growing interest on tactile perception in conditions of active, dynamic touch, the use of EEG to record cortical responses to tactile stimuli encountered via voluntary movement could help elucidate the mechanisms underlying behavioral outcomes obtained via psychophysical approaches, such as participants' ability to recognize planar shapes during haptic exploration (Rohou-Claquin et al., 2025). Furthermore, measuring time-locked responses using scalp EEG is also advantageous to complement results obtained using other neuroimaging techniques, such as functional magnetic resonance imaging (fMRI). Indeed, while fMRI allows to determine the cortical locus of activity associated with sensory processing with high spatial resolution in the order of few millimeters, it does not allow determination of the precise timing of time-locked response at the millisecond scale, due to its temporal resolution being limited, at best, to half a second (Abreu et al., 2018). Our approach involving SEP recordings, on the other hand, allows us to assess cortical responses with a high temporal precision at the millisecond scale. Thanks to the somatotopical organization of S1, our approach also allows to differentiate activity originating from S1 or higher-order areas, albeit with much lower spatial resolution, thus enabling an investigation of the temporal evolution of somatosensory responses and the sequential activation along the somatosensory cortical hierarchy. Our work also opens new possibilities to

elucidate additional cortical mechanisms associated with active dynamic touch, such as movement-related somatosensory gating. Importantly, we show that effectively time-locking the time of finger contact with the physical haptic stimulus allowed us to characterize SEP components of tactile processing in conditions of active touch, which appear consistent in both their latency and topographical distribution with SEPs identified in studies involving passive touch conditions. Future investigations will be necessary to further characterize such components and assess their reproducibility.

CHAPTER 5: General discussion.

In recent years, the study of active touch sensing and multisensory integration in conditions of active, dynamic touch has drawn the interest of researchers across several disciplines. In the engineering and computer science fields, great efforts are being made with the prospect to develop novel haptic technologies, such as tablet-like devices or touch screens to provide tactile feedback in the absence of or with reduced visual feedback. However, relatively little is known about both the behavioral and the neurophysiological mechanisms that underlie interactions between touch and other sensory modalities during haptic exploration of shapes and surfaces. Indeed, one key challenge we encountered when planning the development of EEG studies of multisensory integration in conditions of active, dynamic touch is the fact that the neuroscientific literature is very limited in this regard. Many of the studies carried out in the somatosensory field have employed passive, static touch conditions. At the same time, most of the studies that have employed conditions of active, dynamic touch have only reported behavioral outcomes, and the studies that have investigated cortical responses in conditions of active, dynamic touch were carried out in unimodal tactile conditions (Eldeeb et al., 2020; Henderson et al., 2023; Moungou et al., 2016b). The aim of this doctoral thesis was to develop new approaches to specifically investigate the cortical mechanisms underlying auditory-tactile integration in conditions of active, dynamic touch. Touch itself, whether active or passive, is a complex mechanism encompassing several submodalities: friction, shear forces, tangential and normal forces, vibration, transient skin contacts and local mechanical skin deformation, temperature, wetness, and more, which are combined to give rise to different tactile experiences. For the purpose of this doctoral thesis, we focused on developing EEG approaches aimed at investigating two such experiences of active tactile sensing: perception and processing of textures (**Study 2**), and perception and processing of edges and planar shapes

(**Study 1** and **Study 3**). It is worth mentioning that in **Study 2**, the tactile stimulations were presented passively to participants. This was motivated by the fact that, (1) to date, no studies had used EEG frequency-tagging to investigate the cortical processing of changes in vibrotactile stimuli (even simple, pure vibrations), and (2) that whether S1 is involved in the processing of changes in more complex vibrations (such as white noise) remained an unanswered question. Therefore, for this study, we reasoned that taking a step back and implementing simpler stimulation conditions would allow us to validate the frequency-tagging approach for future investigations involving more naturalistic stimuli and tactile exploration conditions.

This discussion will first present the key findings and interpretations of the studies carried out in this doctoral thesis. Next, future developments of the techniques employed for this doctoral thesis will be discussed, as well as their applications to address unanswered questions related to the cortical processing audio-tactile interactions in conditions of active touch. In the last Section, the different types of stimulations currently available to investigate cortical somatosensory processing and their advantages and disadvantages will be discussed. Lastly, the discussion will aim to define the technical requirements necessary to allow more systematic, interpretable, and reproducible studies on active tactile sensing involving EEG methods.

1. Summary and interpretation of main findings.

In **Study 1**, we used psychophysics to investigate whether auditory feedback concurrently presented with tactile feedback (edge-like transient changes in friction delivered via an ultrasonic haptic display) would improve participants' performance in a task in which they had to localize the position of their exploring digit at the onset of the auditory and/ or tactile stimulation, compared to when

tactile stimuli were presented in isolation. Here, we showed that while localization *precision* (i.e., the slope of the psychometric function) of tactile stimuli was not significantly improved by concurrent presentation of auditory stimuli, localization *accuracy* (i.e., the threshold of the psychometric function) was significantly improved in the bimodal compared to either unimodal stimulation. The threshold parameter in performance psychophysical tasks provides some information about how well participants perform on the task, as it is a measure of how close their perception is to the true value of the stimulation. However, this parameter can be affected by both perceptual and response biases, which is the reason why we focused our specific hypothesis on the slope parameter, which represents how consistent participants are when making their perceptual judgments, and only assessed threshold differences as exploratory analyses. Indeed, we observed a rightward perceptual bias across subjects and across all modalities, which, as discussed in Chapter 2, could be due to an effect of representational momentum, or the tactile ''buzz-lag'' effect, whereby, at the onset of the stimulation, the position of the exploring finger was perceived to be shifted further away in the direction of movement (Cellini et al., 2016). The finding that this bias was significantly reduced under bimodal stimulus presentation partially supports our hypothesis that performance would be enhanced when the haptic feedback was accompanied by concurrent auditory feedback, indexing multisensory gain effects. Such evidence of integration between the tactile and auditory modalities during active sliding movements further motivates us to develop EEG approaches to investigate the possible cortical mechanisms that underlie such interactions.

In **Study 2**, we sought to investigate whether S1 is able to resolve the time-varying frequency composition of different textures, in the absence of differences of gross textural features, such as highly dissimilar envelopes of the vibrations elicited by the finger sliding against a textured surface. Indeed, while the cortical

processing of natural textures has been reported to involve activity originating from S1 (Moungou et al., 2016a), whether the processing of changes in textures also occurs early in the cortical somatosensory hierarchy remains to be determined. Exploiting the somatotopical organization of S1, we stimulated the right index finger and the sole of the right foot, using spectrotemporal vibrotactile sequences delivered in a periodic AAAAB oddball pattern. In accordance with our hypothesis, we showed that the topographical distribution of the periodic oddball responses to spectrotemporal contrasts differed significantly between the two stimulation sites, suggesting that the processing of rapid changes in vibrotactile textures takes place, at least in part, within S1. One key limitation of this study lies in the fact that we did not control for envelope differences between the base and oddball stimuli. In fact, we decided, *a posteriori,* to exclude the data from one of the spectrotemporal sequences we used, as it displayed a larger index of envelope dissimilarity compared to the other sequences. The exploratory analyses we conducted to assess whether envelope differences contributed significantly to the observed responses revealed that indeed this sequence drove stronger oddball responses. While correlational analyses with the remaining sequences showed that envelope dissimilarity was not positively associated with the magnitude of the oddball responses, it is not unreasonable to predict that even small envelope contrasts had at least a partial contribution. However, it is important to remember that we used artificial stimuli in our design, and delivered them in conditions of passive touch. While a potential optimization of the design would be to account for low-level differences between the base and oddball stimuli by keeping the oddball stimuli always the same, while randomizing the base stimuli (as done by De Keyser et al., 2018), in naturalistic conditions we would expect that the somatosensory system does in fact process changes in textures by combining information from different sources, including spectrotemporal and envelope features of the elicited vibrations,

speed, local skin indentation, and shear forces. Furthermore, in conditions of voluntary, free exploration of textures, the exploration strategies and motor control would be adapted continuously to better extract textural information from the surface (Prescott et al., 2011). Thus, while our results do support the hypothesis that S1 is involved in the processing of textures by resolving changes in the distribution of frequency over time of complex vibrations, they do not fully allow us to disentangle the specific contribution and cortical mechanisms of other aspects of texture processing that are part of active tactile exploration.

In **Study 3**, we aimed to develop a novel experimental setup that would allow SEPs characterization in response to edged tactile stimuli encountered by participants performing exploratory sliding movements. This study was motivated by the fact that, to date, SEP responses elicited in such conditions have not been characterized, likely due to the technical challenges of time-locking the onset of contact between the exploring fingertip and the stimulus, a crucial aspect of EEG investigations. To overcome such issues, we used finger position and accelerometer data to re-align the EEG signals to the exact time of contact between the exploring finger and the edged tactile stimulus, thus allowing characterization of time-locked cortical responses. This proof-of-concept study showed that it is possible to record SEPs elicited in response to raised tactile edges, and that the temporal evolution of the topographical pattern of such responses is compatible with previously reports of SEPs in conditions of passive touch, with early responses showing a clear contralateral lateralization, thus suggesting S1 activity, and later responses being more centrally localized, thus indicating recruitment of higher-order somatosensory areas (Allison et al., 1991; Deiber et al., 1986; Desmedt et al., 1987; Desmedt and Bourguet, 1985; Guidotti et al., 2023). The exact latencies of the responses, on the other hand, were less easily comparable with known SEPs. This is not necessarily surprising, given the novelty of the stimulations and conditions

that we implemented. Also, while we time-locked EEG responses to the transient onset of stimulation (i.e., the initial contact of the fingertip with the edge of the tactile stimulus), somatosensory input continued as the pulp of the fingertip continued sliding over the tactile stimulus. Thus, the stimulations we used are not as transient as those used in SEP reports involving passive touch, such as short-lasting vibrations or electrical stimuli. Furthermore, in conditions of active touch, different sensory channels are processed in parallel, including proprioceptive feedback and motor commands (Chapman, 1994; Prescott et al., 2011), which makes a direct comparison with SEPs recorded in passive touch conditions less straightforward. Importantly, besides prompting additional studies to better characterize SEPs associated with edge processing during planar shape exploration, our design opens new avenues to investigate, in humans, whether and how voluntary movement affects the cortical processing of tactile inputs, when the movement is related to and necessary for the perception of tactile stimuli. Suppression or gating of somatosensory signals has been reported in the presence of voluntary movements in both humans and non-human primates (Chapman, 1994; Nakata et al., 2003; Rossini et al., 1999). However, the somatosensory stimuli reported in such studies were unrelated to the movement being performed. Instead, in studies were the two were related, only gating of irrelevant somatosensory information was reported in monkeys, while relevant inputs were passed on through the somatosensory hierarchy (Ageranioti-Bélanger and Chapman, 1992), and SEPs in humans have been shown to be enhanced during touch-relevant movement (Knecht et al., 1993; Wasaka et al., 2017). Measuring SEPs in humans in matched active dynamic and passive dynamic conditions would help further elucidate such mechanisms.

2. Future perspectives to study the cortical mechanisms of audio-tactile integration in conditions of active, dynamic touch.

2.1. EEG frequency-tagging to study the cortical mechanisms of audio-tactile integration during texture exploration.

Despite involving artificial tactile stimuli delivered in conditions of passive touch, **Study 2** opens important avenues for the investigation of the processing of changes in natural textures in conditions of dynamic touch, as well as the effect of sounds on the perception of natural textures. A landmark of audio-tactile interactions in the context of texture perception is the parchment skin illusion (Jousmäki and Hari, 1998). In this phenomenon, the perception of texture roughness can be modulated by modulating the amplitude of the high-frequency components of both sounds elicited by the skin-texture interaction, as well as by complex artificial sounds such as white noise (Guest et al., 2002; Suzuki et al., 2008). While compelling behavioral evidence exists for the illusion, no studies to date have investigated the cortical processes associated with it. Does perception of the illusion modulate activity in early somatosensory areas, or does it recruit higher-order association cortical areas? Using fMRI, it has been shown that cortical areas originally thought to be unisensory actually display patterns of activation also in response to stimuli from other sensory modalities (Liang et al., 2013). In both monkeys and humans, concurrently presented tactile stimuli have also been shown to modulate activity within the primary auditory cortex (Foxe et al., 2002; Kayser et al., 2005; Schürmann et al., 2006). Thus, during the parchment-skin illusion, where auditory feedback modulates the perception of textural stimuli, it is possible that integration of the two modalities would already be observable at the level of S1. To test this hypothesis, future studies could build upon the methodology we used in **Study 2**. First, such investigations should aim to characterize the topographical

distribution of texture-related tactile oddball responses which, based on our results, would likely originate from S1, and of auditory oddball responses, which would be localized along fronto-central scalp electrodes (Nozaradan et al., 2017). Next, including an audio-tactile condition in which only the auditory sequences would include oddball stimuli (AAAAB), while the tactile stimuli would be kept constant (AAAAA) would allow assessing the presence of lateralization of auditory oddball responses contralaterally to the hand receiving the tactile stimulation. If this were the case, it would be an indication of multisensory integration across touch and sound occurring at an early stage along the somatosensory cortical hierarchy. Previous EEG investigations using median nerve stimulation have in fact shown that auditory-somatosensory integration effects are observable 50 ms post-stimulation, and that the topography associated with these responses is consistent with S1 activity (Foxe et al., 2000).

2.2. Measuring SEPs to study the cortical mechanisms of audio-tactile integration during planar shape exploration.

Perception of angles during active exploration relies on two cognitive strategies: the formation of a mental representation of the global structure of the angle, and the local pattern of skin indentation and cutaneous feedback at the angle intersection (Voisin et al., 2002a). Such mental representations represent a ‘’memory trace’’ of the stimulus. Indeed, the ability of participants to recognize shapes previously explored haptically both intra- (by touch) or inter-modally (by vision) relies on the presence of a memory trace acquired through the haptic exploration (Abravanel, 1971). Evidence exists pointing towards a role of S1 as a locus of cortical storage of short-term working memory traces of somatosensory stimuli. Indeed, participants’ performance on a memory task in which they had to compare the frequency of two vibrotactile stimuli presented with a 1500 ms

interval was significantly reduced when a TMS pulse was delivered to the contralateral S1 early (in the first 600 ms) during the interval, while no effect was found when TMS was applied to the ipsilateral S1 (Harris et al., 2002). The study of sensory memory traces using scalp EEG often relies on designs aimed at measuring novelty responses: in the presence of a memory trace of a stimulus, a randomly and infrequently presented stimulus would generate a specific response indexing processing of the deviance between the ''standard'' and ''oddball'' stimuli (Polich, 2007). With regard to cortical processing of novelty, or mismatches between expected and unexpected stimuli, two ERP components have been identified and extensively investigated in the literature: the P300 (Polich, 2007) and the mismatch negativity (MMN) (Näätänen et al., 2007, 2004). The P300 is a positive ERP complex typically recorded around 300 ms following the onset of a sensory stimulus (Polich, 2007). The neural mechanisms underlying the P300 are thought to involve an attention-mediated comparison of the incoming sensory information with the representation of the memory trace of previous sensory information. In the presence of a mismatch between the two, an update in the neural representation of the stimulus will give rise to a P300 response (Polich, 2007). The P300 is a complex of individual ERP components, each relating to different aspects of the processing of novel or unfamiliar stimuli. The P3a is the earliest component of the P300, which is observed around 220-280ms following stimulus onset over centro-frontal scalp electrodes. The P3a is thought to be associated with an involuntary, bottom-up attention shift that occurs in response to a rare ''oddball'' or ''deviant'' stimulus being presented at random intervals within a sequence of frequent ''standard'' stimuli, regardless of whether stimuli are attended or unattended (Polich, 2007). The second P300 component, the P3b, on the other hand, is measured around 300 following stimulus onset over parietal scalp electrodes, and it is thought to involve a voluntary attention orienting response to attended deviant

stimuli. Thus, this component is observed in active oddball paradigm involving overt attention to the stimulation, such as when participants need to either count or respond to deviant stimuli (Polich, 2007).

The MMN is an ERP component which, similarly to the P300, is elicited by rare presentation of deviant stimuli embedded in a sequence of frequent standard stimuli. First described and extensively studied in the auditory modality (Näätänen et al., 2007), a key feature of the MMN is that it occurs in response to discriminable changes in stimulation, and, unlike the P3b, it is elicited irrespective of attention (Näätänen et al., 2004). The processes underlying the MMN response are thought to involve an automatic comparison of the incoming sensory information with the memory trace which is formed upon repetitive presentation of standard stimuli (Näätänen et al., 2007, 2004). In the literature, somatosensory mismatch responses have been reported, with many studies investigating the processing of different low-level contrasts in tactile stimuli, such as their location on the body surface (Shen et al., 2018a, 2018b), their frequency (Butler et al., 2012; Kekoni et al., 1997), intensity (Zhang et al., 2019), and duration (Isenstein et al., 2024). While such findings shed light on the cortical processing of somatosensory mismatches, the fact that they involved somatosensory stimulation delivered in conditions of passive touch limits their ecological interpretation. An intrinsic characteristic of active touch and digit-mediated surface exploration is that the same body surface will come into contact with a changing stimulus or surface. In the case of edge localization during planar shape perception, the physical characteristics of the tactile object may also remain unchanged, while only their location is displaced. In order to differentiate the expected vs. actual location of the edge, integration of motor and proprioceptive inputs associated with the exploratory movement would be necessary, as the tactile information received by the same body location would not be sufficient to signal a change in the surface being explored. The setup we

developed in **Study 3** includes a stepper motor that allows rotating the wooden platform to display different faces. Thus, it will be useful in future designs investigating responses to mismatches in the physical location of edges and planar shapes. In such a design, the same finger and portion of the finger would come into contact with tactile stimuli whose location (or other sensory attributes, such as orientation or material) would be varied. As the results from **Study 2** indicate, concurrent auditory stimulation improves the localization of transient haptic stimuli encountered through exploratory sliding movements, compared to when these are presented in isolation, in that they give rise to a more accurate representation of haptic stimuli in space. Thus, it would be interesting to test whether sound facilitates the formation of mental representation of edges and planar shapes, which would be indexed by P300/MMN responses in bimodal conditions that are significantly different from the sum of the responses elicited in unimodal conditions.

3. Technical considerations: what does the ideal neuroscientific active touch setup look like?

Drawing on the strengths, limitations and challenges of the work carried out in this doctoral thesis, important insights can be gained as to what can be achieved with the tactile stimulation platforms that are currently available, and what their relative advantages and disadvantages are. Crucially, the diverse methodological approaches we used in the experiments we report allowed us to thoughtfully consider the technical necessities associated with investigating multisensory integration in the context of active touch sensing using neuroscientific approaches.

In **Study 2**, we used vibrotactile stimuli delivered in conditions of passive touch. An obvious advantage of using stimulations delivered to participants via an external

source is the ease of controlling the onset, the magnitude, and the duration of the stimulations. This is particularly important for EEG experiments, as the time of stimulus onset can easily be recorded and used to assess time-locked cortical responses. With the aim to assess how voluntary movement affects the temporal perception of somatosensory stimuli, some experiments have employed this approach to deliver vibrotactile stimuli to participants as they were moving their hands (Cellini et al., 2016; Drewing and Vroomen, 2022). However, receiving an electrical or vibrotactile stimulus from an external source which is unrelated to the performed exploratory movement is quite different from the somatosensory input received when the movement is necessary to receive the tactile input. Thus, this type of stimulation, while very well controlled and adaptable, is of limited ecological validity.

In **Study 1**, we used a visuo-tactile ultrasonic haptic display, which modulates the coefficient of friction between the exploring finger pad and the glass of the display, thus generating a tactile sensation (Wiertlewski et al., 2016). Similarly to vibrotactile or electrical stimuli delivered in passive touch conditions, one advantage of such devices lies in the ease of controlling and measuring the timing of stimulation. In a previous experiment (Brahimaj et al., 2023), we used the same haptic display to investigate the perception of temporal synchronicity between tactile and auditory stimuli. In this study, the onset of auditory stimuli was triggered by the voltage output emitted by the haptic display when the exploring finger pad reached a pre-defined region of the plate, via a data acquisition card (Brahimaj et al., 2023). However, a key limitation of such devices is that they cannot locally stimulate a portion of the skin at the finger pad. While the plate can be programmed to vibrate when the finger reaches a specific location by defining an active zone, or taxtel, the amplitude-modulated ultrasonic vibrations necessary to render the haptic feedback are present across the whole surface of the display

(Rekik et al., 2017). Therefore, the generated tactile input does not elicit local skin deformations typically associated with tactile exploration of both rougher textures or planar shapes. Indeed, similarly to the OPTACON sensory substitution device, which convey shapes via an array of vibrating pins (Goldish and Taylor, 1974), such devices would likely not generate activity in SA mechanoreceptors. However, unlike the OPTACON device, they also do not locally modulate FA1 activity, as the whole surface of the finger pad in contact with the display will be subject to the friction modulation induced by the amplitude-modulated ultrasonic vibrations. Therefore, rendering planar shapes using such devices is particularly challenging, as users do not receive input signaling the orientation of the shape's edges, or information about the shape's curvature or angles. A recent investigation has indeed shown that participants' ability to recognize more complex shapes on such devices is not above chance level, and even for a simple straight or sine line it sits at only about 65/70% (Rohou-Claquin et al., 2025). Another potential limitation of devices that rely on tracking fingertip position to generate haptic feedback comes from potential delays between the signal monitoring fingertip position and actual fingertip position and/or delays to trigger stimulation, which is a crucial aspect to consider in EEG investigations. These delays should be precisely quantified and mitigated by engineers and manufacturers of such devices.

In **Study 3**, we designed a more ecological approach, where the edged tactile stimulus explored by participants was a physical stimulus. The tactile input that participants received when contacting the stimulus was therefore more naturalistic, encompassing local skin deformation activating SA fibers, and RA fibers activated by skin motion, as well as friction and slip from the edge's surface. Therefore, it seems that physical stimuli are better suited to generate tactile sensations in conditions of active touch and in the context of planar shape processing as they involve the multiple tactile submodalities that characterize

haptic experiences. However, as previously mentioned, the use of physical tactile stimuli comes with some limitations, particularly in the context of EEG investigations. Perhaps the key limitation lies in the fact that the onset of stimulation is not controlled, nor is the exact manner in which the stimulation is delivered and thus perceived by the subjects. Indeed, the exact pressure, speed, constancy, and movement trajectory before, during, and after contact with the stimulus solely depend on the participants' exploration strategy. In our setup, we took care to record finger vertical displacements and position, to re-align, as precisely as possible, the exact onset of contact between the finger and the stimulus. However, a potential limitation of our approach is that we did not assess the exact dynamic of finger movement and skin deformations. Are the onsets we defined true contacts without finger displacement, or do they represent the moment in which the finger had already surpassed the first edge of the raised tactile stimulus? Answering this question solely using accelerometer recordings is not trivial. Indeed, even if we were to record signals at the moment the finger touched the stimulus prior to overcoming its edge, it is likely that a change in accelerometer signal would still be elicited by the sudden halting of the finger's horizontal displacement. Future efforts should be made to address these issues, possibly using high-speed camera measurements to align local finger geometry at different phases of contact with the physical tactile stimuli (true contact, upward vertical displacement, scanning, downwards vertical displacement) (Delhaye et al., 2014; Janko et al., 2018). The setup we used in **Study 3** presents another important limitation, in that the stimuli were fixed via holes drilled on the parallelepiped wooden platform, which limits the adaptability of the setup. Indeed, since the stimuli are fixed on the exploring platform, testing different types of stimuli or stimuli at different positions would require assembling of a new platform. Therefore, the setup should be adapted in the future to accommodate

interchangeable exploring surfaces and tactile stimuli, such as different shapes, different orientations, or different materials.

Future collaborative efforts between engineering and neuroscience should aim at developing devices that could be easily interfaced with different EEG recording systems. Similarly, to overcome the lack of control over the timing and magnitude of stimulations presented to participants, it will be important for future setups to allow precise recordings of fingertip dynamics during free exploration. Such measurements could include online finger tracking in the x, y, and z axis, to measure velocity, accelerations and decelerations, direction and changes in direction, which are particularly useful to precisely time-lock responses to stimuli and simultaneously assess exploration strategies as the finger approaches the stimuli. At the same time, such precise online measurements would be particularly critical to generate accurate planar shapes in devices which generate haptic feedback depending on finger position during active tactile exploration, such as the EVITA ultrasonic display (Wiertlewski et al., 2016). Similarly, measurements of normal and tangential forces would be useful to relate cortical responses to the forces acting on the fingertip at the moment of contact with the tactile stimuli.

4. General Conclusion

This doctoral thesis contributed to the field of tactile perception in different ways. On the one hand, it allowed us to address important questions with regard to the cortical processing of tactile inputs, including the role that S1 plays in the context of processing of textures and changes in textures, as well as measuring, for the first time, cortical responses to raised edges during active fingertip sliding movements. Our psychophysical investigation also provides evidence for audio-tactile integration in the context of edge localization during active sliding

movements. Importantly, on the other hand, the present work sets the basis for future investigations of audio-tactile integration during haptic exploration, by validating psychophysical and EEG approaches for their future applications to study the behavioral and cortical mechanisms underlying such interactions. Lastly, the different techniques and stimulation types employed here highlighted the limitations of the devices currently available for the study of active tactile sensing, providing us with insights and a deeper appreciation of the technical needs that should be met to systematically investigate touch in ecological conditions.

Bibliography

Abravanel, E., 1971. Active detection of solid-shape information by touch and vision. Perception & Psychophysics 10, 358–360. DOI : 10.3758/BF03207459.

Abreu, R., Leal, A., Figueiredo, P., 2018. EEG-Informed fMRI: A Review of Data Analysis Methods. Frontiers in Human Neuroscience 12, 1-23. DOI: 10.3389/fnhum.2018.00029.

Ageranioti-Bélanger, S.A., Chapman, C.E., 1992. Discharge properties of neurones in the hand area of primary somatosensory cortex in monkeys in relation to the performance of an active tactile discrimination task. Experimental Brain Research 91, 207–228. DOI: 10.1007/BF00231655.

Aggelopoulos, N.C., 2015. Perceptual inference. Neuroscience & Biobehavioral Reviews 55, 375–392. DOI: 10.1016/j.neubiorev.2015.05.001.

Aimonetti, J.-M., Hospod, V., Roll, J.-P., Ribot-Ciscar, E., 2007. Cutaneous afferents provide a neuronal population vector that encodes the orientation of human ankle movements. The Journal of Physiology 580, 649. DOI: 10.1113/jphysiol.2006.123075.

Alain, C., Roye, A., Arnott, S.R., 2013. Middle- and long-latency auditory evoked potentials: what are they telling us on central auditory disorders? In: Celesia, G.G. (Ed.), Handbook of Clinical Neurophysiology, Disorders of Peripheral and Central Auditory Processing. Elsevier, pp. 177–199.

Alais, D., Burr, D., 2004. The Ventriloquist Effect Results from Near-Optimal Bimodal Integration. Current Biology 14, 257–262. DOI: 10.1016/j.cub.2004.01.029.

Alais, D., Burr, D., 2003. The “Flash-Lag” Effect Occurs in Audition and Cross-Modally. Current Biology 13, 59–63. DOI: 10.1016/S0960-9822(02)01402-1.

Allaire, J.J., 2012. RStudio: Integrated Development Environment for R 165–171.

Allison, T., McCarthy, G., Wood, C.C., 1992. The relationship between human long-latency somatosensory evoked potentials recorded from the cortical surface and from the scalp. Electroencephalography and Clinical Neurophysiology/Evoked Potentials Section 84, 301–314. DOI: 10.1016/0168-5597(92)90082-M.

Allison, T., McCarthy, G., Wood, C.C., Jones, S.J., 1991. Potentials evoked in human and monkey cerebral cortex by stimulation of the median nerve. A review of scalp and intracranial recordings. Brain, 114(6), 2465–2503. DOI: 10.1093/brain/114.6.2465.

Augurelle, A.-S., Smith, A.M., Lejeune, T., Thonnard, J.L., 2003. Importance of cutaneous feedback in maintaining a secure grip during manipulation of hand-held objects. Journal of Neurophysiology, 89(2), 665–671. DOI : 10.1152/jn.00249.2002.

Bajcsy, R., 1988. Active perception. Proceedings of the IEEE, 76, 966–1005. DOI: 10.1109/5.5968.

Bays, P.M., Flanagan, J.R., Wolpert, D.M., 2006. Attenuation of Self-Generated Tactile Sensations Is Predictive, not Postdictive. PLOS Biology, 4, e28. DOI: 10.1371/journal.pbio.0040028.

Behrens, T.E.J., Johansen-Berg, H., Woolrich, M.W., Smith, S.M., Wheeler-Kingshott, C. a. M., Boulby, P.A., Barker, G.J., Sillery, E.L., Sheehan, K., Ciccarelli, O., Thompson, A.J., Brady, J.M., Matthews, P.M., 2003. Non-invasive mapping of connections between human thalamus and cortex using diffusion imaging. Nature Neuroscience 6, 750–757. DOI: 10.1038/nn1075.

Bell, J., Bolanowski, S., Holmes, M.H., 1994. The structure and function of pacinian corpuscles: A review. Progress in Neurobiology, 42, 79–128. DOI: 10.1016/0301-0082(94)90022-1.

Bengtsson, F., Brasselet, R., Johansson, R.S., Arleo, A., Jörntell, H., 2013. Integration of Sensory Quanta in Cuneate Nucleus Neurons In Vivo. PLOS ONE, 8, e56630. DOI: 10.1371/journal.pone.0056630.

Bensmaïa, S., Hollins, M., 2005. Pacinian representations of fine surface texture. Perception & Psychophysics 67, 842–854. DOI: 10.3758/BF03193537.

Bensmaia, S.J., Denchev, P.V., Dammann, J.F., Craig, J.C., Hsiao, S.S., 2008. The Representation of Stimulus Orientation in the Early Stages of Somatosensory Processing. Journal of Neuroscience, 28, 776–786. DOI: 10.1523/JNEUROSCI.4162-07.2008.

Bertelson, P., Aschersleben, G., 1998. Automatic visual bias of perceived auditory location. Psychonomic Bulletin & Review, 5, 482–489. DOI: 10.3758/BF03208826.

Bertelson, P., Radeau, M., 1981. Cross-modal bias and perceptual fusion with auditory-visual spatial discordance. Perception & Psychophysics, 29, 578–584. DOI : 10.3758/BF03207374.

Bicchi, A., Scilingo, E.P., Ricciardi, E., Pietrini, P., 2008. Tactile flow explains haptic counterparts of common visual illusions. Brain Research Bulletin, Special Issue: Robotics and Neuroscience, 75, 737–741. DOI: 10.1016/j.brainresbull.2008.01.011.

Bilaloglu, S., Lu, Y., Geller, D., Rizzo, J.R., Aluru, V., Gardner, E.P., Raghavan, P., 2016. Effect of blocking tactile information from the fingertips on adaptation and execution of grip forces to friction at the grasping surface. Journal of Neurophysiology, 115, 1122–1131. DOI: 10.1152/jn.00639.2015.

Birznieks, I., Vickery, R.M., 2017. Spike Timing Matters in Novel Neuronal Code Involved in Vibrotactile Frequency Perception. Current Biology, 27, 1485-1490.e2. DOI: 10.1016/j.cub.2017.04.011.

Björnsdotter, M., Löken, L., Olausson, H., Vallbo, Å., Wessberg, J., 2009. Somatotopic Organization of Gentle Touch Processing in the Posterior Insular Cortex. Journal of Neuroscience, 29, 9314–9320. DOI: 10.1523/JNEUROSCI.0400-09.2009.

Bliss, J.C., Katcher, M.H., Rogers, C.H., Shepard, R.P., 1970. Optical-to-Tactile Image Conversion for the Blind. IEEE Transactions on Man-Machine Systems, 11, 58–65. DOI: 10.1109/TMMS.1970.299963.

Bolanowski, S.J., Jr., Gescheider, G.A., Verrillo, R.T., Checkosky, C.M., 1988. Four channels mediate the mechanical aspects of touch. The Journal of the Acoustical Society of America 84, 1680–1694. DOI: 10.1121/1.397184.

Bradshaw, J.L., Nettleton, N.C., Nathan, G., Wilson, L., 1985. Bisecting rods and lines: Effects of horizontal and vertical posture on left-side underestimation by normal subjects. Neuropsychologia, 23, 421–425. DOI : 10.1016/0028-3932(85)90029-6.

Brahimaj, D., Esposito, G., Courtin, A., Giraud, F., Semail, B., Collignon, O., Mouraux, A., 2023. Temporal detection threshold of audio-tactile delays under conditions of active touch with and without a visual cue. IEEE World Haptics Conference, pp. 354–360. DOI: 10.1109/WHC56415.2023.10224451.

Brandeis, D., Lehmann, D., 1986. Event-related potentials of the brain and cognitive processes: Approaches and applications. Neuropsychologia, Special Issue Methods in Neuropsychology, 24, 151–168. DOI: 10.1016/0028-3932(86)90049-7.

Breitwieser, C., Kaiser, V., Neuper, C., Müller-Putz, G.R., 2012. Stability and distribution of steady-state somatosensory evoked potentials elicited by vibro-tactile stimulation. Medical and Biological Engineering and Computing, 50, 347–357. DOI: 10.1007/s11517-012-0877-9.

Bruns, P., Röder, B., 2010. Tactile capture of auditory localization: an event-related potential study. European Journal of Neuroscience, 31, 1844–1857. DOI: 10.1111/j.1460-9568.2010.07232.x.

Bruns, P., Spence, C., Röder, B., 2011. Tactile recalibration of auditory spatial representations. Experimental Brain Research, 209, 333–344. DOI: 10.1007/s00221-011-2543-0.

Burr, D., Banks, M.S., Morrone, M.C., 2009. Auditory dominance over vision in the perception of interval duration. Experimental Brain Research, 198, 49. DOI: 10.1007/s00221-009-1933-z.

Burton, H., Sinclair, R.J., 1991. Second somatosensory cortical area in macaque monkeys: 2. Neuronal responses to punctate vibrotactile stimulation of glabrous skin on the hand. Brain Research 538, 127–135. DOI: 10.1016/0006-8993(91)90386-A.

Butler, J.S., Foxe, J.J., Fiebelkorn, I.C., Mercier, M.R., Molholm, S., 2012. Multisensory Representation of Frequency across Audition and Touch: High Density Electrical Mapping Reveals Early Sensory-Perceptual Coupling. Journal of Neuroscience, 32, 15338–15344. DOI: 10.1523/JNEUROSCI.1796-12.2012.

Caclin, A., Soto-Faraco, S., Kingstone, A., Spence, C., 2002. Tactile “capture” of audition. Perception & Psychophysics, 64, 616–630. DOI: 10.3758/BF03194730.

Carlson, M., 1981. Characteristics of sensory deficits following lesions of brodmann’s areas 1 and 2 in the postcentral gyrus of *Macaca mulatta*. Brain Research, 204, 424–430. DOI: 10.1016/0006-8993(81)90602-8.

Casado-Palacios, M., Tonelli, A., Campus, C., Gori, M., 2023. Movement-related tactile gating in blindness. Scientific Reports, 13, 16553. DOI: 10.1038/s41598-023-43526-8.

Cellini, C., Scocchia, L., Drewing, K., 2016. The buzz-lag effect. Experimental Brain Research 234, 2849–2857. DOI: 10.1007/s00221-016-4687-4.

Chapman, C.E., 1994. Active versus passive touch: factors influencing the transmission of somatosensory signals to primary somatosensory cortex. Canadian Journal of Physiology and Pharmacology, 72, 558–570. DOI: 10.1139/y94-080.

Chemin, B., Huang, G., Mulders, D., Mouraux, A., 2018. EEG time-warping to study non-strictly-periodic EEG signals related to the production of rhythmic movements. Journal of Neuroscience Methods, 308, 106–115. DOI: 10.1016/j.jneumeth.2018.07.016.

Chemin, B., Mouraux, A., Nozaradan, S., 2014. Body Movement Selectively Shapes the Neural Representation of Musical Rhythms. Psychological Science, 25, 2147–2159. DOI: 10.1177/0956797614551161.

Colon, E., Legrain, V., Mouraux, A., 2014. EEG Frequency Tagging to Dissociate the Cortical Responses to Nociceptive and Nonnociceptive Stimuli. Journal of Cognitive Neuroscience, 26, 2262–2274. DOI: 10.1162/jocn_a_00648.

Colon, E., Legrain, V., Mouraux, A., 2012. Steady-state evoked potentials to study the processing of tactile and nociceptive somatosensory input in the human brain. Clinical Neurophysiology, 42, 315–323. DOI : 10.1016/j.neucli.2012.05.005.

Colon, E., Liberati, G., Mouraux, A., 2017. EEG frequency tagging using ultra-slow periodic heat stimulation of the skin reveals cortical activity specifically related to C fiber thermonociceptors. NeuroImage, 146, 266–274. DOI: 10.1016/j.neuroimage.2016.11.045.

Connolly, J.D., Andersen, R.A., Goodale, M.A., 2003. FMRI evidence for a “parietal reach region” in the human brain. Experimental Brain Research, 153, 140–145. DOI: 10.1007/s00221-003-1587-1.

Connor, C.E., Hsiao, S.S., Phillips, J.R., Johnson, K.O., 1990. Tactile roughness: neural codes that account for psychophysical magnitude estimates. Journal of Neuroscience, 10, 3823–3836. DOI: 10.1523/JNEUROSCI.10-12-03823.1990.

Connor, C.E., Johnson, K.O., 1992. Neural coding of tactile texture: comparison of spatial and temporal mechanisms for roughness perception. Journal of Neuroscience, 12, 3414–3426. DOI : 10.1523/JNEUROSCI.12-09-03414.1992.

Costanzo, R.M., Gardner, E.P., 1980. A quantitative analysis of responses of direction-sensitive neurons in somatosensory cortex of awake monkeys. Journal of Neurophysiology, 43, 1319–1341. DOI: 10.1152/jn.1980.43.5.1319.

Courtin, A., 2022. Catching cold: exploration of the human perception of innocuous cold using chemical sensitization, EEG and psychophysics. (Doctoral Dissertation, UCL - Université Catholique de Louvain).

Courtin, A.S., Delvaux, A., Dufour, A., Mouraux, A., 2023. Spatial summation of cold and warm detection: Evidence for increased precision when brisk stimuli are delivered over larger area. Neuroscience Letters, 797, 137050. DOI: 10.1016/j.neulet.2023.137050.

Courtin, A.S., Maldonado Slootjes, S., Caty, G., Hermans, M.P., Plaghki, L., Mouraux, A., 2020. Assessing thermal sensitivity using transient heat and cold stimuli combined with a Bayesian adaptive method in a clinical setting: A proof of concept study. European Journal of Pain, 24, 1812–1821. DOI: 10.1002/ejp.1628.

Cruccu, G., Aminoff, M.J., Curio, G., Guerit, J.M., Kakigi, R., Mauguiere, F., Rossini, P.M., Treede, R.D., Garcia-Larrea, L., 2008. Recommendations for the clinical use of somatosensory-evoked potentials. Clinical Neurophysiology, 119, 1705–1719. DOI: 10.1016/j.clinph.2008.03.016.

De Keyser, R., Mouraux, A., Quek, G.L., Torta, D.M., Legrain, V., 2018. Fast periodic visual stimulation to study tool-selective processing in the human brain. Experimental Brain Research, 236, 2751–2763. DOI: 10.1007/s00221-018-5331-2.

Deecke, L., Grözinger, B., Kornhuber, H.H., 1976. Voluntary finger movement in man: Cerebral potentials and theory. Biological Cybernetics, 23, 99–119. DOI: 10.1007/BF00336013.

Deflorio, D., Di Luca, M., Wing, A.M., 2022. Skin and Mechanoreceptor Contribution to Tactile Input for Perception: A Review of Simulation Models. Frontiers in Human Neuroscience, 16, 862344. DOI: 10.3389/fnhum.2022.862344.

Deiber, M.P., Giard, M.H., Mauguiere, F., 1986. Separate generators with distinct orientations for N20 and P22 somatosensory evoked potentials to finger stimulation? Electroencephalography and Clinical Neurophysiology/Evoked Potentials Section, 65, 321–334. DOI: 10.1016/0168-5597(86)90012-2.

Del Gratta, C., Della Penna, S., Ferretti, A., Franciotti, R., Pizzella, V., Tartaro, A., Torquati, K., Bonomo, L., Romani, G.L., Rossini, P.M., 2002. Topographic Organization of the Human Primary and

Secondary Somatosensory Cortices: Comparison of fMRI and MEG Findings. NeuroImage 17, 1373–1383. DOI: 10.1006/nimg.2002.1253.

Delhaye, B., Hayward, V., Lefèvre, P., Thonnard, J.L., 2012. Texture-induced vibrations in the forearm during tactile exploration. Frontiers in Behavioral Neuroscience, 6, 37. DOI: 10.3389/fnbeh.2012.00037.

Delhaye, B., Lefèvre, P., Thonnard, J.-L., 2014. Dynamics of fingertip contact during the onset of tangential slip. Journal of The Royal Society Interface, 11, 20140698. DOI: 10.1098/rsif.2014.0698.

Delhaye, B.P., Long, K.H., Bensmaia, S.J., 2018. Neural Basis of Touch and Proprioception in Primate Cortex. Comprehensive Physiology, 8, 1575. DOI: 10.1002/cphy.c170033.

Dépeault, A., Meftah, E.-M., Chapman, C.E., 2013. Neuronal correlates of tactile speed in primary somatosensory cortex. Journal of Neurophysiology, 110, 1554–1566. DOI: 10.1152/jn.00675.2012.

Desmedt, J.E., Bourguet, M., 1985. Color imaging of parietal and frontal somatosensory potential fields evoked by stimulation of median or posterior tibial nerve in man. Electroencephalography and Clinical Neurophysiology/Evoked Potentials Section, 62, 1–17. DOI: 10.1016/0168-5597(85)90030-9.

Desmedt, J.E., Huy Nguyen, T., Bourguet, M., 1987. Bit-mapped color imaging of human evoked potentials with reference to the N20, P22, P27 and N30 somatosensory responses. Electroencephalography and Clinical Neurophysiology/Evoked Potentials, Section 68, 1–19. DOI: 10.1016/0168-5597(87)90065-7.

Diederich, A., Colonius, H., 2004. Bimodal and trimodal multisensory enhancement: Effects of stimulus onset and intensity on reaction time. Perception & Psychophysics, 66, 1388–1404. DOI : 10.3758/BF03195006.

Dionne, J.K., Legon, W., Staines, W.R., 2013. Crossmodal influences on early somatosensory processing: interaction of vision, touch, and task-relevance. Experimental Brain Research, 226, 503–512. DOI: 10.1007/s00221-013-3462-z.

Disbrow, E., Litinas, E., Recanzone, G.H., Padberg, J., Krubitzer, L., 2003. Cortical connections of the second somatosensory area and the parietal ventral area in macaque monkeys. Journal of Comparative Neurology, 462, 382–399. DOI: 10.1002/cne.10731.

Dong, W.K., Chudler, E.H., Sugiyama, K., Roberts, V.J., Hayashi, T., 1994. Somatosensory, multisensory, and task-related neurons in cortical area 7b (PF) of unanesthetized monkeys. Journal of Neurophysiology, 72, 542–564. DOI: 10.1152/jn.1994.72.2.542.

Dowman, R., Schell, S., 1999. Innocuous-related sural nerve-evoked and finger-evoked potentials generated in the primary somatosensory and supplementary motor cortices. Clinical Neurophysiology, 110, 2104–2116. DOI: 10.1016/S1388-2457(99)00203-5.

Drewing, K., Ernst, M.O., 2006. Integration of force and position cues for shape perception through active touch. Brain Research, 1078, 92–100. DOI: 10.1016/j.brainres.2005.12.026.

Drewing, K., Hitzel, E., Scocchia, L., 2018. The haptic and the visual flash-lag effect and the role of flash characteristics. PLOS ONE, 13, e0189291. DOI: 10.1371/journal.pone.0189291.

Drewing, K., Kaim, L., 2009. Haptic shape perception from force and position signals varies with exploratory movement direction and the exploring finger. Attention, Perception, & Psychophysics, 71, 1174–1184. DOI : 10.3758/APP.71.5.1174.

Drewing, K., Vroomen, J., 2022. Moving Hands Feel Stimuli Before Stationary Hands. Haptics: Science, Technology, Applications, Lecture Notes in Computer Science, 12–20. DOI: 10.1007/978-3-031-06249-0_2.

Dykes, R.W., Rasmusson, D.D., Sretavan, D., Rehman, N.B., 1982. Submodality segregation and receptive-field sequences in cuneate, gracile, and external cuneate nuclei of the cat. Journal of Neurophysiology, 47, 389–416. DOI: 10.1152/jn.1982.47.3.389.

Eck, J., Kaas, A.L., Mulders, J.L., Hausfeld, L., Kourtzi, Z., Goebel, R., 2016. The Effect of Task Instruction on Haptic Texture Processing: The Neural Underpinning of Roughness and Spatial Density Perception. Cerebral Cortex, 26, 384–401. DOI: 10.1093/cercor/bhu294.

Edin, B.B., 2001. Cutaneous afferents provide information about knee joint movements in humans. The Journal of Physiology, 531, 289–297. DOI: 10.1111/j.1469-7793.2001.0289j.x.

Edin, B.B., Abbs, J.H., 1991. Finger movement responses of cutaneous mechanoreceptors in the dorsal skin of the human hand. Journal of Neurophysiology, 65, 657–670. DOI: 10.1152/jn.1991.65.3.657.

Eimer, M., Forster, B., 2003. Modulations of early somatosensory ERP components by transient and sustained spatial attention. Experimental Brain Research, 151, 24–31. DOI: 10.1007/s00221-003-1437-1.

Eldeeb, S., Weber, D., Ting, J., Demir, A., Erdogmus, D., Akcakaya, M., 2020. EEG-based trial-by-trial texture classification during active touch. Scientific Reports, 10, 20755. DOI: 10.1038/s41598-020-77439-7.

Ernst, M.O., Banks, M.S., 2002. Humans integrate visual and haptic information in a statistically optimal fashion. Nature, 415, 429–433. DOI: 10.1038/415429a.

Fendrich, R., Corballis, P.M., 2001. The temporal cross-capture of audition and vision. Perception & Psychophysics, 63, 719–725. DOI: 10.3758/BF03194432.

Filbrich, L., Alamia, A., Blandiaux, S., Burns, S., Legrain, V., 2017. Shaping visual space perception through bodily sensations: Testing the impact of nociceptive stimuli on visual perception in peripersonal space with temporal order judgments. PLOS ONE, 12, e0182634. DOI: 10.1371/journal.pone.0182634.

Filimon, F., Nelson, J.D., Huang, R.-S., Sereno, M.I., 2009. Multiple Parietal Reach Regions in Humans: Cortical Representations for Visual and Proprioceptive Feedback during On-Line Reaching. Journal of Neuroscience, 29, 2961–2971. DOI: 10.1523/JNEUROSCI.3211-08.2009.

Fitzgerald, P.J., Lane, J.W., Thakur, P.H., Hsiao, S.S., 2006. Receptive Field (RF) Properties of the Macaque Second Somatosensory Cortex: RF Size, Shape, and Somatotopic Organization. Journal of Neuroscience, 26, 6485–6495. DOI: 10.1523/JNEUROSCI.5061-05.2006.

Fitzgerald, P.J., Lane, J.W., Thakur, P.H., Hsiao, S.S., 2004. Receptive Field Properties of the Macaque Second Somatosensory Cortex: Evidence for Multiple Functional Representations. Journal of Neuroscience, 24, 11193–11204. DOI : 10.1523/JNEUROSCI.3481-04.2004.

Forss, N., Merlet, I., Vanni, S., Hämäläinen, M., Mauguière, F., Hari, R., 1996. Activation of human mesial cortex during somatosensory target detection task. Brain Research, 734, 229–235. DOI: 10.1016/0006-8993(96)00633-6.

Forster, B., Cavina-Pratesi, C., Aglioti, S.M., Berlucchi, G., 2002. Redundant target effect and intersensory facilitation from visual-tactile interactions in simple reaction time. Experimental Brain Research, 143, 480–487. DOI: 10.1007/s00221-002-1017-9.

Fortier-Poisson, P., Langlais, J.-S., Smith, A.M., 2016. Correlation of fingertip shear force direction with somatosensory cortical activity in monkey. Journal of Neurophysiology, 115, 100–111. DOI: 10.1152/jn.00749.2014.

Foxe, J.J., Morocz, I.A., Murray, M.M., Higgins, B.A., Javitt, D.C., Schroeder, C.E., 2000. Multisensory auditory–somatosensory interactions in early cortical processing revealed by high-density electrical mapping. Cognitive Brain Research, 10, 77–83. DOI: 10.1016/S0926-6410(00)00024-0.

Foxe, J.J., Wylie, G.R., Martinez, A., Schroeder, C.E., Javitt, D.C., Guilfoyle, D., Ritter, W., Murray, M.M., 2002. Auditory-Somatosensory Multisensory Processing in Auditory Association Cortex: An fMRI Study. Journal of Neurophysiology, 88, 540–543. DOI: 10.1152/jn.2002.88.1.540.

Freeman, W.J., Holmes, M.D., Burke, B.C., Vanhatalo, S., 2003. Spatial spectra of scalp EEG and EMG from awake humans. Clinical Neurophysiology, 114, 1053–1068. DOI: 10.1016/S1388-2457(03)00045-2.

Freyd, J.J., Finke, R.A., 1984. Representational momentum. Journal of Experimental Psychology: Learning, Memory, and Cognition, 10, 126–132. DOI: 10.1037/0278-7393.10.1.126.

Gabry, J., Češnovar, R., Johnson, A., 2023. cmdstanr: R Interface to "CmdStan."

Gardner, E.P., Palmer, C.I., 1989. Simulation of motion on the skin. I. Receptive fields and temporal frequency coding by cutaneous mechanoreceptors of OPTACON pulses delivered to the hand. Journal of Neurophysiology, 62, 1410–1436. DOI: 10.1152/jn.1989.62.6.1410.

Gescheider, G.A., 1997. Psychophysics: The Fundamentals, 3rd ed. Psychology Press, New York. DOI: 10.4324/9780203774458

Gibson, J.J., 1962. Observations on active touch. Psychological Review, 69, 477–491.

Gillmeister, H., Eimer, M., 2007. Tactile enhancement of auditory detection and perceived loudness. Brain Research, 1160, 58–68. DOI: 10.1016/j.brainres.2007.03.041.

Girard, S., Pelland, M., Lepore, F., Collignon, O., 2013. Impact of the spatial congruence of redundant targets on within-modal and cross-modal integration. Experimental Brain Research, 224, 275–285. DOI: 10.1007/s00221-012-3308-0.

Goldish, L.H., Taylor, H.E., 1974. The Optacon: A Valuable Device for Blind Persons. Journal of Visual Impairment & Blindness, 68, 49–56. DOI: 10.1177/0145482X7406800201.

Groppe, D.M., Urbach, T.P., Kutas, M., 2011. Mass univariate analysis of event-related brain potentials/fields I: A critical tutorial review. Psychophysiology, 48, 1711. DOI: 10.1111/j.1469-8986.2011.01273.x.

Guest, S., Catmur, C., Lloyd, D., Spence, C., 2002. Audiotactile interactions in roughness perception. Experimental Brain Research, 146, 161–171. DOI: 10.1007/s00221-002-1164-z.

Guidotti, M., Beaurieux, C., Marionnaud, P., Bonnet-Brilhault, F., Wardak, C., Latinus, M., 2023. Skin type and nerve effects on cortical tactile processing: a somatosensory evoked potentials study. Journal of Neurophysiology, 130, 547–556. DOI: 10.1152/jn.00444.2022.

Hämäläinen, H., Kekoni, J., Sams, M., Reinikainen, K., Näätänen, R., 1990. Human somatosensory evoked potentials to mechanical pulses and vibration: contributions of SI and SII somatosensory cortices to P50 and P100 components. Electroencephalography and Clinical Neurophysiology, 75, 13–21. DOI: 10.1016/0013-4694(90)90148-D.

Harris, J.A., Miniussi, C., Harris, I.M., Diamond, M.E., 2002. Transient Storage of a Tactile Memory Trace in Primary Somatosensory Cortex. Journal of Neuroscience, 22, 8720–8725. DOI: 10.1523/JNEUROSCI.22-19-08720.2002.

Harvey, M.A., Saal, H.P., Dammann, J.F., Bensmaia, S.J., 2013. Multiplexing Stimulus Information through Rate and Temporal Codes in Primate Somatosensory Cortex. PLOS Biology, 11, e1001558. DOI: 10.1371/journal.pbio.1001558.

Heed, T., Azañon, E., 2014. Using time to investigate space: a review of tactile temporal order judgments as a window onto spatial processing in touch. Frontiers in Psychology, 5 : 76. DOI : 10.3389/fpsyg.2014.00076.

Heid, C., Mouraux, A., Treede, R.-D., Schuh-Hofer, S., Rupp, A., Baumgärtner, U., 2020. Early gamma-oscillations as correlate of localized nociceptive processing in primary sensorimotor cortex. Journal of Neurophysiology, 123, 1711–1726. DOI: 10.1152/jn.00444.2019.

Heller, M.A., 1984. Active and Passive Touch: The Influence of Exploration Time on form Recognition. The Journal of General Psychology, 110, 243–249. DOI: 10.1080/00221309.1984.9709968.

Henderson, J., Mari, T., Hopkinson, A., Byrne, A., Hewitt, D., Newton-Fenner, A., Giesbrecht, T., Marshall, A., Stancák, A., Fallon, N., 2022. Neural correlates of texture perception during active touch. Behavioural Brain Research, 429, 113908. DOI: 10.1016/j.bbr.2022.113908.

Henderson, J., Mari, T., Hopkinson, A., Hewitt, D., Newton-Fenner, A., Giesbrecht, T., Marshall, A., Stancak, A., Fallon, N., 2023. Neural correlates of perceptual texture change during active touch. Frontiers in Neuroscience, 17, 1197113. DOI: 10.3389/fnins.2023.1197113.

Herrmann, C.S., Knight, R.T., 2001. Mechanisms of human attention: event-related potentials and oscillations. Neuroscience & Biobehavioral Reviews, 25, 465–476. DOI: 10.1016/S0149-7634(01)00027-6.

Hogendoorn, H., Kammers, M., Haggard, P., Verstraten, F., 2015. Self-touch modulates the somatosensory evoked P100. Experimental Brain Research, 233, 2845–2858. DOI: 10.1007/s00221-015-4355-0

Hollins, M., 2001. Vibrotactile adaptation impairs discrimination of fine, but not coarse, textures. Somatosensory & Motor Research, 18, 253–262. DOI: 10.1080/01421590120089640.

Hollins, M., Bensmaïa, S.J., Washburn, S., 2001. Vibrotactile adaptation impairs discrimination of fine, but not coarse, textures. Somatosensory & Motor Research, 18, 253–262.

Hollins, M., Bensmaïa, S.J., Roy, E.A., 2002. Vibrotaction and texture perception. Behavioural Brain Research, 135, 51–56. DOI: 10.1016/S0166-4328(02)00154-7.

Hollins, M., Risner, S.R., 2000. Evidence for the duplex theory of tactile texture perception. Perception & Psychophysics, 62, 695–705. DOI : 10.3758/BF03206916.

Holmes, N.P., Tamè, L., 2023. Detection, Discrimination & Localization: The Psychophysics of Touch, in: Holmes, N.P. (Ed.), Somatosensory Research Methods, Neuromethods. Springer US, New York, NY, pp. 3–33.

Hsiao, S., 2008. Central mechanisms of tactile shape perception. Current Opinion in Neurobiology, Sensory systems, 18, 418–424. DOI: 10.1016/j.conb.2008.09.001.

Hubbard, T., 2013. Do the flash-lag effect and representational momentum involve similar extrapolations? Frontiers in Psychology, 4, 290. DOI: 10.3389/fpsyg.2013.00290.

Hubbard, T.L., 2018. Influences on representational momentum, in: Spatial Biases in Perception and Cognition. Cambridge University Press, New York, NY, US, pp. 121–138.

Hubbard, T.L., 2014. The flash-lag effect and related mislocalizations: Findings, properties, and theories. Psychological Bulletin, 140, 308–338. DOI: 10.1037/a0032899.

Hubbard, T.L., 2005. Representational momentum and related displacements in spatial memory: A review of the findings. Psychonomic Bulletin & Review, 12, 822–851. DOI: 10.3758/BF03196775.

Hunt, C.C., 1990. Mammalian muscle spindle: peripheral mechanisms. Physiological Reviews, 70(3), 643-663.

Isenstein, E.L., Freedman, E.G., Molholm, S., Foxe, J.J., 2024. Somatosensory temporal sensitivity in adults on the autism spectrum: A high-density electrophysiological mapping study using the mismatch negativity (MMN) sensory memory paradigm. Autism Research, 17, 1760–1777. DOI: 10.1002/aur.3186.

Iwamura, Y., 1998. Hierarchical somatosensory processing. Current Opinion in Neurobiology, 8, 522–528. DOI: 10.1016/S0959-4388(98)80041-X.

Iwamura, Y., Tanaka, M., Sakamoto, M., Hikosaka, O., 1993. Rostrocaudal gradients in the neuronal receptive field complexity in the finger region of the alert monkey's postcentral gyrus. Experimental Brain Research, 92, 360–368. DOI: 10.1007/BF00229023.

Iwamura, Y., Tanaka, M., Sakamoto, M., Hikosaka, O., 1983. Converging patterns of finger representation and complex response properties of neurons in area 1 of the first somatosensory cortex of the conscious monkey. Experimental Brain Research, 51, 327–337. DOI: 10.1007/BF00237869.

Jain, N., Catania, K.C., Kaas, J.H., 1998. A histologically visible representation of the fingers and palm in primate area 3b and its immutability following long-term deafferentations. Cerebral Cortex, 8, 227–236. DOI: 10.1093/cercor/8.3.227.

Jain, N., Qi, H.-X., Catania, K.C., Kaas, J.H., 2001. Anatomic correlates of the face and oral cavity representations in the somatosensory cortical area 3b of monkeys. Journal of Comparative Neurology, 429, 455–468. DOI: 10.1002/1096-9861(20010115)429:3<455::AID-CNE7>3.0.CO;2-F.

Janko, M., Wiertlewski, M., Visell, Y., 2018. Contact geometry and mechanics predict friction forces during tactile surface exploration. Scientific Reports, 8, 4868. DOI: 10.1038/s41598-018-23150-7.

Jiang, W., Chapman, C.E., Lamarre, Y., 1991. Modulation of the cutaneous responsiveness of neurones in the primary somatosensory cortex during conditioned arm movements in the monkey. Experimental Brain Research, 84, 342–354. DOI: 10.1007/BF00231455.

Jiang, W., Tremblay, F., Chapman, C.E., 1997. Neuronal Encoding of Texture Changes in the Primary and the Secondary Somatosensory Cortical Areas of Monkeys During Passive Texture Discrimination. Journal of Neurophysiology, 77, 1656–1662. DOI: 10.1152/jn.1997.77.3.1656.

Johansson, R.S., Edin, B.B., 1993. Predictive feed-forward sensory control during grasping and manipulation in man, in: Biomedical research (Tokyo). Presented at the Dynamics of perception. International symposium, pp. 95–106.

Johansson, R.S., Vallbo, Å.B., 1983. Tactile sensory coding in the glabrous skin of the human hand. Trends in Neurosciences, 6, 27–32. DOI: 10.1016/0166-2236(83)90011-5.

Johansson, R.S., Vallbo, A.B., 1979. Tactile sensibility in the human hand: relative and absolute densities of four types of mechanoreceptive units in glabrous skin. The Journal of Physiology, 286, 283–300. DOI: 10.1113/jphysiol.1979.sp012619.

Johnson, K.O., 2001. The roles and functions of cutaneous mechanoreceptors. Current Opinion in Neurobiology, 11, 455–461. DOI: 10.1016/S0959-4388(00)00234-8.

Jones, L.A., Smith, A.M., 2014. Tactile sensory system: encoding from the periphery to the cortex. WIREs Systems Biology and Medicine, 6, 279–287. DOI: 10.1002/wsbm.1267.

Jones, L.A., Tan, H.Z., 2013. Application of Psychophysical Techniques to Haptic Research. IEEE Transactions on Haptics 6, 268–284. DOI: 10.1109/TOH.2012.74.

Jousmäki, V., Hari, R., 1998. Parchment-skin illusion: sound-biased touch. Current Biology, 8, R190–R191. DOI: 10.1016/S0960-9822(98)70120-4.

Jurado, C., Larrea, M., Rosero, D., Vizuete, J., Marquardt, T., 2021. Critical Repetition Rates for Perceptual Segregation of Time-Varying Auditory, Visual and Vibrotactile Stimulation. Timing & Time Perception, 10, 122–141. DOI: 10.1163/22134468-bja10043.

Juravle, G., McGlone, F., Spence, C., 2013. Context-dependent changes in tactile perception during movement execution. Frontiers in Psychology, 4, 913. DOI: 10.3389/fpsyg.2013.00913.

Kaas, J.H., 1993. The functional organization of somatosensory cortex in primates. Annals of Anatomy - Anatomischer Anzeiger 175, 509–518. DOI: 10.1016/S0940-9602(11)80212-8.

Kaas, J.H., 1983. What, if anything, is SI? Organization of first somatosensory area of cortex. Physiological Reviews, 63(1), 206-231. DOI: 10.1152/physrev.1983.63.1.206.

Kavounoudias, A., Roll, J.P., Anton, J.L., Nazarian, B., Roth, M., Roll, R., 2008. Proprio-tactile integration for kinesthetic perception: An fMRI study. Neuropsychologia, 46, 567–575. DOI: 10.1016/j.neuropsychologia.2007.10.002.

Kawato, M., 1999. Internal models for motor control and trajectory planning. Current Opinion in Neurobiology, 9, 718–727. DOI: 10.1016/S0959-4388(99)00028-8.

Kayser, C., Petkov, C.I., Augath, M., Logothetis, N.K., 2005. Integration of Touch and Sound in Auditory Cortex. Neuron, 48, 373–384. DOI: 10.1016/j.neuron.2005.09.018.

Kekoni, J., Hämäläinen, H., Rautio, J., Tukeva, T., 1989. Mechanical sensibility of the sole of the foot determined with vibratory stimuli of varying frequency. Experimental Brain Research, 78, 419-424. DOI: 10.1007/BF00228915.

Kekoni, J., Hämäläinen, H., Saarinen, M., Gröhn, J., Reinikainen, K., Lehtokoski, A., Näätänen, R., 1997. Rate effect and mismatch responses in the somatosensory system: ERP-recordings in humans. Biological Psychology, 46, 125–142. DOI: 10.1016/S0301-0511(97)05249-6.

Khalsa, P.S., Friedman, R.M., Srinivasan, M.A., Lamotte, R.H., 1998. Encoding of Shape and Orientation of Objects Indented Into the Monkey Fingerpad by Populations of Slowly and Rapidly Adapting Mechanoreceptors. Journal of Neurophysiology, 79, 3238–3251. DOI: 10.1152/jn.1998.79.6.3238.

Kilteni, K., Engeler, P., Ehrsson, H.H., 2020. Efference Copy Is Necessary for the Attenuation of Self-Generated Touch. iScience, 23(2). DOI: 10.1016/j.isci.2020.100843.

Kim, J., Müller, K.R., Chung, Y.G., Chung, S.C., Park, J.Y., Bülthoff, H., Kim, S.P., 2015. Distributed functions of detection and discrimination of vibrotactile stimuli in the hierarchical human somatosensory system. Frontiers in Human Neuroscience, 8, 1070. DOI: 10.3389/fnhum.2014.01070.

Kim, J.K., Zatorre, R.J., 2011. Tactile–Auditory Shape Learning Engages the Lateral Occipital Complex. Journal of Neuroscience, 31, 7848–7856. DOI : 10.1523/JNEUROSCI.3399-10.2011.

Kim, J.K., Zatorre, R.J., 2010. Can you hear shapes you touch? Experimental Brain Research 202, 747-754. DOI: 10.1007/s00221-010-2178-6.

Kingdom, F.A.A., Prins, N., 2010. Psychophysics: A practical introduction, Psychophysics: A practical introduction. Elsevier Academic Press, San Diego, CA, US.

Kitada, R., Hashimoto, T., Kochiyama, T., Kito, T., Okada, T., Matsumura, M., Lederman, S.J., Sadato, N., 2005. Tactile estimation of the roughness of gratings yields a graded response in the human brain: an fMRI study. NeuroImage, 25, 90–100. DOI: 10.1016/j.neuroimage.2004.11.026.

Knecht, S., Kunesch, E., Buchner, H., Freund, H.-J., 1993. Facilitation of somatosensory evoked potentials by exploratory finger movements. Experimental Brain Research, 95, 330–338. DOI: 10.1007/BF00229790.

Kontsevich, L.L., Tyler, C.W., 1999. Bayesian adaptive estimation of psychometric slope and threshold. Vision Research, 39, 2729–2737. DOI: 10.1016/S0042-6989(98)00285-5.

Kornhuber, H.H., Deecke, L., 1985. The starting function of the SMA. Behavioral and Brain Sciences 8, 591–592. DOI: 10.1017/S0140525X00045210.

Krubitzer, L.A., Kaas, J.H., 1992. The somatosensory thalamus of monkeys: Cortical connections and a redefinition of nuclei in marmosets. Journal of Comparative Neurology, 319, 123–140. DOI: 10.1002/cne.903190111.

Krubitzer, L.A., Kaas, J.H., 1990. The organization and connections of somatosensory cortex in marmosets. Journal of Neuroscience, 10, 952–974. DOI: 10.1523/JNEUROSCI.10-03-00952.1990.

LaMotte, R.H., Srinivasan, M.A., 1996. Neural encoding of shape: responses of cutaneous mechanoreceptors to a wavy surface stroked across the monkey fingerpad. Journal of Neurophysiology, 76, 3787–3797. DOI: 10.1152/jn.1996.76.6.3787.

Langdon, A.J., Boonstra, T.W., Breakspear, M., 2011. Multi-frequency phase locking in human somatosensory cortex. Progress in biophysics and molecular biology, 105, 58–66. DOI: 10.1016/j.pbiomolbio.2010.09.015.

Lederman, S.J., 1981. The perception of surface roughness by active and passive touch. Bulletin of the Psychonomic Society, 18, 253–255. DOI: 10.3758/BF03333619.

Lederman, S.J., 1979. Auditory Texture Perception. Perception, 8, 93–103. DOI: 10.1068/p080093.

Lederman, S.J., Gati, J., Servos, P., Wilson, D., 2001. fMRI-derived cortical maps for haptic shape, texture, and hardness. Cognitive Brain Research, 12, 307–313.

Lederman, S.J., Klatzky, R.L., 1993. Extracting object properties through haptic exploration. Acta psychologica, 84, 29–40. DOI : 10.1016/S0926-6410(01)00041-6.

Lederman, S.J., Klatzky, R.L., Morgan, T., Hamilton, C., 2002. Integrating multimodal information about surface texture via a probe: relative contributions of haptic and touch-produced sound sources, in: Proceedings 10th Symposium on Haptic Interfaces for Virtual Environment and Teleoperator Systems. HAPTICS 2002. pp. 97–104. DOI: 10.1109/HAPTIC.2002.998946.

Leinonen, L., Hyvärinen, J., Nyman, G., Linnankoski, I., 1979. I. Functional properties of neurons in lateral part of associative area 7 in awake monkeys. Experimental Brain Research, 34, 299–320. DOI: 10.1007/BF00235675.

Lenc, T., Lenoir, C., Keller, P.E., Polak, R., Mulders, D., Nozaradan, S., 2024. Measuring self-similarity in empirical signals to understand musical beat perception. Journal of Neuroscience, 61(2): 316637. DOI: 10.1111/ejn.16637.

Lenc, T., Merchant, H., Keller, P.E., Honing, H., Varlet, M., Nozaradan, S., 2021. Mapping between sound, brain and behaviour: four-level framework for understanding rhythm processing in humans and non-human primates. Philosophical Transactions of the Royal Society B: Biological Sciences, 376, 20200325. DOI: 10.1098/rstb.2020.0325.

Lenz, F.A., Dostrovsky, J.O., Tasker, R.R., Yamashiro, K., Kwan, H.C., Murphy, J.T., 1988. Single-unit analysis of the human ventral thalamic nuclear group: somatosensory responses. Journal of Neurophysiology, 59, 299–316. DOI: 10.1152/jn.1988.59.2.299.

Lenz, F.A., Seike, M., Lin, Y.C., Baker, F.H., Rowland, L.H., Gracely, R.H., Richardson, R.T., 1993. Neurons in the area of human thalamic nucleus ventralis caudalis respond to painful heat stimuli. Brain Research, 623, 235–240. DOI: 10.1016/0006-8993(93)91433-S.

Liang, M., Mouraux, A., Hu, L., Iannetti, G.D., 2013. Primary sensory cortices contain distinguishable spatial patterns of activity for each sense. Nature Communications, 4, 1979. DOI: 10.1038/ncomms2979.

Liu-Shuang, J., Norcia, A.M., Rossion, B., 2014. An objective index of individual face discrimination in the right occipito-temporal cortex by means of fast periodic oddball stimulation. Neuropsychologia 52, 57–72. DOI: 10.1016/j.neuropsychologia.2013.10.022.

Long, K.H., Lieber, J.D., Bensmaia, S.J., 2022. Texture is encoded in precise temporal spiking patterns in primate somatosensory cortex. Nature Communications, 13, 1311. DOI: 10.1038/s41467-022-28873-w.

Loutit, A.J., Vickery, R.M., Potas, J.R., 2021. Functional organization and connectivity of the dorsal column nuclei complex reveals a sensorimotor integration and distribution hub. Journal of Comparative Neurology, 529, 187–220. DOI: 10.1002/cne.24942.

Macefield, G., Gandevia, S. C., & Burke, D. (1989). Conduction velocities of muscle and cutaneous afferents in the upper and lower limbs of human subjects. Brain, 112(6), 1519–1532. DOI: 10.1093/brain/112.6.1519.

Mackevicius, E.L., Best, M.D., Saal, H.P., Bensmaia, S.J., 2012. Millisecond Precision Spike Timing Shapes Tactile Perception. Journal of Neuroscience, 32, 15309–15317. DOI: 10.1523/JNEUROSCI.2161-12.2012.

Manfredi, L.R., Saal, H.P., Brown, K.J., Zielinski, M.C., Dammann, J.F., Polashock, V.S., Bensmaia, S.J., 2014. Natural scenes in tactile texture. Journal of Neurophysiology, 111(9): 1792–1802. DOI: 10.1152/jn.00680.2013.

Maris, E., Oostenveld, R., 2007. Nonparametric statistical testing of EEG- and MEG-data. Journal of Neuroscience Methods, 164, 177–190. DOI: 10.1016/j.jneumeth.2007.03.024.

Matusz, P.J., Dikker, S., Huth, A.G., Perrodin, C., 2019. Are We Ready for Real-world Neuroscience? Journal of Cognitive Neuroscience, 31, 327–338. DOI: 10.1162/jocn_e_01276.

Merz, S., Meyerhoff, H.S., Frings, C., Spence, C., 2020. Representational momentum in vision and touch: Visual motion information biases tactile spatial localization. Attention, Perception & Psychophysics, 82, 2618–2629. DOI: 10.3758/s13414-020-01989-1.

Miller, J., 1982. Divided attention: Evidence for coactivation with redundant signals. Cognitive Psychology, 14, 247–279. DOI: 10.1016/0010-0285(82)90010-X.

Miller, L.E., Longo, M.R., Saygin, A.P., 2019. Tool use modulates somatosensory cortical processing in humans. Journal of Cognitive Neuroscience, 31, 1782–1795. DOI: 10.1162/jocn_a_01452.

Mizrachi, N., Nelinger, G., Ahissar, E., Arieli, A., 2022. Idiosyncratic selection of active touch for shape perception. Scientific Reports, 12, 2922. DOI: 10.1038/s41598-022-06807-2.

Morein-Zamir, S., Soto-Faraco, S., Kingstone, A., 2003. Auditory capture of vision: examining temporal ventriloquism. Cognitive Brain Research, 17, 154–163. DOI: 10.1016/S0926-6410(03)00089-2.

Moscatelli, A., Bianchi, M., Ciotti, S., Bettelani, G.C., Parise, C.V., Lacquaniti, F., Bicchi, A., 2019. Touch as an auxiliary proprioceptive cue for movement control. Science Advances, 5(6), eaaw3121. DOI: 10.1126/sciadv.aaw3121.

Moungou, A., Thonnard, J.-L., Mouraux, A., 2016a. EEG frequency tagging to explore the cortical activity related to the tactile exploration of natural textures. Scientific Reports, 6, 20738. DOI : 10.1038/srep20738.

Moungou, A., Vezzoli, E., Lombart, C., Lemaire-Semail, B., Thonnard, J., Mouraux, A., 2016b. A novel method using EEG to characterize the cortical processes involved in active and passive touch. IEEE Haptics Symposium (HAPTICS), pp. 205–210. DOI: 10.1109/HAPTICS.2016.7463178.

Mountcastle, V.B., LaMotte, R.H., Carli, G., 1972. Detection thresholds for stimuli in humans and monkeys: comparison with threshold events in mechanoreceptive afferent nerve fibers innervating the monkey hand. Journal of Neurophysiology, 35(1), 122-136. DOI: 10.1152/jn.1972.35.1.122.

Mountcastle, V.B., Talbot, W.H., Sakata, H., Hyvärinen, J., 1969. Cortical neuronal mechanisms in flutter-vibration studied in unanesthetized monkeys. Neuronal periodicity and frequency discrimination. Journal of Neurophysiology, 32(3), 452-484. DOI: 10.1152/jn.1969.32.3.452.

Mouraux, A., Iannetti, G.D., 2009. Nociceptive Laser-Evoked Brain Potentials Do Not Reflect Nociceptive-Specific Neural Activity. Journal of Neurophysiology, 101, 3258–3269. DOI: 10.1152/jn.91181.2008.

Mouraux, A., Iannetti, G.D., Colon, E., Nozaradan, S., Legrain, V., Plaghki, L., 2011. Nociceptive Steady-State Evoked Potentials Elicited by Rapid Periodic Thermal Stimulation of Cutaneous Nociceptors. Journal of Neuroscience, 31, 6079–6087. DOI: 10.1523/JNEUROSCI.3977-10.2011.

Muniak, M.A., Ray, S., Hsiao, S.S., Dammann, J.F., Bensmaia, S.J., 2007. The Neural Coding of Stimulus Intensity: Linking the Population Response of Mechanoreceptive Afferents with Psychophysical Behavior. Journal of Neuroscience, 27, 11687–11699. DOI : 10.1523/JNEUROSCI.1486-07.2007.

Murray, E.A., Mishkin, M., 1984. Relative contributions of SII and area 5 to tactile discrimination in monkeys. Behavioural Brain Research, 11, 67–83. DOI: 10.1016/0166-4328(84)90009-3.

Murray, M.M., Foxe, J.J., Higgins, B.A., Javitt, D.C., Schroeder, C.E., 2001. Visuo-spatial neural response interactions in early cortical processing during a simple reaction time task: a high-density electrical mapping study. Neuropsychologia, 39, 828–844. DOI : 10.1016/S0028-3932(01)00004-5.

Muzyka, I.M., Estephan, B., 2019. Somatosensory evoked potentials. Handbook of Clinical Neurology, Clinical Neurophysiology: Basis and Technical Aspects. Elsevier, pp. 523–540.

Näätänen, R., Escera, C., 2000. Mismatch Negativity: Clinical and Other Applications. Audiology and Neurotology, 5, 105–110. DOI: 10.1159/000013874.

Näätänen, R., Paavilainen, P., Rinne, T., Alho, K., 2007. The mismatch negativity (MMN) in basic research of central auditory processing: A review. Clinical Neurophysiology 118, 2544–2590. DOI: 10.1016/j.clinph.2007.04.026.

Näätänen, R., Pakarinen, S., Rinne, T., Takegata, R., 2004. The mismatch negativity (MMN): towards the optimal paradigm. Clinical Neurophysiology 115, 140–144. DOI: 10.1016/j.clinph.2003.04.001.

Nakata, H., Inui, K., Wasaka, T., Nishihira, Y., Kakigi, R., 2003. Mechanisms of Differences in Gating Effects on Short- and Long-Latency Somatosensory Evoked Potentials Relating to Movement. Brain Topography, 15, 211–222. DOI: 10.1023/A:1023908707851.

Nelson, A.J., Staines, W.R., Graham, S.J., McIlroy, W.E., 2004. Activation in SI and SII; the influence of vibrotactile amplitude during passive and task-relevant stimulation. Cognitive Brain Research, 19, 174–184. DOI: 10.1016/j.cogbrainres.2003.11.013.

Nelson, C.A., McCleery, J.P., 2008. Use of Event-Related Potentials in the Study of Typical and Atypical Development. Journal of the American Academy of Child & Adolescent Psychiatry, 47, 1252–1261. DOI: 10.1097/CHI.0b013e318185a6d8.

Norcia, A.M., Appelbaum, L.G., Ales, J.M., Cottereau, B.R., Rossion, B., 2015. The steady-state visual evoked potential in vision research: A review. Journal of Vision, 15, 4. DOI: 10.1167/15.6.4.

Nozaradan, S., 2014. Exploring how musical rhythm entrains brain activity with electroencephalogram frequency-tagging. Philosophical Transactions of the Royal Society B: Biological Sciences, 369, 20130393. DOI: 10.1098/rstb.2013.0393.

Nozaradan, S., Mouraux, A., Cousineau, M., 2017. Frequency tagging to track the neural processing of contrast in fast, continuous sound sequences. Journal of Neurophysiology, 118, 243–253. DOI: 10.1152/jn.00971.2016.

Nozaradan, S., Peretz, I., Missal, M., Mouraux, A., 2011. Tagging the Neuronal Entrainment to Beat and Meter. Journal of Neuroscience, 31, 10234–10240. DOI: 10.1523/JNEUROSCI.0411-11.2011.

Otto, T.U., Mamassian, P., 2017. Multisensory Decisions: the Test of a Race Model, Its Logic, and Power. Multisensory Research, 30(1), 1-24. DOI: 10.1163/22134808-00002541.

Park, G., Choi, S., 2011. Perceptual space of amplitude-modulated vibrotactile stimuli, IEEE World Haptics Conference 2001, pp. 59–64. DOI: 10.1109/WHC.2011.5945462.

Pei, Y.C., Denchev, P.V., Hsiao, S.S., Craig, J.C., Bensmaia, S.J., 2009. Convergence of Submodality-Specific Input Onto Neurons in Primary Somatosensory Cortex. Journal of Neurophysiology, 102, 1843–1853. DOI: 10.1152/jn.00235.2009.

Pei, Y.C., Hsiao, S.S., Bensmaia, S.J., 2008. The tactile integration of local motion cues is analogous to its visual counterpart. Proceedings of the National Academy of Sciences, 105, 8130–8135. DOI: 10.1073/pnas.0800028105.

Plöchl, M., Gaston, J., Mermagen, T., König, P., Hairston, W.D., 2016. Oscillatory activity in auditory cortex reflects the perceptual level of audio-tactile integration. Scientific Reports, 6, 33693. DOI: 10.1038/srep33693.

Ploner, M., Schmitz, F., Freund, H.-J., Schnitzler, A., 2000. Differential Organization of Touch and Pain in Human Primary Somatosensory Cortex. Journal of Neurophysiology, 83, 1770–1776. DOI: 10.1152/jn.2000.83.3.1770.

Polich, J., 2007. Updating P300: An integrative theory of P3a and P3b. Clinical Neurophysiology, 118, 2128–2148. DOI: 10.1016/j.clinph.2007.04.019.

Pons, T.P., Garraghty, P.E., Cusick, C.G., Kaas, J.H., 1985. The somatotopic organization of area 2 in macaque monkeys. Journal of Comparative Neurology, 241, 445–466. DOI: 10.1002/cne.902410405.

Prescott, T.J., Diamond, M.E., Wing, A.M., 2011. Active touch sensing. Philosophical Transactions of the Royal Society B: Biological Sciences, 366, 2989–2995. DOI: 10.1098/rstb.2011.0167.

Prins, N., 2012. The Adaptive Psi Method and the Lapse Rate. Journal of Vision, 12, 322. DOI: 10.1167/12.9.322.

Prins, N., 2013. The psi-marginal adaptive method: How to give nuisance parameters the attention they deserve (no more, no less). Journal of Vision, 13, 3. DOI: 10.1167/13.7.3.

Prins, N., Kingdom, F.A.A., 2018. Applying the Model-Comparison Approach to Test Specific Research Hypotheses in Psychophysical Research Using the Palamedes Toolbox. Frontiers in Psychology 9, 1250. DOI: 10.3389/fpsyg.2018.01250.

Proske, U., 1997. The Mammalian Muscle Spindle. Physiology, 12, 37–42. DOI: 10.1152/physiologyonline.1997.12.1.37.

Proske, U., Gandevia, S.C., 2012. The Proprioceptive Senses: Their Roles in Signaling Body Shape, Body Position and Movement, and Muscle Force. Physiological Reviews, 92, 1651–1697. DOI: 10.1152/physrev.00048.2011.

Pruett, J.R., Sinclair, R.J., Burton, H., 2000. Response Patterns in Second Somatosensory Cortex (SII) of Awake Monkeys to Passively Applied Tactile Gratings. Journal of Neurophysiology, 84, 780–797. DOI: 10.1152/jn.2000.84.2.780.

R Core Team, R: A language and environment for statistical computing, 2021.

Raab, D.H., 1962. Division of Psychology: Statistical Facilitation of Simple Reaction Times. Transactions of the New York Academy of Sciences, 24, 574–590. DOI: 10.1111/j.2164-0947.1962.tb01433.x

Randolph, M., Semmes, J., 1974. Behavioral consequences of selective subtotal ablations in the postcentral gyrus of *Macaca mulatta*. Brain Research, 70, 55–70. DOI: 10.1016/0006-8993(74)90211-X.

Regan, D., 1989. Distinctions between the transient and steady-state response of a system. in: Human Brain Electrophysiology: Evoked Potentials and Evoked Magnetic Fields in Science and Medicine, pp. 34–42.

Regan, D., 1966. Some characteristics of average steady-state and transient responses evoked by modulated light. Electroencephalography and Clinical Neurophysiology, 20, 238–248. DOI: 10.1016/0013-4694(66)90088-5.

Rekik, Y., Vezzoli, E., Grisoni, L., Giraud, F., 2017. Localized Haptic Texture: A Rendering Technique based on Taxels for High Density Tactile Feedback, in: Proceedings of the 2017 CHI Conference on Human Factors in Computing Systems, pp. 5006–5015. DOI: 10.1145/3025453.3026010.

Retter, T., Rossion, B., Schiltz, C., 2021. Harmonic amplitude summation for frequency-tagging analysis. Journal of Cognitive Neuroscience, 33(11), 2372-2393. DOI: 10.1162/jocn_a_01763.

Rincon-Gonzalez, L., Buneo, C.A., Tillery, S.I.H., 2011. The Proprioceptive Map of the Arm Is Systematic and Stable, but Idiosyncratic. PLOS ONE, 6, e25214. DOI: 10.1371/journal.pone.0025214.

Rincon-Gonzalez, L., Naufel, S.N., Santos, V.J., Helms Tillery, S., 2012. Interactions Between Tactile and Proprioceptive Representations in Haptics. Journal of Motor Behavior, 44, 391–401. DOI: 10.1080/00222895.2012.746281.

Rohde, M., Dam, L.C.J. van, Ernst, M.O., 2016a. Statistically Optimal Multisensory Cue Integration: A Practical Tutorial. Multisensory Research, 29, 279–317. DOI: 10.1163/22134808-00002510.

Rohou-Claquin, B., Kaci, A., Lemaire-Semail, B., Gueorguiev, D., 2025. Recognition of 2D Shapes with Varying Complexity and Thickness on an Ultrasonic Tactile Display. EuroHaptics 2024, pp. 48–60. DOI: 10.1007/978-3-031-70061-3_5.

Roland, P.E., 1987. Somatosensory detection of microgeometry, macrogeometry and kinesthesia after localized lesions of the cerebral hemispheres in man. Brain Research Reviews, 12, 43–94. DOI: 10.1016/0165-0173(87)90018-X.

Romo, R., Hernández, A., Zainos, A., Salinas, E., 2003. Correlated Neuronal Discharges that Increase Coding Efficiency during Perceptual Discrimination. Neuron, 38, 649–657. DOI : 10.1016/S0896-6273(03)00287-3.

Rossini, P.M., Q. Cracco, R., B. Cracco, J., J. House, W., 1981. Short latency somatosensory evoked potentials to peroneal nerve stimulation: Scalp topography and the effect of different frequency filters. Electroencephalography and Clinical Neurophysiology, 52, 540–552. DOI: 10.1016/0013-4694(81)91429-2.

Rossini, P.M., Babiloni, C., Babiloni, F., Ambrosini, A., Onorati, P., Carducci, F., Urbano, A., 1999. "Gating" of human short-latency somatosensory evoked cortical responses during execution of movement. A high-resolution electroencephalography study. Brain Research, 843, 161–170. DOI: 10.1016/S0006-8993(99)01716-3.

Rossion, B., 2014. Understanding face perception by means of human electrophysiology. Trends in Cognitive Sciences, 18, 310–318. DOI: 10.1016/j.tics.2014.02.013.

Rossion, B., Boremanse, A., 2011. Robust sensitivity to facial identity in the right human occipito-temporal cortex as revealed by steady-state visual-evoked potentials. Journal of Vision, 11, 16. DOI: 10.1167/11.2.16.

Rossion, B., Torfs, K., Jacques, C., Liu-Shuang, J., 2015. Fast periodic presentation of natural images reveals a robust face-selective electrophysiological response in the human brain. Journal of Vision, 15, 18. DOI: 10.1167/15.1.18.

Ruben, J., Schwiemann, J., Deuchert, M., Meyer, R., Krause, T., Curio, G., Villringer, K., Kurth, R., Villringer, A., 2001. Somatotopic Organization of Human Secondary Somatosensory Cortex. Cerebral Cortex, 11, 463–473. DOI: 10.1093/cercor/11.5.463.

Saal, H.P., Bensmaia, S.J., 2014. Touch is a team effort: interplay of submodalities in cutaneous sensibility. Trends in Neurosciences, 37, 689–697. DOI: 10.1016/j.tins.2014.08.012.

Saal, H.P., Delhaye, B.P., Rayhaun, B.C., Bensmaia, S.J., 2017. Simulating tactile signals from the whole hand with millisecond precision. Proceedings of the National Academy of Sciences, 114, E5693–E5702. DOI: 10.1073/pnas.1704856114.

Saal, H.P., Wang, X., Bensmaia, S.J., 2016. Importance of spike timing in touch: an analogy with hearing? Current Opinion in Neurobiology, Systems neuroscience, 40, 142–149. DOI: 10.1016/j.conb.2016.07.013.

Salinas, E., Hernández, A., Zainos, A., Romo, R., 2000. Periodicity and Firing Rate As Candidate Neural Codes for the Frequency of Vibrotactile Stimuli. Journal of Neuroscience, 20, 5503–5515. DOI: 10.1523/JNEUROSCI.20-14-05503.2000.

Schubert, R., Blankenburg, F., Lemm, S., Villringer, A., Curio, G., 2006. Now you feel it--now you don't: ERP correlates of somatosensory awareness. Psychophysiology, 43, 31–40. DOI: 10.1111/j.1469-8986.2006.00379.x.

Schürmann, M., Caetano, G., Hlushchuk, Y., Jousmäki, V., Hari, R., 2006. Touch activates human auditory cortex. NeuroImage, 30, 1325–1331. DOI: 10.1016/j.neuroimage.2005.11.020.

Sciutti, A., Squeri, V., Gori, M., Masia, L., Sandini, G., Konczak, J., 2010. Predicted sensory feedback derived from motor commands does not improve haptic sensitivity. Experimental Brain Research, 200, 259–267. DOI: 10.1007/s00221-009-1996-x.

Semmes, J., Turner, B., 1977. Effects of cortical lesions on somatosensory tasks. Journal of Investigative Dermatology, 69, 181–189. DOI: 10.1111/1523-1747.ep12497948.

Shaw, N., 1986. The Origin of the N20 Component of the Somatosensory Evoked Potential in Man. Australian Journal of Experimental Biology and Medical Science, 64, 471–475. DOI: 10.1038/icb.1986.50.

Shen, G., Smyk, N.J., Meltzoff, A.N., Marshall, P.J., 2018a. Using somatosensory mismatch responses as a window into somatotopic processing of tactile stimulation. Psychophysiology, 55, e13030. DOI: 10.1111/psyp.13030.

Shen, G., Smyk, N.J., Meltzoff, A.N., Marshall, P.J., 2018b. Neuropsychology of Human Body Parts: Exploring Categorical Boundaries of Tactile Perception Using Somatosensory Mismatch Responses. Journal of Cognitive Neuroscience, 30, 1858–1869. DOI: 10.1162/jocn_a_01313.

Shore, D.I., Gray, K., Spry, E., Spence, C., 2005. Spatial Modulation of Tactile Temporal-Order Judgments. Perception, 34, 1251–1262. DOI: 10.1068/p3313.

Simões-Franklin, C., Whitaker, T.A., Newell, F.N., 2011. Active and passive touch differentially activate somatosensory cortex in texture perception. Human Brain Mapping, 32, 1067–1080. DOI: 10.1002/hbm.21091.

Smith, M.C., Deacon, P., 1984. Topographical anatomy of the posterior columns of the spinal cord in man. The long ascending fibres. Brain, 107(3), 671–698. DOI: 10.1093/brain/107.3.671.

Snyder, A.Z., 1992. Steady-state vibration evoked potentials: description of technique and characterization of responses. Electroencephalography and Clinical Neurophysiology/Evoked Potentials, Section 84, 257–268. DOI: 10.1016/0168-5597(92)90007-X.

Srinivasan, M.A., Whitehouse, J.M., LaMotte, R.H., 1990. Tactile detection of slip: surface microgeometry and peripheral neural codes. Journal of Neurophysiology, 63, 1323–1332. DOI: 10.1152/jn.1990.63.6.1323.

Stan Development Team, 2017. shinystan: Interactive visual and numerical diagnostics and posterior analysis for Bayesian models, R package version 2.4. 0.

Stan Development Team, RStan: the R interface to Stan, R package version 2, 2016.

Stein, B.E., Stanford, T.R., 2008. Multisensory integration: current issues from the perspective of the single neuron. Nature Reviews Neuroscience, 9, 255–266.

Stippich, C., Freitag, P., Kassubek, J., Sörös, P., Kamada, K., Kober, H., Scheffler, K., Hopfengärtner, R., Bilecen, D., Radue, E., Vieth, J., 1998. Motor, somatosensory and auditory cortex localization by fMRI and MEG. Neuroreport, 9, 1953–1957. DOI: 10.1097/00001756-199806220-00007.

Sutton, S., Braren, M., Zubin, J., John, E.R., 1965. Evoked-Potential Correlates of Stimulus Uncertainty. Science, 150, 1187–1188. DOI: 10.1126/science.150.3700.1187.

Suzuki, Y., Gyoba, J., Sakamoto, S., 2008. Selective effects of auditory stimuli on tactile roughness perception. Brain Research, 1242, 87–94. DOI: 10.1016/j.brainres.2008.06.104.

Talbot, W.H., Darian-Smith, I., Kornhuber, H.H., Mountcastle, V.B., 1968. The sense of flutter-vibration: comparison of the human capacity with response patterns of mechanoreceptive afferents from the monkey hand. Journal of Neurophysiology, 31(2), 301-334. DOI: 10.1152/jn.1968.31.2.301.

Taoka, M., Toda, T., Hihara, S., Tanaka, M., Iriki, A., Iwamura, Y., 2016. A systematic analysis of neurons with large somatosensory receptive fields covering multiple body regions in the secondary somatosensory area of macaque monkeys. Journal of Neurophysiology, 116, 2152–2162. DOI: 10.1152/jn.00241.2016.

ten Donkelaar, H.J., Broman, J., van Domburg, P., 2020. The Somatosensory System, Clinical Neuroanatomy: Brain Circuitry and Its Disorders. Springer International Publishing, pp. 171–255. DOI: 10.1007/978-3-030-41878-6_4.

Tobimatsu, S., Zhang, Y.M., Kato, M., 1999. Steady-state vibration somatosensory evoked potentials: physiological characteristics and tuning function. Clinical Neurophysiology, 110, 1953–1958. DOI: 10.1016/S1388-2457(99)00146-7.

Tuthill, J.C., Azim, E., 2018. Proprioception. Current Biology, 28, R194–R203. DOI: 10.1016/j.cub.2018.01.064.

Tuunanen, P.I., Kavec, M., Jousmäki, V., Usenius, J.-P., Hari, R., Salmelin, R., Kauppinen, R.A., 2003. Comparison of BOLD fMRI and MEG characteristics to vibrotactile stimulation. NeuroImage, 19, 1778–1786. DOI : 10.1016/S1053-8119(03)00256-8.

Vallbo, A.B., Johansson, R.S., 1984. Properties of cutaneous mechanoreceptors in the human hand related to touch sensation. Human Neurobiology, 3, 3–14.

van den Broeke, E.N., Mouraux, A., Groneberg, A.H., Pfau, D.B., Treede, R.D., Klein, T., 2015. Characterizing pinprick-evoked brain potentials before and after experimentally induced secondary hyperalgesia. Journal of Neurophysiology, 114, 2672–2681. DOI: 10.1152/jn.00444.2015.

Varnava, A., McCarthy, M., Beaumont, J.G., 2002. Line bisection in normal adults: direction of attentional bias for near and far space. Neuropsychologia, 40, 1372–1378. DOI: 10.1016/S0028-3932(01)00204-4.

Vaughan, H.G., 1982. The neural origins of human event-related potentials. Annals of the New York Academy of Sciences, 388, 125–138. DOI: 10.1111/j.1749-6632.1982.tb50788.x.

Vercillo, T., Gori, M., 2015. Attention to sound improves auditory reliability in audio-tactile spatial optimal integration. Frontiers in Integrative Neuroscience, 9, 34. DOI: 10.3389/fnint.2015.00034.

Verrillo, R.T., 1985. Psychophysics of vibrotactile stimulation. The Journal of the Acoustical Society of America, 77, 225–232. DOI: 10.1121/1.392263.

Vezzoli, E., Sednaoui, T., Amberg, M., Giraud, F., Lemaire-Semail, B., 2016. Texture Rendering Strategies with a High Fidelity - Capacitive Visual-Haptic Friction Control Device. 10th International Conference, EuroHaptics 2016, London, UK, Proceedings, Part 10, pp. 251-260. DOI: 10.1007/978-3-319-42321-0_23.

Vialatte, F.B., Dauwels, J., Maurice, M., Yamaguchi, Y., Cichocki, A., 2009. On the synchrony of steady state visual evoked potentials and oscillatory burst events. Cognitive Neurodynamics, 3, 251–261. DOI: 10.1007/s11571-009-9082-4.

Vingerhoets, G., 2014. Contribution of the posterior parietal cortex in reaching, grasping, and using objects and tools. Frontiers in Psychology, 5, 151. DOI : 10.3389/fpsyg.2014.00151.

Voisin, J., Benoit, G., Chapman, C.E., 2002a. Haptic discrimination of object shape in humans: two-dimensional angle discrimination. Experimental Brain Research, 145, 239–250. DOI: 10.1007/s00221-002-1117-6.

Voisin, J., Lamarre, Y., Chapman, C.E., 2002b. Haptic discrimination of object shape in humans: contribution of cutaneous and proprioceptive inputs. Experimental Brain Research, 145, 251–260. DOI: 10.1007/s00221-002-1118-5.

Voss, M., Ingram, J.N., Haggard, P., Wolpert, D.M., 2006. Sensorimotor attenuation by central motor command signals in the absence of movement. Nature Neuroscience, 9, 26–27. DOI: 10.1038/nn1592.

Vroomen, J., De Gelder, B., 2004. Temporal Ventriloquism: Sound Modulates the Flash-Lag Effect. Journal of Experimental Psychology: Human Perception and Performance, 30, 513–518. DOI: 10.1037/0096-1523.30.3.513.

Wang, X., Merzenich, M.M., Sameshima, K., Jenkins, W.M., 1995. Remodelling of hand representation in adult cortex determined by timing of tactile stimulation. Nature, 378, 71–75. DOI: 10.1038/378071a0.

Wasaka, T., Kida, T., Kakigi, R., 2017. Facilitation of information processing in the primary somatosensory area in the ball rotation task. Scientific Reports, 7, 15507. DOI: 10.1038/s41598-017-15775-x.

Weber, A.I., Saal, H.P., Lieber, J.D., Cheng, J.-W., Manfredi, L.R., Dammann, J.F., Bensmaia, S.J., 2013. Spatial and temporal codes mediate the tactile perception of natural textures. Proceedings of the National Academy of Sciences, 110, 17107–17112. DOI: 10.1073/pnas.1305509110.

Whitehead, K., Papadelis, C., Laudiano-Dray, M.P., Meek, J., Fabrizi, L., 2019. The Emergence of Hierarchical Somatosensory Processing in Late Prematurity. Cerebral Cortex, 29, 2245–2260. DOI: 10.1093/cercor/bhz030.

Whitney, D., Murakami, I., Cavanagh, P., 2000. Illusory spatial offset of a flash relative to a moving stimulus is caused by differential latencies for moving and flashed stimuli. Vision Research, 40, 137–149. DOI: 10.1016/S0042-6989(99)00166-2.

Whitsel, B.L., Petrucelli, L.M., Sapiro, G., 1969. Modality representation in the lumbar and cervical fasciculus gracilis of squirrel monkeys. Brain Research, 15, 67–78. DOI: 10.1016/0006-8993(69)90310-2.

Wiertlewski, M., Fenton Friesen, R., Colgate, J.E., 2016. Partial squeeze film levitation modulates fingertip friction. Proceedings of the National Academy of Sciences, 113, 9210–9215. DOI: 10.1073/pnas.1603908113.

Wiesendanger, M., Miles, T.S., 1982. Ascending pathway of low-threshold muscle afferents to the cerebral cortex and its possible role in motor control. Physiological Reviews, 62, 1234–1270. DOI: 10.1152/physrev.1982.62.4.1234.

Winter, R., Harrar, V., Gozdzik, M., Harris, L.R., 2008. The relative timing of active and passive touch. Brain Research, 1242, 54–58. DOI: 10.1016/j.brainres.2008.06.090.

Yamada, T., Kimura, J., Nitz, D.M., 1980. Short latency somatosensory evoked potentials following median nerve stimulation in man. Electroencephalography and Clinical Neurophysiology, 48, 367–376. DOI: 10.1016/0013-4694(80)90129-7.

Yau, J.M., Connor, C.E., Hsiao, S.S., 2013. Representation of tactile curvature in macaque somatosensory area 2. Journal of Neurophysiology, 109, 2999–3012. DOI: 10.1152/jn.00804.2012.

Yau, J.M., Pasupathy, A., Fitzgerald, P.J., Hsiao, S.S., Connor, C.E., 2009. Analogous intermediate shape coding in vision and touch. Proceedings of the National Academy of Sciences, 106, 16457–16462. DOI: 10.1073/pnas.0904186106.

Zahouani, H., Vargiolu, R., Boyer, G., Pailler-Mattei, C., Laquièze, L., Mavon, A., 2009. Friction noise of human skin in vivo. Wear, 17th International Conference on Wear of Materials, 267, 1274–1280. DOI: 10.1016/j.wear.2009.03.007.

Zampini, M., Torresan, D., Spence, C., Murray, M.M., 2007. Auditory–somatosensory multisensory interactions in front and rear space. Neuropsychologia, 45(8), 1869–1877. DOI: 10.1016/j.neuropsychologia.2006.12.004.